Analysis of low-voltage energy supply networks in x-by-wire autonomous electric vehicles and the thermal integration of the NV storage.

TU Delft

Audi

Pietro Trevisan

Analysis of low-voltage energy supply networks in x-by-wire autonomous electric vehicles and the thermal integration of the NV storage.

by

Pietro Trevisan

Master Thesis

in partial fulfillment of the requirements for the degree of

Master of Science
in Mechanical Engineering

at the Department Maritime and Transport Technology of Faculty Mechanical, Maritime and Materials Engineering of Delft University of Technology.
To be defended publicly on Thursday October 12th, 2023 at 13.00

Student number:	5630827
MSc track:	Multi-Machine Engineering
Report number:	2023.MME.8862
Supervisor:	Prof. Dr. Ir. Henk Polinder

Acknowledgements

With this project my academic journey comes to an end and I want to take a moment to express my gratitude to all the people that helped me get where I am now.

First, I want to thank my university supervisor Dr. Ir. Henk Polinder for helping me find this project, which allowed me to work with one of my dreams company. Also, thank you for guiding me through this last months and be part of this project, regardless of our initial agreements.
To my company supervisor Dr. Ir. Thomas Hackner, despite your busy schedule you were always able to make space for me and help me with insightful tips and comments.
To Alejandro, with your knowledge and skills you were always there to support me in finding solutions to my problems. More importantly, I owe you a thanks for your kindness and understanding, you helped me get up when I was at my lowest and stress and fear were getting the best of me.

I want to thank my parents, who made this whole dream possible and always pushed me to be the best version of myself, you are my greatest inspiration. To my brother, Antonio, you are my endless motivation. Your achievements have always been the reason why I strive, as I have always wished to reach your level of excellence.
To my housemates, Nico and Ale, with whom I shared my toughest moments. Thank you for supporting and baring me at all times, even when my mind was not in the right place.
To my friends in the Netherlands, Carlone, Zizo, Taso, Lidewij, Benny, Ansh, Ines, Albi. If I finished this project is also thanks to you that helped me put a smile on my face and release the stress.
Finally to my friends in Italy, Bhc and Fango, for always being there for me to talk and making me feel like I never left.

Abstract

With the rapid advancement of technology, we are moving towards a society that is increasingly driven by computer intelligence. At the same time, we are facing pressing environmental issues that are pushing us towards cleaner solutions. One industry that is heavily influenced by these two factors is the automotive industry, where autonomous electric vehicles are gaining more popularity. Audi AG, one of the biggest car manufacturer companies, is now trying to take a step forward in this market by implementing two low-voltage energy sources into the system to improve automation features. The main obstacle to the introduction of these energy sources is the strong influence that temperature has on them. Both high and low temperatures are detrimental to the battery's lifespan and performance and, in extreme conditions, they may completely impede the energy source from supplying energy or lead to thermal runaway. Therefore, effective thermal regulation of the energy source is fundamental to ensure battery availability and enhance efficiency. The objective of this research is to develop a new thermal regulating system for low-voltage energy sources in autonomous electric vehicles.

Contents

Nomenclature

Abbreviations

AV	Autonomous Vehicle
BTMS	Battery Thermal Management System
DDT	Dynamic Driving Tasks
EDLC	Electrical Double Layer Capacitors
EES	Electrical Energy Sources
EV	Electric Vehicle
HV	High Voltage
ICE	Internal Combustion Engines
LAB	Lead Acid Batteries
LIB	Lithium Ion Battery
LV	Low Voltage
MM	Magnetocaloric Material
PCM	Phase Change Material
SAE	Society of Automotive Engineers
SC	Supercapacitors
TR	Thermal Regulator

List of symbols

ΔT	Temperature interval [°C]
Δt	Time interval [s]
ϵ	Emissivity
A_{rad}	Radiation heat exchanged emitting area [m^2]
cs_{case}	Specific heat capacity of the case [J/kg°C]
i_P	Current delivered to the Peltier module [A]
k_{cell}	Cell thermal conductivity [W/mK]
k_{HPext}	Heat pipe external thermal conductivity [W/mK]
k_{HPint}	Heat pipe internal thermal cunductivity [W/mK]
m_case	Case mass [kg]
Q_c	Heat absorbed by the Peltier module [W]
Q_g	Heat generated by the Peltier module [W]
Q_{cond}	Heat ecxchanged through conduction [W]
Q_{conv}	Heat exchanged through convection W]
Q_{gen}	Battery internal heat generated [W]
Q_{rad}	Heat ecxchanged through radiation [W]
T_{case}	Case temperature [°C]
T_{cell}	Cell temperature [°C]
T_{cold}	Temperature of the cold side of the Peltier module [°C]
T_{final}	Final temperature of the case for the Peltier's control architecture [°C]
T_{hot}	Temperature of the hot side of the Peltier module [°C]
T_{ideal}	Ideal temperature of the case for the Peltier's control architecture [°C]
T_{start}	Starting temperature of the case for the Peltier's control architecture [°C]
U_{OCV}	Open circuit voltage [V]
A	Heat exchange surface [m^2]
i	Current [A]
it	Discharged capacity [Ah]
Q	Capacity [Ah]
SoC	State of Charge [%]
th	Thickness [m]
V	Voltage [V]

1 Introduction

The origin of electric vehicles can be traced back to the 1830s, when the first battery-powered tricycle was designed and built. This invention led to the increase of research on battery integration in the automotive sector, and by the end of the 19th century several companies had started to produce electric vehicles (EV). In the 21st century, EVs came to the forefront of the automotive industry thanks to the technological advancements and the need for a cleaner solution. Moreover, further change has been brought to the automotive sector with the introduction of autonomous vehicles (AV). These intelligent vehicles are designed to improve traffic control and overall road safety through vehicle communication and coordination, along with optimal energy consumption. Furthermore, AVs are designed to give great comfort to the user, with the final scope of removing any liability from the driver, who would then become a simple passenger in the cabin.

The company Audi AG wants to advance in this market, which requires overcoming a safety issue. In fact, x-by-wire connections must replace the mechanical ones to carry out the automation features, thus energy must always be available. In order to do so, two new low-voltage (LV) electrical energy sources (EES) are added to the power grid. The temperature of these sources must be regulated to assure their functionality and performance. Thus, the scope of this project is to develop a new design for a thermal regulator (TR). To do so, a simulation model has to be used to evaluate overall functioning and performance of the energy source alone in different conditions. This allows to gather some data in terms of heating and cooling requirements, from which it is possible to develop a new design for the TR and then simulate its influence on the energy source's performance.

The report is divided into five sections. Chapter 1 provides an initial introduction to autonomous vehicles, focusing on the five levels defined by the Society of Automotive Engineers (SAE). The project scope is presented as defined in collaboration with the company Audi AG, followed by the research questions and methodology used to address them. A literature review is conducted and presented in Chapter 2, including an analysis of two energy sources, focusing on their functioning and the influence temperature has on them. The review also includes an investigation of existing thermal regulating technologies and simulation models for EES with thermal considerations. The design process followed is then reported in Chapter 3, where three initial designs for the new components are introduced and assessed for selection of the best option. To evaluate the EES behavior and the TR performance, a simulation model is developed, as presented in Chapter 4. Finally, the results obtained with the simulation model are shown and discussed in Chapter 5, followed by conclusions and suggestions for future development indicated in Chapter 6.

1.1. Autonomous vehicles

With the development of new technologies, more intelligent and autonomous systems have been created and integrated into vehicles. As discussed in [1], AVs have been shown to be more efficient than human-driven vehicles, offering smoother acceleration and more accurate path planning. AVs also seem to be safer, in fact Bella et al. [1] reported a study where out of 128 accidents analyzed between 2014 and 2018, 63% occurred while the vehicle was in autonomous mode. However, the research showed that most of these accidents were not caused by the AVs but they were initiated by other parties, such as conventional vehicles, motorcycles, bikers, or pedestrians. AVs can assist the human driver or completely

take over the dynamic driving tasks (DDT), which include the operational and tactical functions required to operate a vehicle in traffic. Examples of DDTs are vehicle motion on the road, thus the lateral and longitudinal control of the car position in the lane, environment monitoring, which refers to the detection of surrounding objects, and maneuver planning, as in deciding what actions should the vehicle do to reach the destination [2].

Different AVs offer different levels of automation. Based on the features provided, the Society of Automotive Engineers divides these vehicles into six levels [2], as follows:

- Level 0: No Driving Automation - all tasks are performed by the human operator.
- Level 1: Driver Assistance - the automation system controls either the lateral or longitudinal motion of the vehicle, but not both simultaneously.
- Level 2: Partial Driving Automation - both lateral and longitudinal control are performed by the automation system for a sustained period of time, but within specific operating conditions.
- Level 3: Conditional Driving Automation - all DDTs are performed by the automation system for a sustained period of time and within specific operating conditions, but the human operator must be ready to overtake in case of DDT fallback.
- Level 4: High Driving Automation - same as level 3, with the added feature that the fallback is also performed by the system.
- Level 5: Full Driving Automation - all the DDT and DDT fallback are performed by the system for a sustained period of time with no limitations on operating conditions.

1.2. Audi AG's project

Currently, the highest level of automation in the automotive sector is level 2 according to the SAE classification method. According to a representative of Audi AG, one of the world's leading producers of premium cars, the company wants to advance into the world of autonomous vehicles to achieve level 3/4 on the SAE scale. The addition of new automation features requires to substitute all the mechanical connections with x-by-wire connections. This leads to a safety issue as electricity must always be available in the vehicle. To overcome this obstacle, the company has decided to introduce to the power grid two emergency low-voltage energy sources. The full system is presented in Figure 1.1, where the yellow section represents the high-voltage (HV) grid, used for traction, and the blue and green sections represent the low-voltage (LV) grids, which supply power for the automation features. By having two grids for the automation features, redundancy is obtained, which is beneficial for safety.

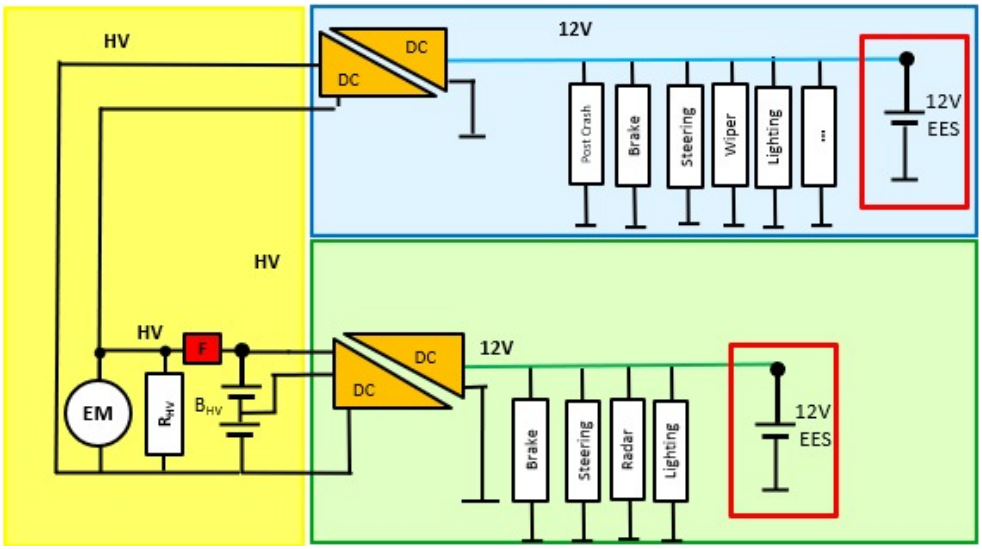

Figure 1.1: Power grid visualization, divided into HV (yellow), primary LV (blue), and secondary LV (green) section. The red rectangles indicate the new low-voltage energy sources.

The system works in normal operating conditions by utilizing the HV battery and the DC-DC converter to power all grids. In case of emergency situations, the LV supplies will have to take over. In particular, the considered emergency situations refer to conditions where the HV cannot power the LV nets because of connection issues, such as failure of the DC-DC converter. Both low and high temperatures can affect energy source performance, overall functioning, and safety. Given that it must be possible to use the vehicle in all environmental conditions, thermal regulation of the energy sources is necessary.

The primary LV energy source (blue EES in Figure 1.1) has to take over to power the automation features in case the HV battery fails to supply power to the LV nets. The primary LV energy source is also used with the car at rest for cooling, pre-heating of the cabin or the supplies, communication, etc. This implies that it is not required to deliver large amount of instant power but rather provide large amounts of energy, for which high energy density is required and it is important to maintain the EES in a close-to-optimal operating temperature range.

If the primary LV battery fails during use of the vehicle, the secondary LV energy source is activated to bring the vehicle to safety on the side of the road and zero speed, which requires high power delivery and therefore the main concern is high power density. As this source is only used for short periods, it is decided to maintain it only in a working range and not an optimal one.

A preliminary research has suggested to limit the possibility of implementation into the LV nets to lithium-ion batteries (LIB), lead-acid batteries (LAB), and supercapacitors (SC) because of their advantages [3]. LIBs have high levels of specific energy, which indicates the amount of energy stored per unit of mass, ranging between 120-240 Wh/kg [4]. This means they can store considerable amounts of energy for later use, making them available for applications where energy over time is more important than large amounts of instantaneous power. Also, lots of research has been done as this technology is been used in many different sectors, for which multiple designs have been developed to implement it in different applications [5] [6].

Supercapacitors show great levels of specific power, which represents the amount of power output per unit mass, which can go up to about 40 kW/kg, almost 100 times more than batteries. Because of this SCs have been used in applications that require the source to withstand fast charge/discharge cycles.

LABs have been available since the mid-1800s, for which this technology has also been improved consistently, making the cheapest battery type available, with good overall performance and reliability [7]. LABs show lower level of power and energy density compared to SCs and LIBs, about 30 Wh/kg and 150 W/kg respectively. LABs tend to experience capacity loss if they undergo incomplete charging cycles, which can be the case in EVs. Even though they have a much wider working temperature range, they are discarded from the selection as LIBs and SCs are considered a better fit for this application [3].

This initial introduction to the project can be summarized by a main research question, which itself can be broken down into different subquestions. This division is presented in the following section.

1.3. Research objective

The research objective is presented hereafter as a main question, followed by a number of subquestions and considerations.

Main question:

What types of electrical energy storage systems should be used in the low voltage nets and how can they be efficiently thermally regulated and integrated into the autonomous electric vehicle?

Thermal regulation is necessary given temperature is one of the most influential factors in an energy source's working performance and reliability. High efficiency of the thermal regulator in terms of time and power needed to heat/cool the supply is also a goal of the project.

Subquestions:

- What are the system specifications in terms of power and energy requirements for the low-voltage nets?
- How can the low-voltage electrical energy sources be assessed for correct selection for this application?
- What are the effects of temperature on the electrical energy sources in the electric autonomous vehicle?
- What are acceptable working temperature ranges for the low-voltage nets energy sources?
- How can the thermal regulators of the low-voltage electrical energy sources for autonomous electric vehicles be assessed for correct selection?
- How can acceptable levels of efficiency of the thermal regulator be achieved in terms of time and energy required to make the energy source reach the desired temperature?
- What control architecture should be used for monitoring the thermal regulators of the low-voltage energy sources?

The questions listed above identify the main concerns of the project. However, it is necessary to consider further aspects, such as understanding from the industry why existing technologies, used for the main battery, cannot efficiently regulate the low-voltage energy sources. From this, it is then possible to establish the flaws and limitations of the state-of-the-art technologies, thus identifying the needed improvements. Also, the temperature profile of the low-voltage energy sources is needed to understand the level of heating/cooling required. To do so, a simulation model of the energy source, considering thermal influence, must be developed, and is therefore also important to understand what type of model best fits this scenario.

1.4. Methodology

In this section, the methodology followed to answer the research questions is presented.

At first, a literature review on the topic is carried out to select the proper EES for this application based on system requirements, considering lithium-ion batteries and supercapacitors. Other than discussing their functioning and possible designs, the research also includes an explanation of what causes heating in the supplies and the effect different temperatures have on them. Thus, the study explains why there is a need for thermal regulators and defines specific working temperature ranges for the selected supplies. Following, the review analyzes different types of modelling methods for EES with thermal considerations to provide a framework upon which to develop a new simulation model. Finally, already existing methods for thermal regulation are analysed to establish a starting point for the development of the new designs as improvement and combination of the existing technologies. The developed model is used to gather the levels of cooling and heating required by the supplies, which worked as initial requirements for design process. Three design options are then created and the best option is selected according to specific assessment parameter and methodology. The best option is finally tested and further optimized. A graphic representation of the process followed throughout the project is presented in Figure 1.2.

The literature review is presented in Chapter 2, followed by the new component's design process and assessment in Chapter 3. The simulation model development is described in Chapter 4 and the obtained results are discussed in Chapter 5. Finally, the conclusions and suggestions for future development are addressed in Chapter 6.

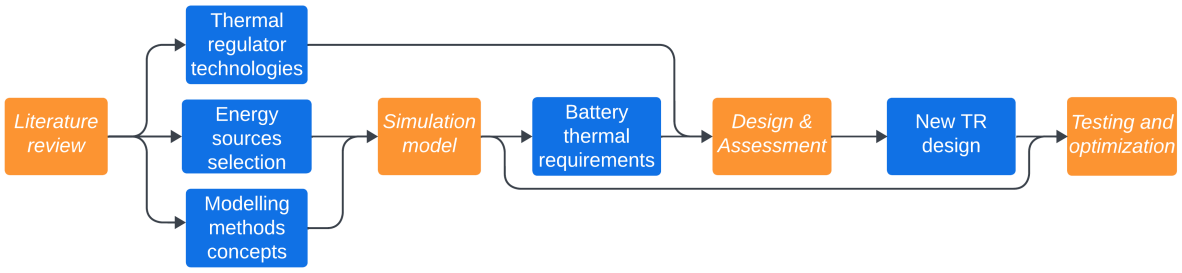

Figure 1.2: Visualization of the workflow followed during the project. The orange boxes represent the process and the blue ones the output of each process.

2

Literature review

This chapter presents the literature review that was conducted. It begins by introducing the system requirements and thermal specifications to justify the selection of LIBs and SCs. After describing the different designs, functioning, and temperature influence for the energy sources, the review focuses on the analysis of various modelling methods for EES including thermal considerations, which can serve as sources of inspiration for the creation of a new simulation model. Finally, the review concentrates on existing thermal regulation methods that can serve as starting points for the development of the new component.

2.1. Electrical Energy Sources

This review has the objective of outlining the advantages and disadvantages of LIBs and SCs, considering different designs to evaluate their use in this application. The following sections also describe the effects that different temperatures have on the considered energy sources, allowing to define specific working temperature ranges.

2.1.1. Requirements and challenges

As described above, the system is divided into low and high-voltage nets and this research focuses on the two low-voltage energy supplies. To execute the automation features, the low-voltage energy sources are required to have a 12V nominal voltage for an average load of 30A. The primary one should have a capacity of 40 or 60Ah based on the vehicle's dimensions. The project will focus on a 40 Ah energy source, which means an energy requirement of 480Wh, while the average power required is around 360 W. This high energy value is due to the fact that the primary low-voltage battery must also work with the car at rest, thus higher amounts of energy are important rather than high power density. On the other hand, the secondary low-voltage battery is used only in emergency situations to move the vehicle to safe conditions. Because of this, it is required that the secondary supply must be able to deliver energy for 2 minutes with an ambient temperature of -20°C to bring the vehicle to the side of the road and zero speed. The loads required are on average 30A with peaks of 1-2 seconds of 200A, for peaks of about 2400 W and energy requirement of 12 Wh.

The low-voltage emergency energy sources must be available and ready to function for the vehicle to start. However, when the vehicle is not being operated, the energy sources can be maintained at temperatures outside the operating range. Therefore, considering user comfort, it is necessary to quickly bring the EES to a working temperature when the vehicle has to be used. It is decided that, regardless of the system temperature, the maximum waiting time between the vehicle start and its actual use must be 2 minutes.

A summary of the requirements described is presented in Table 2.1.

	Energy [Wh]	Power [W]	Availability	Temperature range
Primary LV EES	480	360	Always	Close-to-optimal
Secondary LV EES	12	2400	Always	Working range

Table 2.1: System requirements in terms of energy, power, when is the EES required to be available when operating the vehicle, and desired EES temperature range when operating the vehicle.

Both energy sources are subject to strong temperature variations which can have negative effects on the performance, durability, and safety of the power supplies, making thermal regulation essential. High temperatures can result from external ambient temperature, internal heat generation within the cell, and heat dissipation from nearby components. Under extreme conditions, thermal runaway can occur, a dangerous condition in which overheating causes the battery temperature to rapidly increase, leading to a positive feedback loop of further overheating [7]. As vehicles may be used in multiple locations, cold temperatures are also a challenge that must be addressed. Low temperatures can have negative effects on the power supplies, such as increasing the viscosity of the electrolyte, making it more difficult for ions to move through the battery, or even impeding the overall operation of the energy source.

The primary low-voltage energy source must be regulated to work inside a close-to-optimal temperature range to increase efficiency. On the other hand, the secondary supply is not required to work at its highest efficiency but rather is fundamental for the source to be available at any given condition to assure the possibility of taking the vehicle to safety.

The following sections provide an analysis of lithium-ion batteries and supercapacitors. Along with their functioning, different designs are presented to highlight their advantages and disadvantages, and determine the best option for this application. Moreover, the effects of temperatures on each supply are considered to understand why thermal regulation is important, to identify an acceptable temperature range, and to understand the conditions that must be avoided to ensure safety and functionality. Lead-acid batteries were initially considered as possible solution, although they were discarded from the selection because, as mentioned above, they do not meet the energy or power requirements, thus they cannot be used in this application [3].

The coming sections have the objective of giving the information necessary to assess the best supply for the specific application. The energy sources in the two low-voltage nets do not have to be the same and can work independently from one another. The final decision is to implement LIB and SC for the primary and secondary low-voltage energy sources, respectively.

2.1.2. Lithium-ion batteries

The commercialization of lithium-ion batteries began in 1991 and quickly became a popular power source due to their advantages. LIBs are lightweight and compact thanks to their high energy density, and they offer good power density, relatively long life, and fast charging capabilities. However, there are also some downsides to consider, such as their cost and the emissions produced during recycling and manufacturing [5, 6].

LIBs can be classified into three main geometries: cylindrical cells, prismatic cells, and pouch or coffee-bag cells. While EV producers like Tesla prefer cylindrical cells to reduce cost, most manufacturers prefer the other shapes for their higher energy density [5, 8, 9].

Lithium-ion batteries have four main components: anode, cathode, electrolyte, and separator. The negative electrode (anode) is made of graphite, while the positive electrode is composed of lithium metal oxides, typically mixed with manganese, nickel, phosphorous or cobalt. The electrolyte, which allows the flow of lithium ions, is made of lithium salts and solvents, and the separator is a porous membrane embedded in the electrolyte to prevent the risk of a short circuit by avoiding contact between the anode and cathode. Copper current collectors are also present and connected to the electrodes. Lithium cobalt

oxide batteries present higher capacity compared to lithium manganese oxide batteries, which are then discarded. Lithium-ion phosphate batteries on the other hand are safer, cheaper, with higher energy density, and can work on a wider temperature range than the other types mentioned. Finally, lithium mixed nickel-manganese-cobalt oxide batteries have the highest energy density out of the possible types, although they show low thermal stability for which they cannot be considered for this application [10]. Therefore, the best design is lithium-ion phosphate batteries for the primary low-voltage net as the main concern is high energy density and thermal stability over price and power density.

In LIBs, lithium-ions travel through the electrolyte to supply or store electricity. During the charging process, the electrons are forced to leave the cathode and move to the anode externally, while the lithium ions detach from the cathode and travel through the electrolyte in the same direction, also going to the anode. Specifically, lithium metal oxide is reduced in the cathode, which is what causes the release of lithium-ions. This process is called intercalation. On the other hand, deintercalation refers to the same process but reverted in discharge operation, meaning ions and electrons are removed from the anode and returned to the cathode. The electrons travel in the outside circuit, powering the external load [5, 11]. A schematic of the process is presented in Figure 2.1. In this example, the cathode is made with cobalt.

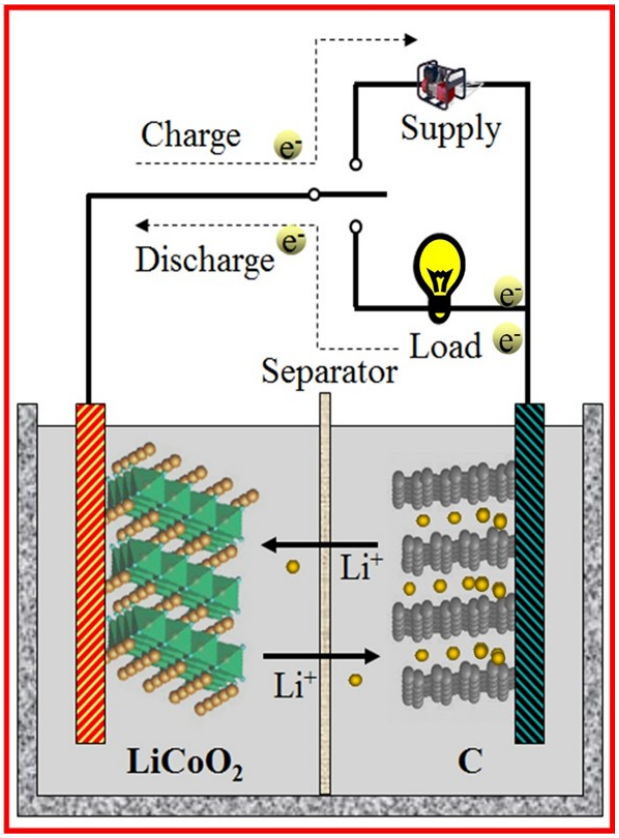

Figure 2.1: Schematic of a lithium-ion battery working process.

Because of the working process described, heat can be generated inside a lithium-ion battery through three mechanisms: Joule heating, entropic heating, and electrode reactions. The latter is a result of the transfer of ions between the electrodes and electrolyte. Just as in other types of batteries, entropic heating is partially reversible, meaning an endothermic reaction will cool the system by absorbing heat [12].

When stored at high temperatures, lithium-ion batteries experience a loss of available lithium ions, resulting in a decrease in capacity. Furthermore, when in use, high temperatures promote degradation and the growth of the solid electrolyte interface (SEI). The SEI is a thin layer that forms on the electrodes and

typically serves as a protective barrier, preventing further reaction between the electrodes and electrolyte and maintaining battery performance and capacity. However, when too thick, the SEI blocks the ions flow in between electrodes and increases the internal resistance, which reduces the capacity and increases the self-discharge rate and the risk of thermal runaway. Moreover, at even higher temperatures, the SEI may dissolve, thus leaving the electrodes with no protection.

Low temperatures also affect the battery, causing loss of active material and altering battery chemistry, reducing efficiency. The rate of lithium ion diffusion decreases due to the increased viscosity of the electrolyte, leading to the formation of a layer of lithium over the SEI, causing degradation and a drop in efficiency. This effect is exacerbated by fast charging, as more lithium ions move, causing the layer to grow larger and more quickly. At low temperatures, the reactions become more difficult to occur, and at extreme conditions, the electrolyte may freeze, completely blocking ion flow [5, 12, 13].

There is no unanimous opinion on the optimal temperature range for LIBs as it is strongly dependent on the geometry and chemistry, although, according to Galatro et al. [12], their aging behavior can be classified into three categories: low temperature (<20°C), high temperature (>40°C), and intermediate temperature (between 20 and 40°C). While not officially defined as the optimal range for operation, the intermediate temperature domain is considered best for minimizing battery aging and degradation. It is therefore recommended to maintain the battery between 20 and 40°C for higher performance and longevity. As this battery type can be considered for application as the primary low-voltage net where high energy density is required, it is best to use it around the optimal temperature range to increase efficiency while assuring functioning.

2.1.3. Supercapacitors

Supercapacitors (SCs) are also potential electric storage devices for the automotive industry. Patented in 1957, they are suitable for applications that require high efficiency and power density, serving as a balance between normal capacitors and batteries. Supercapacitors are durable with a long lifespan and fast charge/discharge time, 100 times faster than that of batteries [4]. In fact, they are already used in cars for collecting the energy from regenerative braking, which comes in high density levels, and for providing energy boosts for quick accelerations. Additionally, their good thermal stability at low temperatures makes them ideal for cold weather engine start. However, these devices are not currently used alone in EVs and are usually paired with other power sources. This is due to their low energy density, around 10-20 times less than that of LIBs, which is not practical for the automotive market. Building on these considerations, supercapacitors can be a good fit as the secondary low-voltage energy source as high power density and thermal stability are fundamental.

Supercapacitors are composed of electrodes, electrolyte, current collectors, and separator. The electrolyte, which is a solution of cations, anions, and solvents, can either be an organic or aqueous solution and serves as a charge transfer medium. The separator must allow ion transfer while preventing contact between the electrodes, and the material used depends on the electrolyte chosen. For instance, polymer separators are usually used with organic electrolytes while glass fiber is preferred for aqueous ones.

Supercapacitors can be divided into three main types based on their operating process: electrical double layer capacitors (EDLC), Redox-capacitors, and Hybrid Supercapacitors [14]. EDLCs utilize physical processes while redox-capacitors use redox reactions. Hybrid Supercapacitors store energy by combining the mechanisms of the other two.

In EDLCs, charge is stored due to the Coulomb force between positive and negative charges. When connected to a power source, electrons move from the cathode to the anode, causing positively charged ions in the electrolyte to move toward the anode and negatively charged ions toward the cathode. This results in a uniform distribution of ions and the formation of an electric double layer at the electrolyte-electrode interface, as shown in Figure 2.2, which presents the charged configuration. There is no charge shifting between electrodes and electrolyte which makes the process highly reversible. In fact, when discharging,

the electrons move from the anode to the cathode through the external load, recreating the initial conditions.

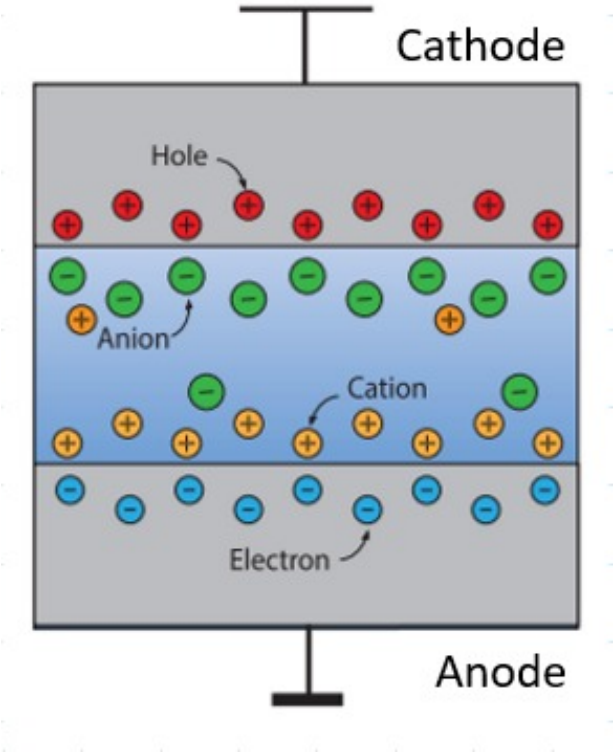

Figure 2.2: EDLC configuration at charged state.

Redox-capacitors' charge and discharge processes are similar to those of batteries. In fact, when charging, the electric field that forms makes the ions in the electrolyte move towards the electrode-electrolyte interface, activating a redox reaction that makes them enter the oxide in the electrode and release electrons that get accumulated. On the other hand, when connected to a load, the ions return to the electrolyte through a chemical reaction opposite to the one just mentioned and electrons are released into the outer circuit[14]. This redox process gives redox-capacitors higher energy density than EDLC.

Hybrid supercapacitors use both EDLC and reodx processes. As discussed in [15], they can be divided into internal parallel and internal series hybrid supercapacitors based on the materials used for the electrodes. Parallel ones combine battery and capacitive materials, providing high energy density and the possibility to work with current levels that are usually too high for battery materials. The series one combine supercapacitor and battery type electrodes. The newest version uses lithium-ion batteries and EDLC technology. The former is used for the anode and the latter for the cathode, creating lithium-ion capacitors. The fact that both processes are used assures higher capacitance and energy density, while maintaining the typical power density values. Thus, an internal parallel hybrid supercapacitor is favored for integration in the low-voltage emergency system.

Considering thermal effect, organic electrolytes used in supercapacitors have a high flammability risk and can release toxic gases at high temperatures, making them unsuitable for use at high temperatures. Also, aqueous electrolytes have a low boiling point and should not be used at temperatures higher than 70°C. Also, the high power density allows for fast charge/discharge rates and high current levels, which can result in the generation of large amounts of heat, which although can also be dissipated relatively quickly. High temperatures can accelerate the degradation of the electrical power source, particularly through aging of the electrode material and decomposition of the electrolyte. Low temperatures can also affect the performance of supercapacitors as the viscosity of the electrolyte can be increased by low

temperatures, potentially leading to freezing in extreme conditions. This obstructs the flow of electrons and ions, negatively impacting the performance of the device [14].

The temperature range for supercapacitors is then broader than that of LIBs, as the main limits are temperatures higher than 70°C or close to the electrolyte's freezing point, which is on average -20°C. This large temperature range is optimal for the application in the secondary emergency low-voltage net where the requirement is not high efficiency but even just availability of the supply.

2.1.4. Conclusions

Thanks to this review, it is defined that prismatic lithium-ion batteries can be used as primary emergency LV energy sources because of their high energy density, while supercapacitors shall be implemented in the secondary net due to their high power density. In particular, lithium-ion phosphate LIBs should be used because of their reliability, low-cost, and higher energy density compare to other LIBs model. The selected temperature range for these batteries in [20°C, 40°C], which represents a close-to-optimal working range. Concerning SCs, an internal parallel hybrid supercapcitor is suggested to improve energy density while maintaing high level of power density. The selected temperature range for this technology is [-20°C, 70°C]. Given the much narrower temperature range, the project will focus on LIBs since if the new design can maintain them in the working range than it is assured it will work with SCs as well.

The analysis also showed that cold temperatures are more challenging as the EES could be inoperable because of freezing of the electrolyte. In fact, the most common thermal regulators are usually electrically powered because more efficient in transferring heat, therefore if the energy source is inoperable the regulation will not take place. On the other hand, high temperature are more dangerous, although the EES can still function and therefore activate the regulators to enter a safe working range.

2.2. Modelling methods

This section investigates different models for simulation of EES with thermal considerations. The scope is to analyse various methods to understand the techniques used to simulate the behavior of the energy source considering the effect of temperature on the performance. Promising methods can than be used to form the basis for a new model. An initial characterization of the models is done, followed by a conceptualization of different methods used to recreate the energy source thermal behavior and overall heat distribution in the system.

Based on literature, there are two main types of electrical energy source models: physical and abstract. Physical models consider the electrochemical reactions inside the battery to describe its behavior, while abstract models are based on governing equations to recreate the behavior of the energy source, without relating the output to the internal processes. Abstract models are preferred as they allow a complete characterization of the energy source without the need to recreate the complex internal reactions of the energy source.

Lavety, Keshri, and Chaudhari [16] utilized an equivalent electrical circuit model to simulate a lead-acid battery, considering temperature influence. This method characterizes the behavior of different energy sources without the need to understand the internal chemical reactions of the supply. In fact, the model does not have a correlation with the process inside the battery, thus it can be used for all energy sources, which can be useful for the model that needs to be deloped as it must be able to simulate different EESs.

Gartner [17] modified a general Shepherd's model to simulate battery behavior as a function of temperature, based on the characteristic discharge/charge curve of the energy source. The model is not related to the battery's internal processes, thus can be used for any electrical source. The author added temperature-dependent parameters and a correction coefficient in the characteristic equation to include a non-constant charge/discharge rate. The model is extended to the whole module by considering heat transfer through convection, conduction, and radiation. An assumption of uniform temperature distribution

for each thermal body is done based on the Biot's number, and the implementation uses the electrical resistance analogy. These thermal consideration can then be used for the new simulation model.

Same et al. [18] studied the effect of different thermal factors on battery behavior, such as ambient temperature, charge/discharge rate, entropic heat coefficient, thermal conductivity, and heat transfer coefficient. The objective is to understand how these factors influence the supply's thermal behavior and how to reduce the temperature by changing these factors, defining which are more relevant and thus must be considered in the new model.

Using electrochemical impedance spectroscopy, Al Sakka et al. [19] defined the thermal resistance and capacitance of a cylindrical-cell supercapacitor. They used the latter to simulate the thermal behavior of the energy source through electrical analogy in Matlab. Convection between ambient air and the external surface of the supercapacitor and general conduction are the only heat transfer methods considered, while other convection cases and radiation are neglected. These analysis can be useful to evalute which heat transfer modes must be considered and which ones can be neglected to simplify the model.

2.2.1. Conclusions

Considering that the EES behavior must be simulated without relating to its internal processes, it is decided to use abstract models. The model must not be limited to the study of internal heat generation but rather include the influence of temperature on the EES performance, for which the models offered by Gartner [17] and Lavety, Keshri, and Chaudhari [16] are used as they do not correlate with a specific power source and they consider the actual influence of temperature on the electrical model. Moreover, the model offered by Gartner [17] considers all types of heat transfer modes, which is necessary to obtain realistic results and integrate thermal regulators. However, to simplify the model, it is decided to consider the notions offered by Al Sakka et al. [19] to appropriately integrate only the essential heat transfer modes to the model.

2.3. Thermal regulators

As mentioned in Section 2.1, temperature affects the performance of electrical energy source and therefore they must be maintained in specific ranges. To do so, thermal regulators are used to cool and heat the energy source to bring it into the desired range. This section provides an overview of existing techniques used for thermal regulation in general, not strictly in the automotive market, divided into cooling, heating, and systems that can do both. With this analysis of the state-of-the-art sector, it is possible to understand the advantages and disadvantages of the different methods. This evaluation allows the identification of suitable technologies for this application and serves as a foundation for the design of the new component. In fact, the new design can be initially developed based on existing methodologies and subsequently optimized according to the specific needs of this project.

2.3.1. Cooling methods

The most popular cooling method for battery thermal managment system (BTMS), both through natural (e.g. ambient wind) and forced convection (e.g. with a fan), is air cooling. The former is cheaper as it does not require a power source to function, although it has been proven to provide weaker heat dissipation. On the other hand, forced convection seems more promising as it shows higher heat transfer capability, but careful design must be developed to avoid its main drawback, which is the formation of temperature gradients in the battery pack. However, according to Zhang et al. [13], a well-designed geometry for both the incoming and outgoing duct can increase the temperature distribution balance by up to 93%. To further improve air cooling performance, it is also possible to recycle the pre-conditioned cold air used to cool down the cabin temperature for user comfort. By doing so, the power consumption is reduced as the air utilized has already being cooled down.

Using liquid as the cooling medium provides better efficiency compared to the air method due to its higher heat transfer coefficient, which allows for a more compact system. For instance, water and oil can have a heat transfer coefficient up to 3 times higher than that of air. Other examples of liquids used for this applica-

tion are glycol and acetone [13]. The heat transfer rate increases with liquid velocity. Further improvements in thermal conductivity and heat transfer rate can be obtained by dissolving nanoparticles of thermally conductive materials into the liquid, creating a nanofluid that offers higher efficiency. Solid particles have better conductivity than the fluid itself, and the smaller the particle, the higher the mixture's conductivity [20].

2.3.2. Heating methods

By integrating a heater into an air cooling system, a heating effect can be obtained. Energy from the battery powers the heater and, as mentioned before, this will also internally warm up the battery through Joule heating. The heater is positioned between the battery pack and a fan to warm up the air that will then get in contact with the battery. A visualization of the air heating (and cooling) system is shown in Figure 2.3. Two main downsides can be identified for this system. First, energy consumption is increased, and second, in extreme ambient conditions, the battery might not be able to start up, making it impossible to heat up with the air method. Air-based regulating systems have been implemented in different vehicles like Audi Q5 and Nissan Leaf. Nevertheless, the system's low efficiency due to the low cooling capacity of air led to the transaction to liquid-based BTMS [21]. Although, the vehicles mentioned used the system to regulate the main battery, but it could then be used to regulate the low-voltage battery, specifically the secondary one where the only objective is to obtain a working temperature and not an optimal one.

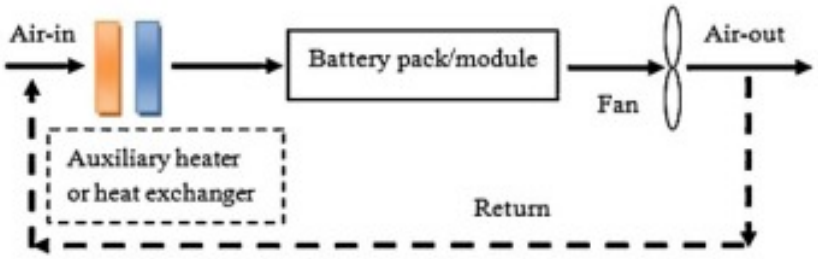

Figure 2.3: Schematic of an air-based thermal regulator

Just like for the air system, a liquid system can be used for heating as well by integrating a water heater. A visualization of a water-based TR is shown in Figure 2.4 Liquid-based thermal regulators can be found in multiple vehicles, for example, the Audi e-tron GT uses separate coolant circuits, each at its own temperature level, for battery, drive train components' and cabin thermal management, while a high-voltage heater is installed for low environmental temperatures. A similar architecture is used in the Q4 e-tron model, where only two coolant circuits are used instead Alexander Schmuck. A comparable system is also implemented by the company BMW, for instance in the iX models. This car model has three cooling/heating circuits that can also be connected with electrical valves. The excess heat generated in the drive train is used in cold conditions to warm up the power source [23]. Another example is Tesla's liquid-based cooling system, which also uses a mixture of water and glycol. This thermal regulating system is installed below the battery and works as a heat sink [24].

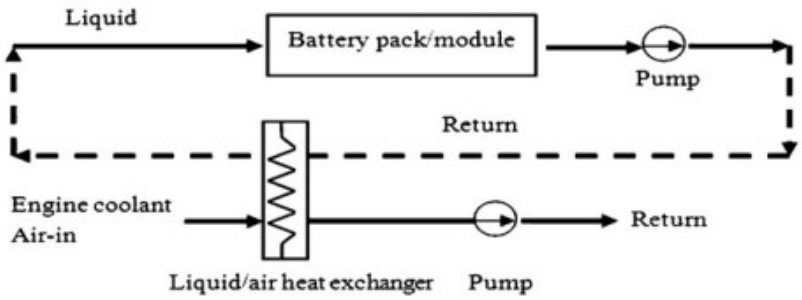

Figure 2.4: Schematic of a water-based thermal regulator

Another heating method is to use the Joule effect. This can be obtained by simply activating the energy source or by adding a load (resistance) in the battery pack. By doing so, it is possible to warm up the pack by making current flow through the resistance, thus inducing the Joule effect, which will then warm up the energy source from the inside.

2.3.3. Cooling and heating methods

This section discusses methods that are applicable to both cooling and heating tasks, which can be useful for this application as both conditions can occur. Initially, two passive methods are introduced: phase change materials (PCM) and heat pipes. Subsequently, the focus shifts to active systems, where regulating methods based on thermoelectric and magnetocaloric effects are analyzed.

Phase change materials

PCMs are environmentally friendly materials that work by the latent heat storage process. This means they can absorb heat from the energy source when at high temperatures by melting, thus reducing the energy source temperature. This heat can then be released onto the battery when it reaches lower temperature by solidification of the PCM, passively heating it up. Some examples of phase change materials are hydrated salts, stearic acid, polyethylene glycol, paraffin, graphene, and composites of the latter [13]. In general, a good PCM should be able to absorb large amounts of heat, have a high thermal conductivity, and the phase change temperature shall be within the battery temperature range. It should be chemically stable, not flammable, with small volume variation during phase change, and with no risk of hazardous gases release [25].

PCMs have the advantage of being a passive method, thus no extra energy consumption is required. They can be produced in arbitrary shapes, therefore they can be used for any kind of battery geometry. Moreover, PCMs can be used for thermal insulation, which is advantageous both in warm and cold ambient conditions as the material can be used to maintain the battery temperature about 10°C higher or lower than the surrounding initial temperature [26]. Even if this insulation effect works for short periods of time, it can be useful by combining the PCM with an active method. By doing so, the insulation can help reduce energy consumption as the active method does not have to be activated as much.

Considering now disadvantages, PCMs normally show a poor heat transfer coefficient, although this can be fixed by introducing fins to increase the contact surface area, allowing better heat transfer, or by adding thermally conductive materials to the mix. Also, the materials need time to solidify/melt, therefore they cannot assure quick cyclical thermal regulation as the material might still be melted when there is still heat coming from the power source that must be removed (the same and opposite scenario for low ambient temperatures). A possible solution is to combine PCM with another method, such as liquid-based, to guarantee the right PCM conditions at any time. However, this will then require energy consumption.

Heat pipes

A heat pipe system also works autonomously without the need for external energy sources. It uses fluid as a medium and its evaporation/condensation to transfer heat spontaneously between two points. The difference from PCM material is that heat pipes do not store heat but they only transfer it from one point to

another. Specifically, the internal fluid exchanges heat with the heat load and evaporates. The phase change creates a pressure difference in the system for which the vapor moves to the condenser, where heat is exchanged with the outside and the fluid goes back to liquid condition, and so on. Lately, micro heat pipes have been developed, which offer higher thermal conductivity and performance. Also, low cost, small dimensions, and lightweight are great advantages of the system. However, temperature gradients can occur inside the communication channel, which can then be transferred onto the EES.

Thermoelectric methods

Thermoelectric methods take advantage of thermoelectric effects, which produce heat from electricity and vice-versa; these phenomena are the Peltier and Seebeck effects. In the first case, when two different conductive materials are connected to one another and to an electrical energy source, the junction will absorb or release heat depending on the direction of the current flow. By doing so, both cooling and heating can be obtained with the same system, contrary to common electric heating. The Seebeck effect is equal and opposite to the Peltier effect. When the two conductive materials are exposed to different temperatures, current starts flowing in the circuit, generating electricity. The application of Peltier module is not spread to the automotive system because of the low efficiency. They are rather used for regulation of medical equipment where precise temperature control is required, or cooling of computer's hardware were there is small space available.

Magnetocaloric effect

Another method for regulating temperature is the magnetocaloric effect. When subject to a magnetic field, the magnetic spins inside the magnetocaloric material (MM) will align, increasing the material temperature. In Figure 2.5 the process for heating or cooling with this method is presented [27].

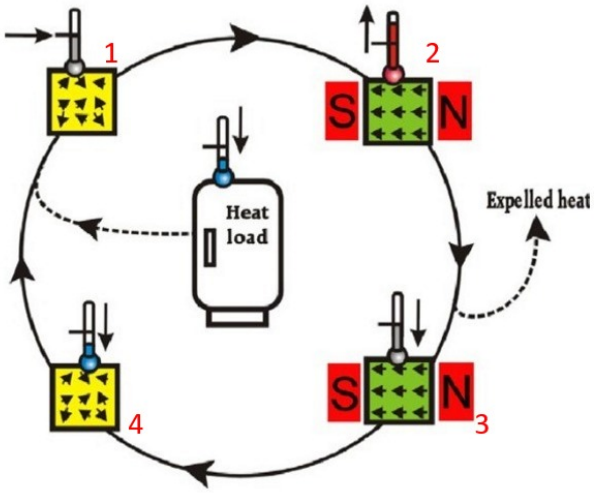

Figure 2.5: Schematic of the magnetocaloric cycle.

Considering the material at room temperature (step 1), the material is magnetized, which leads to alignment of the spins, thus a temperature increase (step 2). The magnetic field is kept constant and the material is left to cool down to room temperature (step 3), at which point the magnetic field is removed. The de-organization of the spins leads to a decrease in internal energy through heat release, for which the material reaches a temperature lower than the initial one (step 4). The material can now cool down the heat load (thus the EES) and the cycle can be repeated. If heating is required instead, only step 1 and 2 are necessary, then the material can release heat into the cold EES. These systems are still under development and improvement, but they are now used for refrigerators or systems that require extremely low temperatures, given that the system can go as low as 0 K. The main limitation to these systems is their low heating capability.

2.3.4. Conclusions

This section underlined the advantages and disadvantages of different technologies used for thermal regulation, dividing them into systems used for cooling, for heating, and for both. Methods that can both heat and cool are preferred to reduce complexity, given that both are required for this project. Nevertheless, this review showed that all the methods analysed have some type of limit, and therefore it is decided to design a hybrid system that uses a mix of technologies out of the ones analysed. Also, it is decided that the new component shall include both active and passive systems. The active ones show an overall better performance, while passive systems are useful to improve the effect of the active ones while maintaining the same level of energy consumption. The next chapter shows the integration into the design process of the technical notions gathered from this review.

3

Thermal regulator

This chapter has the scope to introduce the final design for the new component based on the information gathered in the literature review. Once fully designed, it is then possible to implement the new TR into the simulation and evaluate its performance.

Initially, three designs are presented, followed by an explanation of the parameters utilized to evaluate the designs. The assessment is then presented and the best option is selected. The starting design was then tested in the simulation described in Chapter 4 and showed to be able to maintain the battery in the desired temperature range. It was then decided to improve the design and the optimization process utilized is presented at the end of this chapter.

3.1. Designs introduction

In this section, three different designs are introduced, indicating their functioning and how they are integrated with the energy source. The main pros and cons useful for the theoretical assessment are presented as well.

Selecting the appropriate thermal regulator for the specific application can be challenging. In fact, according to [28], the battery thermal management system is one of the leading causes of unscheduled maintenance in a vehicle, indicating that the operating conditions are not always optimal. From the literature review, it was decided to include both passive and active methods in the new design to counterbalance their disadvantages: low thermal regulation capacity and energy consumption, respectively. The following designs are selected for different reasons. The Smart Battery design is considered because it assures the availability of the energy source at any time, increasing user comfort by eliminating waiting time during cold start-ups. The Magnetic Regulator design offers an upcoming technology of regulation that has higher efficiency compared to the traditional gas-based methods [29]. The Magnetic Regulator design instead is considered for its compactness and simplicity.

3.1.1. Design 1 - Smart battery

This design utilizes multiple methods, an active one, based on self-heating, and two passive ones, heat sinks, and air from the outside.

One of the main challenges of this project is to find a solution that allows leaving the vehicle at low temperatures (down to -20°C) and still ensuring the functioning of the low-voltage supplies. To overcome this obstacle, controller-based self-heating is considered. This technology utilizes the principle of the Joule effect for heating the energy source. The objective is to heat the battery through self-heating and maintain it at a working temperature. First, a trigger temperature (T_{trig}) and minimum accepted low working temperature (T_{ok}) are defined based on the selected supply. When the temperature falls below T_{trig}, a controller activates the battery until T_{ok} is reached. The goal is to keep the energy source in a temperature range high enough to ensure the functioning of the supply without dissipating too much energy in taking the supply to higher unnecessary temperatures. When the controller detects that T_{trig} is reached, it will make the battery run at low voltage levels, to heat it from the inside. Given that the heat generation inside a battery is proportional to the difference between its open circuit voltage and the voltage output, low levels

of voltage are preferred to heat the supply to T_{ok}. This process is used also when the vehicle is parked to reduce the waiting time when it needs to be operated. The HV battery will then recharge the LV battery through the DC-DC converter.

A heat sink is used to increase the overall surface of the energy source, allowing it to release more heat and thus reducing the peak temperatures reached in operating conditions. The heat sink is composed of multiple fins attached to the supply that augment its surface and thus facilitate heat transfer with the outside.

Passive air cooling is also considered for this application. This method consists of gathering air from the outside and conveying it into a duct to the energy source. This method can be critical and less performing in hot ambient temperatures. Nevertheless, in these circumstances, air-conditioning is normally activated to cool down the cabin for comfort. Thus, the energy source air cooling ducts can be coupled with the ones used for AC in the cabin, lowering the air temperature, and thus increasing cooling efficiency. The same and opposite can be done in cold conditions to deliver warm air to the battery for heating purposes. By doing so, the energy consumption from the self-heating method is reduced as heat also comes from the passive air heating method.

A visualization of the design is shown in Figure 3.1.

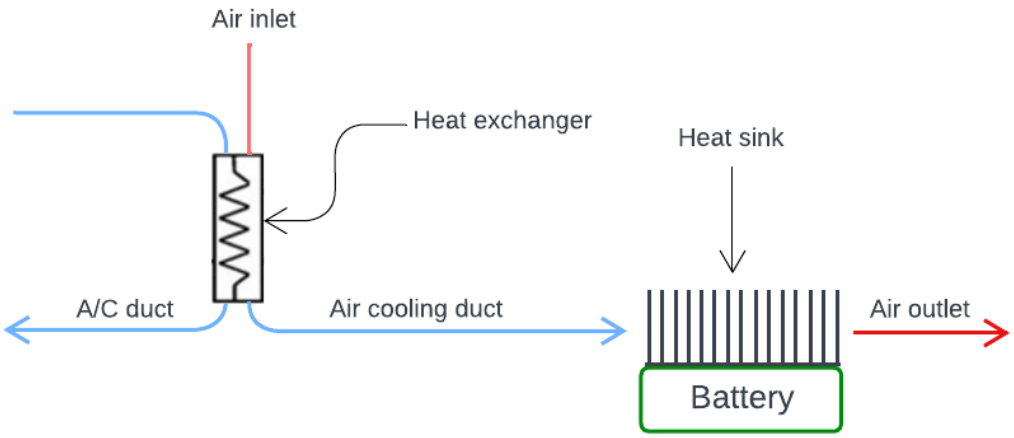

Figure 3.1: Schematic of the Smart Battery design.

3.1.2. Design 2 - Magnetic regulator

This design considers two main phenomena: the magnetocaloric effect and the Seebeck effect.

The magnetocaloric cycle can be used as described in Section 2.3.3 for both heating and cooling. To achieve this result, an outer layer of magnetocaloric material that surrounds the energy source case is installed. It is necessary to install a system to magnetize/demagnetize the MM, therefore, a rotary mechanism must be integrated as it can change the MM magnetization at different points, thus creating a continuous heat exchange. To do so, the layer of MM must be split into different parts to allow different magnetizated/demagnetized points. In cooling conditions, the magnetizer must move in steps, allowing the MM to cool down, while still magnetized, so that lower temperatures can be reached when the MM is demagnetized and energy is released. On the other hand, when heating is needed, the magnetizer can simply rotate around the MM at a low speed. The MM's shape must cover the energy source uniformly and will therefore have an almost rectangular shape. Therefore, a mechanism that changes the motion of the magnetizer from a circular one to a more rectangular one is needed.

From the technology just described, it is evident that the MM will be at different temperatures at different points. Therefore, it is possible to take advantage of this temperature gradient to generate electricity with the Seebeck effect, which can then be used to partly power the rotary system or to recharge the energy source.

A visualization of the design is shown in Figure 3.2.

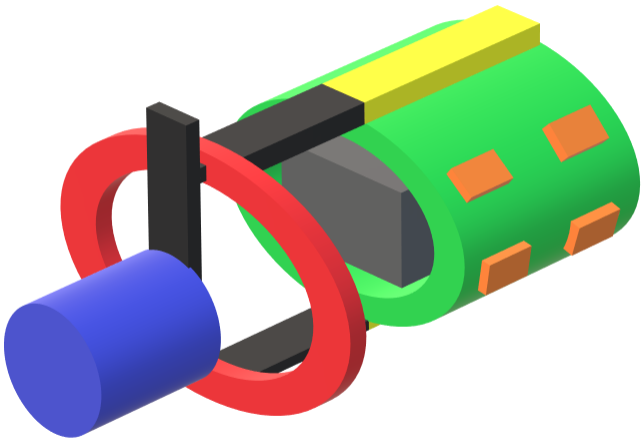

Figure 3.2: Schematic of the Magnetic Regulator design. The motor is in blue, the motion correction element in red, the mechanical arms in black, the magnetizers in yellow, the magnetocaloric material in green, the battery in grey, and the Seebeck modules in orange.

3.1.3. Design 3 - Peltier regulator

The third design is based on the combination of heat pipes and the Peltier effect.

Peltier modules are installed on the battery case and can be used for both cooling and heating. The power needed to activate the Peltier modules is drawn from the HV battery. By doing so, it can be assured the energy source is at the correct temperature when it must be activated. If the HV source cannot deliver energy anymore, the modules must rely on the LV energy source itself.

The heat pipes system is introduced to transfer heat from the HV energy source to the LV one. In fact, during usage of the vehicle, the HV battery warms up and the heat generated is normally removed and then dissipated. Although, it is possible to take advantage of this waste heat and re-invest it by implementing heat pipes. Heat pipes can be used to gather the heat from the HV source and transfer it to the LV source. By doing so, a heating effect is obtained, which reduces the amount of energy required by the Peltier modules in heating conditions. It is assumed that the distance between the HV and LV battery is of 600 mm, which will then be the length of the heat pipes.

A visualization of the design is shown in Figure 3.3.

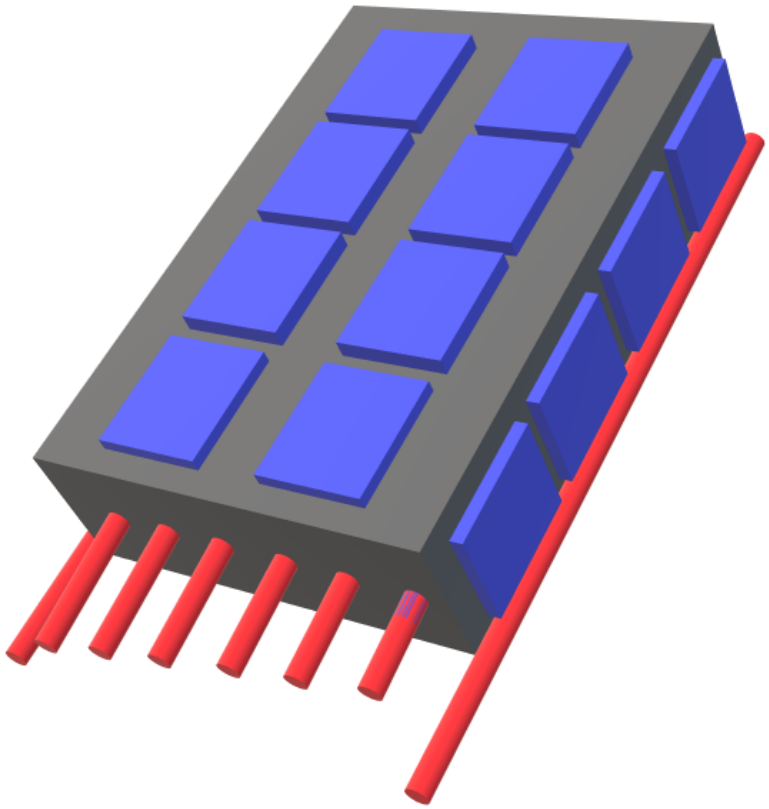

Figure 3.3: Schematic of the Peltier Regulator design. The battery is in grey, the Peltier modules in blue, and the heat pipes in red.

The presented designs must be evaluated in order to select the best solution for this application. The selection process is presented in the following section.

3.2. Design selection

This section shows the process followed for the selection of the best design out of the three described above. In particular, four different parameters are defined and a weight is assigned based on the parameter's relevance. The different designs are then evaluated and compared for each parameter, showing which one is more optimal for this application.

3.2.1. Assessment parameters

The best option out of the three proposed has to be selected for this application. The evaluation should consider both the functioning of the component and the preferences of the customer. Four parameters have been identified, and for each parameter, a weight is assigned to represent its importance in the assessment. The parameters are defined as follows:

- Thermal efficiency: it represents how well the system works and is performing in this application. Given that the goal of the component is to cool/heat the energy supply, is fundamental that the heat transferred to/from the supply is at the right level. Also, good thermal efficiency indicates low power requirements, thus, in the case of an active method, the capability to function and regulate for longer.

  For this parameter, three different conditions are considered. The most critical scenario is at low temperatures with the energy source inactive. As shown in Section 2.1, in these condition there is a

risk the EES will freeze and become inoperable. The system is also evaluated at normal operating temperatures to verify its correct functioning. Finally, high temperatures with the energy source running are considered a critical condition that could lead to failure. The three scenarios have different weights on the overall parameter final value based on their relevance, specifically, the first one is considered of the highest importance, followed by the starting high-temperature configuration. Finally, functioning at normal operating conditions is considered as basic as it is valuable but also partly assured by the other two cases.

This parameter is considered the most important one since it shows whether the system is capable of bringing the battery to the desired temperature, and thus indicates if the TR is working correctly. Because of this, its weight is 4.

- Cost of ownership: it is the best way to fully assess the price of a component as it not only considers the initial selling price but also all the costs that must be sustained throughout the system lifespan. For this purpose, a lifespan of 10 years is considered.

  Four indices are considered for the cost of ownership. First, the energy consumed to regulate the energy source's temperature. This value is approximated considering three hours of vehicle usage for five days a week. The approximate manufacturing cost is also considered as it strongly influences the selling price. Also, the expected maintenance costs are considered, defined as the costs required for one maintenance cycle times the amount of expected maintenance required throughout the considered lifespan. Finally, the weight of the component is also considered as it is strictly related to the vehicle's efficiency. It has been demonstrated that a 10% weight reduction can lead to an improvement of 13.7% in the driving range [30].

  The cost of ownership is an important factor as the company wants to minimize costs. A weight of 3 was selected after a discussion with Audi AG employees.

- Response time: this parameter measures the time required to reach the desired temperature range at cold starts. Specifically, it indicates the waiting time between the vehicle activation and the moment the LV energy source reaches a working temperature when starting at -20°C.

  A weight of 2 is assigned to this parameter as it is only important for user comfort.

- Maintenance requirements: this parameter represents the expected total amount of maintenance required for the component throughout its lifespan. Although this aspect is partly considered in the cost of ownership, it is essential to assess it individually as it is possible for the component's maintenance to be extremely cheap but required frequently. In this case, the number of times it needs to be worked on would not fully appear in the cost of ownership and would then not be considered.

  The weight assigned to this parameter is 1.

By considering and evaluating these parameters, the most suitable option for development can be determined for the new component. The following subsection presents the methodology used to evaluate the designs with the presented parameters, followed by the actual assessment.

3.2.2. Assessment methodology

To conclude the selection of the optimal solution for the new thermal regulator design, we utilize the previously outlined assessment criteria. Specifically, we compare these criteria between the different designs to establish a ranking. Points are then assigned based on their ranking: the highest-ranked design receives 3 points, the second-highest receives 2 points, and the third-highest receives 1 point. These points are then weighted by the respective parameter's relevance and summed together. The parameter with the highest cumulative points is the preferred choice. In the event of a tie, the parameter displaying better performance in the two most critical criteria, namely thermal efficiency and cost of ownership, will be considered the best option.

To facilitate understanding, an example is given. Let us consider three designs, for each one is shown whether it was the best (1st), second best (2nd), or last (3rd) for each parameter, and the corresponding points. The best option for this configuration is highlighted (the results do not refer to the actual assessment).

	Thermal efficiency	Cost of ownership	Time response	Maintenance requirements
Weight	4	3	2	1
Design 1	1st→3 pts	2nd→2 pts	3rd→1 pt	2nd→2 pts
Design 2	2nd→2 pts	1st→3 pts	2nd→2 pts	3rd→1 pt
Design 3	3rd→1 pt	3rd→1 pt	1st→3 pts	1st→3 pts

Table 3.1: Assessment example.

From Table 3.1, the following total scores are obtained for each design:

- Design 1: 3x4 + 2x3 + 1x2 + 2x1 = 22
- Design 2: 2x4 + 3x3 + 2x2 + 1x1 = 22
- Design 3: 1x4 + 1x3 + 3x2 + 3x1 = 16

Given that the first two designs have the same score, a tiebreaker is necessary. As mentioned above, the latter is based on the total value accumulated with the most important parameters, which equals 18 for design 1 and 17 for design 2, making design 1 the best option.

3.2.3. Assessment

Hereafter, the assessment for the selection of the best design is presented. The process is divided into different subsections, one for each assessment parameter, which are themselves divided into three paragraphs, one for each design. For each parameter, a visual summary of the evaluation is given. Through the presented data, assumptions, and notions, it is possible to determine the most optimal design for this application.

Thermal efficiency

The thermal efficiency parameter considers the capability of the component to bring the energy source to the desired temperature range. The parameter considers three conditions: heating at low temperatures, maintaining the correct range while operating, and cooling at high temperatures.

- Smart battery: at low temperatures with the vehicle at rest, the battery is kept in an acceptable working range thanks to the control architecture, by which functioning is assured. Further heating is also delivered from the air system if the vehicle is active and the user is heating the cabin. The main downside to the heating efficiency is the presence of the heat sink: the latter enhances heat release by increasing the overall surface of the energy source, thus accelerating the cooling of the supply. Furthermore, repetitive and short activations of the energy source at are detrimental to the supply, even further when at low temperatures.

  Considering now normal operating temperatures, heating is still effective thanks to the self-heating technique. On the other hand, cooling with heat sinks has been proven to significantly remove heat from a cell, for which it could be extended to the overall energy supply [31]. The heat generated inside the cell is released at a higher rate thanks to the heat sink and this phenomenon is increased by the air cooling. Moreover, the heat sink helps maintain temperature uniformity in the energy source, reducing the temperature gradient up to 42% compared to the battery without heat sink [32].

  Finally, at high temperatures, the system can only rely on the heat sink and air cooling combo, which can be effective but not accurately controlled.

- Magnetic regulator: the magnetocaloric effect can be used for both cooling and heating. The cooling efficiency of this method is 20 to 50% higher than conventional gas compression techniques [33]. The main downside is the heating efficiency, which is significantly lower than the cooling one. Nevertheless, the magnetocaloric effect takes place around the curie's temperature of the material, which is on average around 20°C. Therefore, the system must always be maintained at such a temperature, thus maintaining the battery in the correct temperature range.

- Peltier regulator: at low ambient temperatures and vehicle at rest, the system relies on the Peltier effect, which can stabilize the temperature of the energy source regardless of the ambient temperature and has great heating/cooling capabilities [34]. The heat pipes do not influence the system as the HV battery would also be at the same temperature, thus there would be no heat coming from the HV battery. Otherwise, if the vehicle is being used, the heat pipes systems are also heating the supply by transferring heat from the HV battery to the LV one, reducing energy consumption. The same discussion can be done for normal operating conditions.

  At high temperatures, the system must instead solely on the Peltier effect, which has great cooling efficiency. Alaoui [35] proved the ability of a Peltier-based battery thermal management system to maintain the temperature of the energy source about 10°C lower than without the BTMS, assuring safe operations. These results are only a counterbalance between power usage and cooling needs, as in fact, the Peltier regulator can generate temperatures from -40°C up to 200°C, for which thermal efficiency is assured. In this condition, the heat pipe system is useless as heat needs to be removed from the energy source.

Given all the above considerations, the Peltier regulator results to be the best option in terms of thermal efficiency. The heat pipes allow to passively heat the energy source when operating, while at critical temperatures the Peltier effect can be used, assuring always the capability to cool or heat the EES to the desired temperature range. Also, given that this system is based mostly on thermoelectric methods, the temperature of the energy source can be accurately controlled and maintained in the desired temperature range.
The Magnetic Regulator is considered second best as it always maintains the energy source at a working temperature but has low heating efficiency.
The Smart Battery finally is classified as last, as the heating efficiency is obstructed by the presence of the heat sinks, which make the energy source retain heat for short periods, thus requiring constant regulation for low-temperature conditions. Also, when cooling is required, the system has to fully rely on the passive system, therefore it cannot be assured that the battery will be maintained in the desired range.

The following table summarizes the notions mentioned above as a comparison in between the different designs' performance in different conditions.

	Smart Battery	Magnetic Regulator	Peltier Regulator
Low temperature	High	Low	High
Room temperature	Medium	High	High
High temperature	Medium	High	High
Score	2nd	3rd	1st

Table 3.2: Thermal efficiency summary

Cost of ownership
The cost of ownership considers energy consumption, manufacturing costs for series production, maintenance costs, and component weight.

- Smart battery: considering energy consumption, the self-heating technique based on the control architecture is the least efficient option. In fact, by using the simulation model developed and

analyzed in Chapter 4, when at -20°C it is necessary to use up to 80% of the total capacity to bring it to 0°C with 4C discharge rate, which corresponds to approximately 384 Wh. It is also necessary to consider the effect of the heat sink which makes the system release heat more quickly, thus making it necessary to repeat the heating cycle more often, increasing energy usage.

Manufacturing-wise, it is assumed that four heat sinks must be installed on top of the battery. Considering the TDK-Lambda Heatsink produced by RS, a total price of 200 € is met. The price for the air duct also needs to be considered. Given that the air duct needs to be coupled with the air-conditioning system, it is assumed that a 1.5 m long pipe is needed. Considering the Stairville Aluminium Pipe from Thomann, the price increases by 25€, leading to a total cost of approximately 230€.

One concern for maintenance is dust accumulation on the heat sinks, which reduces the overall heat transfer capacity of the elements. However, it is assumed that the air cooling system will remove the dust itself. On the other hand, the air cooling system requires cleaning of the duct every 3-5 years according to the NADCA (National Air Duct Cleaners Association). Thus, three maintenance cycles would be required with low costs.

Finally, it is important to consider the weight variation recorded with the installation of the BTMS. The air duct is assumed to be around 1.5 kg and the heat sinks weigh 0.5 kg each, for an approximate total of 3.5 kg extra.

	Energy consumption	Manufacturing costs	Maintenance costs	Weight
Smart battery	384 Wh	230 €	Low	3.5 kg

Table 3.3: Cost of ownership summary for Smart battery.

- Magnetic regulator: it is assumed to use four Nd2Fe14B permanent magnets as magnetizers, each 70 mm wide for a total weight of about 4 kg. The rotary system is used at an angular speed of $\pi/4$ rad/s to spin a 10 cm arm on which the magnets are mounted. With these assumptions, the total energy required can be calculated. First, the torque is defined as the product of the weight to move and the distance at which the weight is positioned, giving approximately 4 Nm. By multiplying the torque by the angular speed we obtain the power needed for this movement, which we assume has to be done over three hours, for a total of approximately 10 Wh of energy. To add on, it is necessary to consider that various stoppages and position-holding manoeuvres are needed to magnetize the magnetocaloric material, thus the actual energy requirements could be a bit higher. The Seebeck generator helps reduce the impact on the energy source by generating electricity itself. Considering using 10 modules of the model GM250-71-14-16 produced by the company RS, for an average temperature difference between the modules plate of 20°C for three hours, the total energy generation is 1.5 Wh. Thus, the total energy consumption would be approximately 8.5 Wh.

  The manufacturing costs for this design are much higher than the first one. First of all, the four magnets mentioned above cost 140 € each, for a total of 560 €. Furthermore, considering the power requirements defined above, a small stepper motor is required to rotate the magnetizing system, which requires a torque of approximately 4 Nm. A commercial motor produced by Nanotec that satisfies these requirements costs 140 €. The MM must surround the full battery, thus, considering Gadolinium since it is one of the most used materials for this application, with a thickness of 4 mm and a price of 20 €/kg, the total is about 60 €. The Seebeck modules mentioned above cost 30 € each, for a total of 300€. Finally, given the cubic shape of the energy source, the MM around it would not be spherical, thus a correction element is needed to change the motion of the magnetizers to follow the shape of the MM. Thus, even the overall manufacturing costs are about 1100 €.

Considering maintenance, the system utilizes a rotary system, which requires bearings and gears for power transmission, which themselves require maintenance, even just for lubrication. Furthermore, the extra motion-correction element is subject to varying loads and vibrations, for which further checks are required. In case of failure of the motion-correction element, full replacement of the latter would be needed. Maintenance is then often required with medium costs.

Finally, the overall weight is also high. The MM itself would weigh approximately 3 kg and the magnetizers 4 kg; the mechanical arm (that connects the magnetizers to the gears), the correction element, and power transmission gears are assumed to have a total weight of 3 kg. The stepper motor mentioned above weighs 3 kg, and all the Seebeck modules about 1kg, for a total of approximately 14 kg.

	Energy consumption	Manufacturing costs	Maintenance costs	Weight
Magnetic regulator	8.5 Wh	1100 €	High	14 kg

Table 3.4: Cost of ownership summary for Magnetic regulator.

- Peltier regulator: the energy usage of the Peltier modules can be assumed from their technical sheets. Alaoui [35] utilized six modules per each cell. Although, the considered cells in the research had a capacity of 60 Ah, thus higher temperatures would be reached because of higher discharge rates utilized. Thus, considering the lower capacity of the cell in this project and the lower heat generation, fewer modules are considered. The modules used are offered by the company RS, model ET-127-20-25-RS, with dimensions of 55x55x55 mm, for a total of 24 modules that can be used to cover the outside surface of the energy source and still leave space for the heat pipes. The assumed actual usage time is 0.5 h over a time span of 3 h since the modules will not be constantly activated. Assuming then an average current and voltage required of 3 A and 6V, respectively, the total energy consumption is about 216 Wh.

  The heat pipes considered are model 124681 from DigiKey, which can transfer up to 48 W of heat (end to end). Assuming eight heat pipes will be used (six on the inside between cells and two on the outside) a total price of approximately 120 € is required. The Peltier modules cost about 50 €/module, for a total of 1200 €, leading to initial costs of around 1320 €.

  Maintenance requirements for this design are almost none. The manufacturing company states that for the considered Peltier module, the mean time between failure is 125000 hours. Given the usage on which the cost of ownership is considered, which is 3 h/day, 5 days/week for 10 years, maintenance shall never be required. Analogously, heat pipes also require low maintenance, assuring up to 30 years of functioning [36], thus extremely low to no maintenance is expected. Nevertheless, if needed, the process would require changing the entire heat pipe or the modules, for which high costs are expected for one single cycle. Nevertheless, these conditions would then only be met in case of breakage of the system, which has not been considered for the other cases and should therefore not influence the evaluation.

  The total weight of the Peltier modules is around 1.5 kg as each one weighs approximately 0.0625 kg. The heat pipes weigh approximately 0.163 kg each, for a total of around 3 kg.

	Energy consumption	Manufacturing costs	Maintenance costs	Weight
Peltier regulator	216 Wh	1320 €	Null	3 kg

Table 3.5: Cost of ownership summary for Peltier regulator.

The Smart battery has the worst cost of ownership due to the high energy consumption as it requires to use almost the whole battery even for just one heating cycle. It does have lower manufacturing costs and maintenance costs, which although are strongly countered by the energy consumption.
The Magnetic regulator high manufacturing costs, maintenance costs, and weight make it the second best as these factors are balanced by the low energy consumtpion.
The best option is the Peltier regulator. The energy consumption is high, although it is important to consider that most energy comes from the HV battery since the LV has to take place only when and if the the first one fails. Furthermore, this decision is also supported by the low weight and the fact that no maintenance costs are required.

Following, a visual summary of the cost of ownership analysis is presented. The Maintenance costs table does not show absolute data as it has the only scope of showing approximate prediction. 2-3 cycles are expected for the Smart battery, 0 for the Peltier regulator, and a larger amount (not specifically defined) for the Magnetic regulator. Thus, the overall maintenance costs are expected to be higher for the second design, followed by the Smart battery, and no costs are expected for the Peltier regulator.

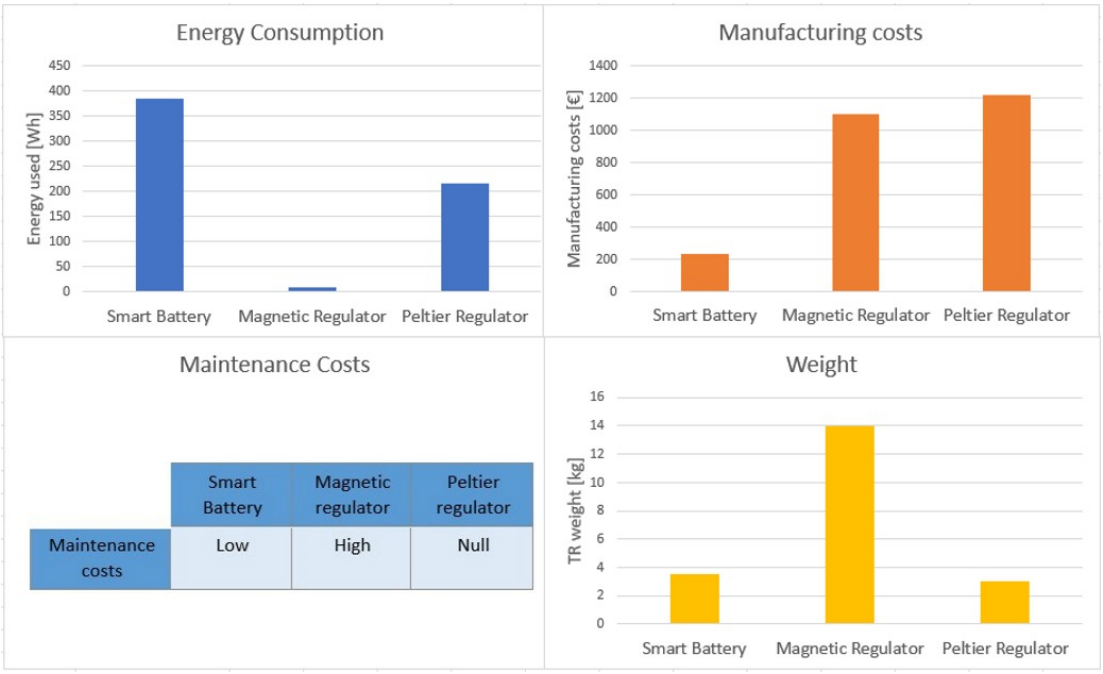

Figure 3.4: Cost of ownership summary.

Time response
The time response indicates how long the user must wait before being able to operate the vehicle when starting at -20°C.

- Smart battery: the self-heating technique based on a control architecture assures the availability of the supply at all times. The controller activates the energy source whenever it goes below a predefined threshold, maintaining it always in a working range.
- Magnetic regulator: given the low-temperature increase in temperature of the material through the magnetocaloric effect, the time required to bring the supply to the correct temperature is higher than that of the other two designs. However, since the MM must be maintained close to its Curie's temperature, the system must constantly work, for which the supply will always be at the right temperature.
- Peltier regulator: the Peltier modules can warm up the energy source at a high rate, although it is not constantly used like the methods in designs 1 and 2, for which a higher response time is

considered. It is expected the design will take approximately 2 minutes to bring the battery to a working temperature when starting at -20°C.

The Smart battery results to be the best option considering the comfort of the user in terms of waiting time before being able to operate the vehicle. The same can be said for the Magnetic regulator, although, when considering a single heating cycle, it requires more time to heat the supply than the first design, for which it is considered second. The last design has a fast heating rate but it does not always maintain the battery at a working temperature range, hence it is considered to be the slowest option.

The following table summarizes these results indicating the immediate availability of the energy source when considering the first two designs, while it is assumed the Peltier regulator will take about two minutes to bring the supply to a working range.

	Smart Battery	Magnetic Regulator	Peltier Regulator
Availability	Immediate	Immediate	$\approx$2 min
Score	1st	2nd	3rd

Table 3.6: Time response summary.

Maintenance requirements
This parameter considers how many maintenance cycles are expected for the component for 10 years.

- Smart battery: the expected maintenance requirements for this design are approximately 2-3 cycles over 10 years.
- Magnetic regulator: maintenance requirements for this system are not precisely defined, but it is assumed that higher maintenance will be needed when compared to the other two options.
- Peltier regulator: from literature, as stated in Section 3.2.3, no maintenance shall be required for this design at all.

The Peltier regulator qualifies as the best option in terms of maintenance requirements as no maintenance is expected. The Smart battery shows low needs of maintenance, for an expected maximum of 3 times over 10 years, while the Magnetic regulator is less durable because of the rotary system and the load and vibrations it generates and thus requires more frequent maintenance.

In the following graph, the maintenance cycles expected for the Magnetic regulator are indicated as 10, although this is not an absolute value and is used only for visual comparison to the other designs' requirements.

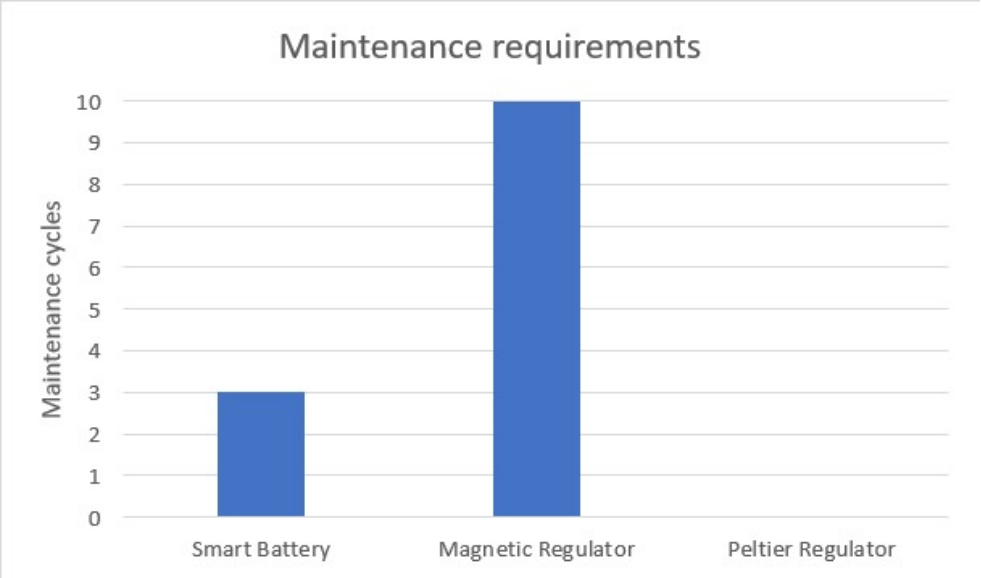

Figure 3.5: Maintenance requirements summary.

Assessment performance
The finalization of the assessment consists of assigning the corresponding points to each design and evaluating the overall performance considering the weights for each parameter. This process is presented hereafter, from which the Peltier regulator results to be the best option and therefore will be further developed into details and simulated.

	Thermal efficiency	Cost of ownership	Time response	Maintenance requirements	Score
Weight	4	3	2	1	
Smart battery	3rd→1 pt	3rd→1 pt	1st→3 pts	2nd→2 pts	15
Magnetic regulator	2nd→2 pts	2nd→2 pts	2nd→2 pts	3rd→1 pt	19
Peltier regulator	1st→3 pts	1st→3 pts	3rd→1 pt	1st→3 pts	26

Table 3.7: Assessment performance evaluation for selection of the best design.

3.3. Design optimization

An iterative design process was used to propose a more cost-effective and energy-efficient system. The initial design was over-dimensioned with 24 Peltier modules and 8 heat pipes. This design showed high response time and low energy consumption; however, the manufacturing cost could be brought down.

Considering the heat pipes system, the external heat pipes are removed from the design as they have little to no influence in the heating process of the battery system. This is due to the strong heat exchange with the surrounding air, for which almost all the heat transferred by the external heat pipes was dispersed to the surroundings and not delivered to the LV energy source.

Considering the Peltier modules, the key conditions analysed when optimizing the design were:

- At -20°C with no usage of the energy source.
- At 50°C with 30 A discharge rate.

The first case is considered for user comfort as the time needed to bring the energy source to a working temperature corresponds to the time the user must wait before being able to operate the vehicle. The

second case represents a condition in which the vehicle is being operated and the energy source must be activated while at high temperatures and therefore needs cooling to increase its efficiency. In this last case, both the energy used and the time needed to bring the vehicle to the optimal range are considered. The simulation model described in Chapter 4 is used to obtain the results for the two cases mentioned. The results for the design optimization are presented in Table 3.8:

	-20°C, i = 0A		50°C, i = 30A	
Number of modules	E_{ok} [Wh]	Δt_1 [s]	E [Wh]	Δt_2 [s]
24	10.5	53	180	36
23	10.7	52	176.8	38
22	10.26	59	173	40
21	10.25	66	168	41
20	10.08	67	168	43
19	9.96	75	169	47
18	9.53	76	170	47
17	10	73	169	50
16	9.8	75	169	52
15	9.7	96	169	55
14	9.2	119	168	59
13	9.2	102	168	63

Table 3.8: Values for design optimization. E_{ok} and Δt_1 indicate the energy and time required to bring the energy source to 0°C. Δt_2 indicates the time to bring the energy source to 35°C. E indicates the energy used to maintain the energy source in the working range throughout the whole discharge time.

Based on the above selection criteria, the design consisting of 20 modules was selected (highlighted in yellow in Table 3.8). Despite not being the best performer in any individual category, there are three main reasons to support this selection. First, the energy consumption criteria were discarded as the variation in between the cases was negligible. Second, considering the time required to bring the EES to a working temperature when starting at -20°C, it was decided to accept only the configurations with a maximum deviation of 15 s from the optimal one. Thus, all the configurations with 19 modules or less were discarded. With these two points in mind, the focus fell on the manufacturing costs. The chosen design was within tolerable deviation in each category, while also being cost-effective and leading to a 200€ reduction in manufacturing costs. Considering also the price of the external heat pipes removed, the total saving is of 230 €.

3.4. Conclusions

This chapter described the process followed to design a new thermal regulator. Other then introducing the considered initial design, it defined the assessment parameters used to evaluate each design to select the optimal one, which was then further optimized.

The Peltier regulator behavior and influence on the battery performance can now be evaluated through the simulation model presented in the following chapter.

4

Simulation model

This chapter describes the simulation model developed for this project. As mentioned in Section 1.4, the initial scope of the model is to obtain heating and cooling requirements of the energy source by simulating its thermal and electrical behavior without a temperature regulator. The gathered data was used as a starting point for the design process of the new component, which is then implemented into the model to evaluate its functioning and performance.

Several steps must be taken to develop the simulation. First, the functioning of a single cell is modelled considering electrical and thermal behavior, in particular the internal heat generation and the influence of temperature on the performance. The model is then extended to the whole battery by considering multiple cells and their connections. Finally, different types of heat transfer modes are included to evaluate the temperature distribution in the system. A visualization of the process is presented in Figure 4.1.

This chapter first discusses the requirements for the simulation and the layers considered, followed by a depiction of the main assumptions and how the geometry of the battery is recreated in the model. The electrical model and the thermal model are then presented and the integration of the thermal regulator into the model is explained. Finally, the method used to verify the model accuracy is described.

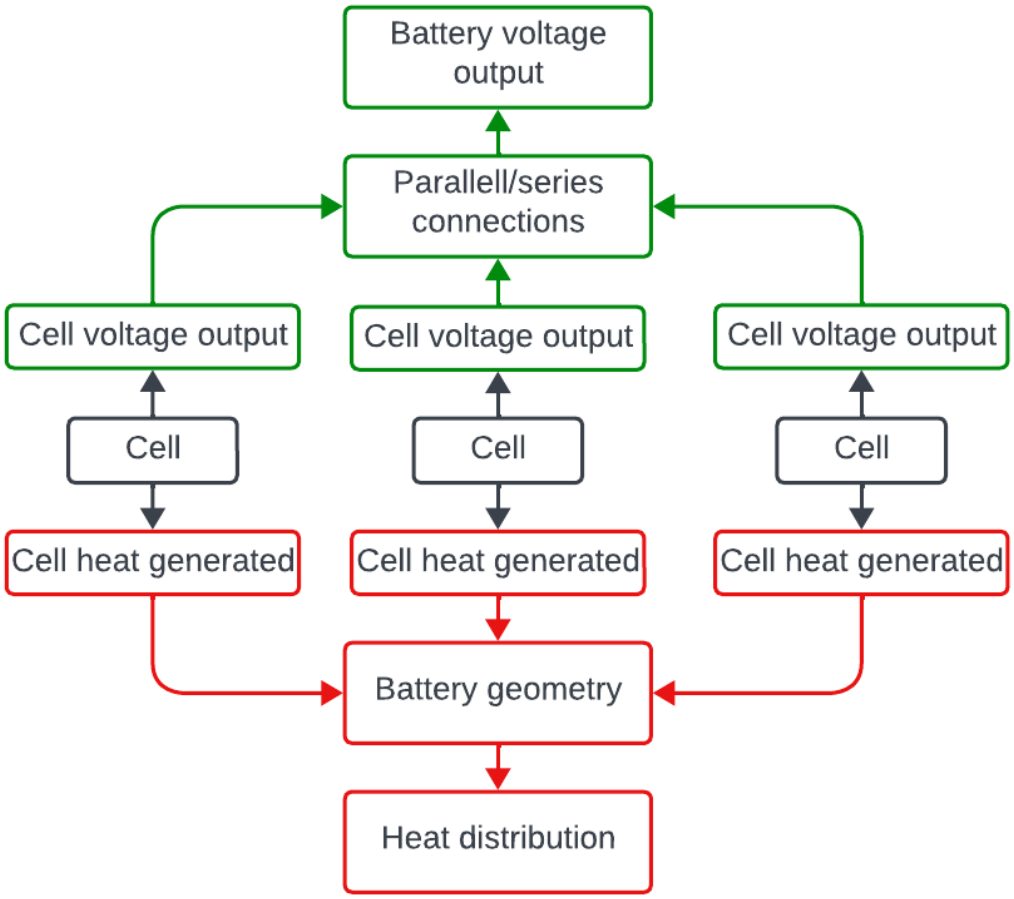

Figure 4.1: Schematic of model development process. In red the thermal behavior, in green the electrical one.

4.1. Requirements and layers

It is decided that the following requirements must be met for this simulation:

- Realistic: the literature review presented in Chapter 2 highlights that most simulations of electrical energy sources only focus on the amount of heat generated by the supply and the risk for thermal runaway, neglecting the impact of temperatures on the supply's performance, in particular the reduced performance and the risk of freezing at low temperatures. In contrast, this simulation aims to consider heat distribution within the system to determine the output voltage of each cell based on its current temperature, demonstrating the thermal influence on the supply's efficiency and functioning.

- Modular: the simulation should be designed in a modular manner, allowing for the addition or removal of different components without impeding its overall functioning. This flexibility is necessary as it must be possible to simulate the functioning of the energy source both with and without the thermal regulator. Thus, it should be allowed to modify the functions that define the effects of new components on the rest of the system without requiring extensive changes to the existing code. Achieving modularity involves dividing each step of the cycle into separate functions.

- Flexible: based on the literature review, it has been determined that a lithium-ion battery and a supercapacitor should be employed in the low-voltage net, thus it must be possible to evaluate the performance of both with one single simulation. Also, different dimensions, geometry, and internal

connections might be considered, so they should all be implementable in the code. To achieve this, the energy source simulation shall not relate to the processes that happen inside the supply but rather to a governing equation that generates the output voltage of the selected supply based on its technical specifications.

The system under consideration is divided into three layers: the cells, the case, and the hood air. As shown in Figure 4.2, it is important to note that the hood air layer represents the air surrounding the battery within the vehicle rather than the outside (ambient) air. This distinction is necessary because the temperature around the battery in a vehicle can differ from the external environment. For instance, considering the battery positioned under the hood on a hot summer day, the air temperature surrounding the battery will be higher than the external air temperature.

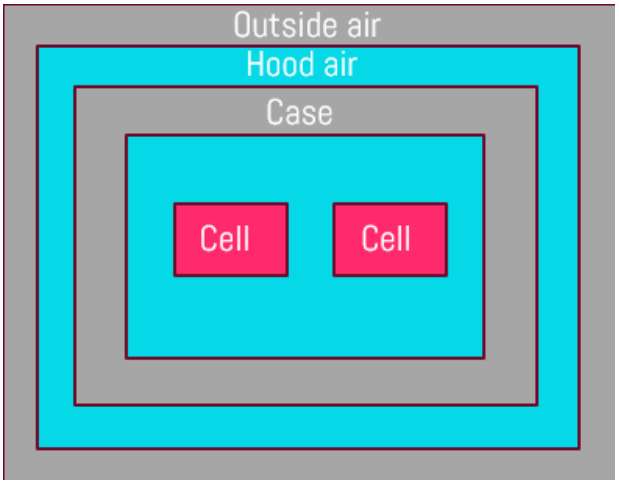

Figure 4.2: Simulation layers.

4.2. Assumptions and geometry

Before delving into the description of the simulation process, it is necessary to understand the main assumptions and how the system considers battery geometry. The main assumptions are the following:

- The hood air temperature is assumed to remain constant throughout the process.
- Each cell acts independently. Nevertheless, they work simultaneously and they are all required to deliver the same current level, which is defined based on the total current required and the cells' connections, either parallel or in series.
- For each cell the output voltage is calculated and the total output voltage is defined based on the cells' connections, either parallel or in series.
- All elements are considered as a lumped thermal mass, thus each element only has one average temperature.
- Heat exchange between cells is neglected as they are all approximately at the same temperature.
- Heat exchange between the cells and the case happens through conduction.
- Heat exchange between the case and the hood air happens through convection and radiation.
- When included, heat exchange between the Peltier modules and the case happen through conduction.

- When included, heat exchange between the Peltier modules and the hood air happen through convection and radiation.

- When included, heat exchange between the heat pipes and the cells happen through conduction.

In order to recreate both the electrical and thermal behavior of the battery, its internal geometry must be defined. Given that the simulation must be able to function for different geometries, it is necessary to define a system that can be extended to energy sources with different numbers of cells and types of connections. For this purpose, the cells are divided into modules which are then distributed and connected according to the source's geometry. Inside each module, the cells are distributed vertically (columns), horizontally (rows), and in depth (depth). Analogously, the modules are then organized into columns, rows, and depth. An example of this is shown in Figure 4.3, where each module has three rows, two columns, and four cells in depth and overall the power supply has three rows, two columns, and two modules in depth. The depicted geometry dis used as reference only.

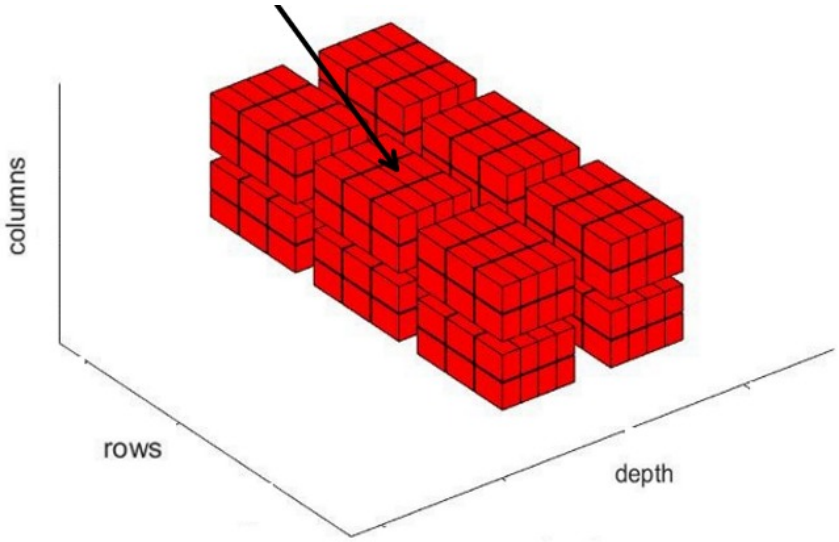

Figure 4.3: Example of the representation of the energy source geometry. This example does not refer to the battery actually considered for the project.

Each cell has an identification number defined as module number - row in the module - depth in the module - column in the module. By doing so, it is possible to use different geometries by only defining the distance between cells, the distance between levels, the distance from the cells to the case, and the overall number of cells and modules and their distribution. Levels are numbered from bottom to top and from left to right. Once a row is completed, the next one (so the next depth) starts counting from the bottom left corner, and so on. To give an example of the use of the identification number, if we consider the cell pointed in Figure 4.3, the ID is 4232 (level 4, row 2, depth 3, column 2).

The battery considered for the simulation is a LiFePo4 4s7p 12.8V 42Ah battery produced by LiTech Power [37], which uses model 32700 6 Ah cells [38]. The case is made of aluminum which has a thermal conductivity of 237 W/mK and specific heat capacity of 800 J/kgK. The overall cell thermal conductivity is assumed equal to 1.37 W/mK [39]. The cylindrical cells geometry is recreated in the model as a rectangular shape with height and width of 0.026 m and length of 0.0656 m, each with a mass of 0.048 kg and specific heat capacity of 1150 J/kgK [40].

4.3. Simulation process

A basic outline of the model is shown in Figure 4.4, followed by an explanation of the process.

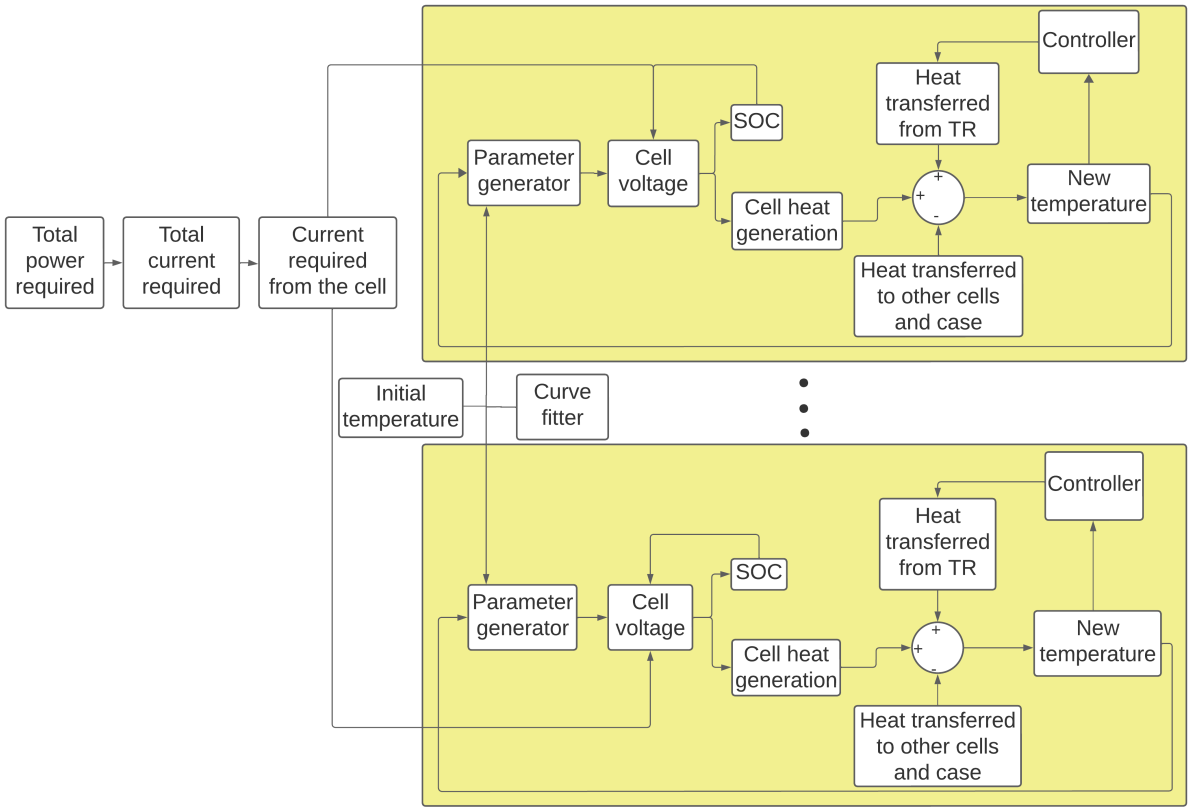

Figure 4.4: Simulation process.

The two yellow rectangles each represent one cell. To facilitate understanding, only two cells are presented, although the actual amount of cells can be changed as wished.

Based on the technical specifications and the selected governing equation, Equation 4.1, the model defines the initial parameters to fit the model to the selected cell. In particular, the function ”Curve fitter” considers the C-rate dependent discharge curves of the chosen cell, generating a set of parameters to tune the governing equation. The equation considered is the one proposed by Meng et al. [41], which defines the output voltage as a function of the state of charge and current required and is a combination of the Shepherd, Unnewehr, and Nerst model. Equation 4.1 does not consider the internal processes to recreate the behaviour of the battery but simply considers its technical data to simulate the output voltage. It can be used for batteries with similar behavior, otherwise, if another type of EES is simulated, the equation must be changed.

$$V = x_1 - x_2 \cdot i - x_3/SoC - x_4 \cdot SoC + x_5 \cdot log(SoC) + x_6 \cdot log(1 - SoC) \tag{4.1}$$

where:

- i = current required by the sytem [A]
- SoC = battery’s state of charge [-]

Parameter x_1 is a constant that generates an offset based on the cell’s nominal voltage. The second element, $x_2 \cdot i$, instead relates the curve to the specific C-rate. In fact, based on the current level, the term will adjust the curve by either raising or lowering the overall curve. The other parameters instead are gains used to adjust the influence of the state of charge on the various parts of the curve. In Figure 4.5, the elements’ influence on the curve is shown. Each element in the equation has matching color with the corresponding part of the curve it influences.

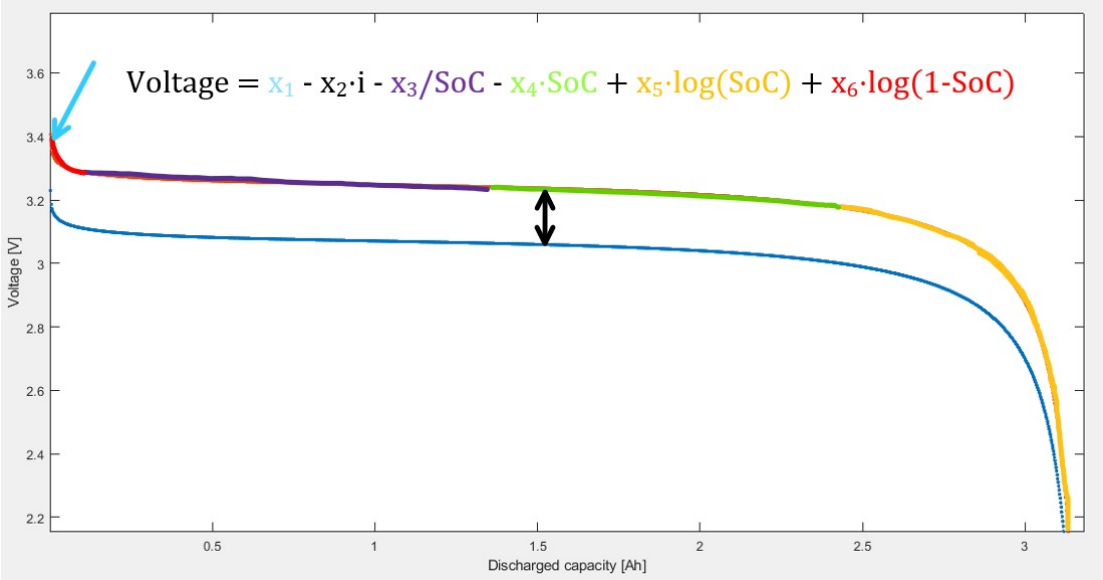

Figure 4.5: C-rate dependent equation explanation.

A second set of parameters is defined in the ”Parameter generator” function, which considers the temperature dependent discharge curves of the cell to tune the governing equation considering temperature influence. These parameters are selected after a process of trial and error and result in a modified version of Equation 4.1, which is the following:

$$V = w_1 \cdot x_1 - x_2 \cdot i - x_3/SoC - x_4 \cdot SoC + w_2 \cdot x_5 \cdot log(SoC) + x_6 \cdot log(1 - SoC) - w_3 \cdot log(Q - it) \quad (4.2)$$

where:

- i = current required by the system [A]
- SoC = battery’s state of charge [-]
- Q = battery’s capacity [Ah]
- it = battery’s discharge capacity [Ah]

The first temperature-dependent parameter w_1 adjusts the curve’s offset to the decrease in voltage output with the decrease of the cell’s temperature (and vice versa). Parameter w_2 instead is used to adjust the curve descent, specifically on the second logarithmic side. By inserting this parameter directly on the logarithm, the steepness of the second descent varies with temperature, showing a less marked decrease for lower temperatures. Finally, term $w_3 \cdot log(Q - it)$ calibrates the simulation with the behavior of the cell at low temperatures where the descent starts earlier than at higher temperatures [42].

In particular, the function ”Parameter generator” generates five values for each parameter, w_1, w_2, and w_3, one for each temperature for which there is a discharge curve. Then, throughout the simulation, based on the instant temperature of the selected cell, the value of the parameters are updated through linear interpolation of the initial sets of values.

The voltage output of the cell is calculated based on cell’s temperature, state of charge, and current required. Based on the output voltage, the current delivered is evaluated with Ohm’s law and the discharged capacity is calculated utilizing Coulomb counting, according to the following equation:

$$it(t) = it(t - 1) + i \cdot \Delta t/3600 \quad (4.3)$$

where:

- it = battery's discharged capacity [Ah]
- i = battery's current output [A]
- Δt = time for which i is delivered [s]

The heat generated by the cell is then calculated as a modification to the method described by Ismail et al. [43]. The entropic heat generation is excluded from the model as it influences less than 1% of the total heat generation. Moreover, a correction factor of 0.1 is added to tune the model to the specific cell type. The formula used is the following:

$$Q_{gen} = i \cdot (Uocv - V) \cdot 0.1 \tag{4.4}$$

where:

- i = battery's current output [A]
- U_{OCV} = battery's open circuit voltage [V]
- V = battery's voltage output [V]

The new temperature reached by the cells is evaluated and heat exchange is considered, according to Gartner [17] model. Conduction heat exchange is considered between the heat pipes and the cells, the Peltier modules and the case, and between the case and the cell. It was initially considered to model heat transfer between the case and the cells through convection as well, however the Raleigh number for this heat transfer mode was lover than 1000, for which heat exchange is purely through conduction. Conduction heat transfer from element A to element B is modelled as shown in Equation 4.5:

$$\begin{aligned} Q_{cond} &= \frac{k_{eq} \cdot A \cdot (T_A - T_B)}{th}, \\ k_{eq} &= \frac{1}{\frac{1}{k_A} + \frac{1}{k_B}} \end{aligned} \tag{4.5}$$

where:

- A = conducting area [m^2]
- T_A, T_B = temperature of element A and B [°C]
- th = material thickness [m]
- k_A, k_B = thermal conductivity of material A and B [W/mK]

Convection heat transfer is considered between the hood air and the case and between the hood air and the Peltier modules, and therefore is modelled only as external natural convection. Convection heat transfer between one body and the air is modelled as follows:

$$\begin{aligned} Ra &= \frac{g \cdot \beta (T_{body} - T_{air}) L^3 \cdot Pr}{v^2}, \\ \Psi &= \left[1 + \left(\frac{0.492}{Pr} \right)^{9/16} \right]^{-16/9}, \\ Nu &= 0.68 + 0.670 \cdot (Ra\Psi)^{1/4}, \\ Q_{conv} &= k_{eq} \cdot A \cdot Nu \cdot (T_A - T_B), \\ k_{eq} &= \frac{1}{\frac{th}{k_A} + \frac{th}{k_B}} \end{aligned} \tag{4.6}$$

where:

- Ra = Raleigh number [-]
- g = gravitational acceleration [m/s^2]
- β = volumetric coefficient of expansion (equal to 1/T for an ideal gas) [K]
- L = space in between elements [m]
- v = kinematic viscosity [m/s^2]
- Pr = Prandtl number, equal to 0.69 for air between 150-600 K [-]
- A = area of the surface [m^2]
- T_{body}, T_{air} = temperature of the exchanging body and of the hood air [°C]
- k_{body}, k_{air} = thermal conductivity of the exchanging body and of hood air [W/mK]
- th = material thickness [m]

Finally, radiation heat transfer is considered between the hood air and the case and between the hood air and the Peltier modules and is modelled as follows:

$$Q_{rad} = \sigma \epsilon A_{rad}(T_{body}^4 - T_{air}^4) \tag{4.7}$$

where:

- σ = Stefan-Boltzmann constant 5.67·10^{-8}
- ϵ = emissivity of the body, assumed equal to 0.8 [-]
- A_{rad} = radiating area of the body [m^2]
- T_{body}, T_{air} = temperature of the body and of hood air [°C]

4.4. TR implementation

To verify the influence of the TR on the battery performance, two main case studies are considered, specifically with the battery inactive and starting at -20°C and 50°C. In order to do so, the TR effect must be simulated in the model. This section shows the implementation of the new TR design into the simulation model. The design, composed of a mix of active (Peltier modules) and passive (heat pipes) systems, must be integrated with the energy source in order to analyze its influence on the thermal behaviour and overall performance of the supply. The different parts are added separately so the effect of both can be individually assessed.

4.4.1. Heat pipes

The new thermal regulator utilizes heat pipes as a passive heat transfer system to recover waste heat from the high-voltage battery. In fact, the heat removed from the main energy source while functioning is transported by the heat pipes to the LV battery, heating it up when in cold conditions.

The optimized design considers using 6 heat pipes in between parallel cells. The design is shown in Figure 4.6, where the heat pipes are in blue and the battery case is presented only on the sides to facilitate understanding.

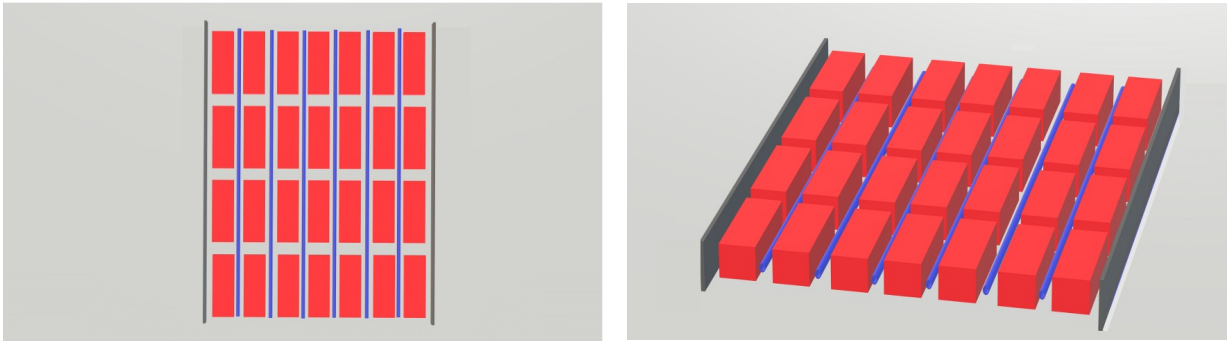

Figure 4.6: Heat pipes system visualization.

The heat pipes considered have a heat transfer power of 48W and are 600 mm long with a 12 mm diameter and weigh about 0.16 kg each. Water is used as the transfer medium. The internal heat transfer coefficient is 24387 W/mK and the outer material is copper.

The following assumptions are made to integrate the heat pipes system into the model. To facilitate understanding, the two ends of the heat pipes will be mentioned as the HV side (the one in contact with the HV battery, thus the hot side) and the LV side (in contact with the LV battery, thus the cold side).

- Heat transfer inside the heat pipe is unidirectional, from the HV side to the LV side.
- The minimum temperature on the LV side of the heat pipes, from hereafter named T_{HP}, is met in correspondence with the entrance in the LV energy source. The rest of the pipe, meaning the part that goes inside the LV EES, is at a lower temperature, thus T_{HP} is actually the maximum temperature on the LV side. Because of this the results will be more conservative as lower amounts of heating will come from the HPs.
- The HV side temperature of the heat pipe is modelled to reach 30°C after 10 minutes, as follows:

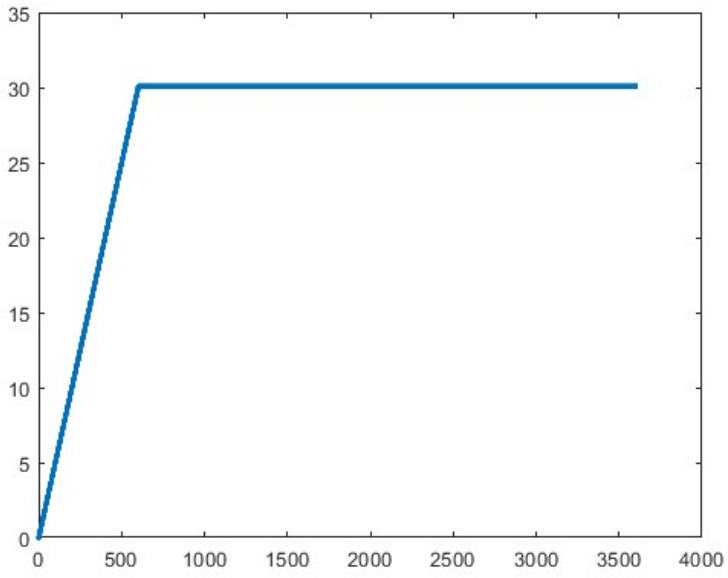

Figure 4.7: Heat pipes hot side temperature trend.

- Heat exchange is implemented through conduction.
- The area through which heat transfer happens equals half the outer surface of the heat pipe that goes along the element it is exchanging with. Thus, the length considered is the single cell length. The exchanging area is half the total surface area as heat transfer is considered to happen only through the surface facing the other exchanging body.
- As indicated by the manufacturers, heat transfer inside the heat pipe only happens for a temperature gradient between the LV and HV side of at least 10°C. Below this gradient, heat transfer is negligible [44].
- Heat transfer for the heat pipes happens as follows: the pipe, at temperature T_{HP}, first exchanges with the first cell on its left. After heat is exchanged, the HP temperature decreases, then the pipe exchanges with the cell on its right, the HP temperature decreases, and then the process proceeds for the next cells in depth. As heat is exchanged with one pipe, the cells temperatures are updated. Once one heat pipe finishes exchanging, the heat transfer for the next one starts with the (influenced) cells at the new temperature.
- Each heat pipe exchanges heat only with the (eight) cells it is directly in contact with.

Implementation
The following steps are followed in the simulation to integrate the effect of the heat pipes system, considering the assumptions mentioned above.

1. The internal heat transfer from the HV to the LV side of the heat pipe is calculated.
2. The new maximum temperature T_{HP} on the LV side is calculated according to the transferred heat.
3. Heat transfer between the heat pipes and the cells is calculated.
4. The overall heat exchanged from one heat pipe is evaluated and the new maximum temperature on the LV side (after heat transfer completes) is calculated.
5. The new temperature of the cells is calculated based on the heat exchanged with the heat pipes.

4.4.2. Peltier module

The Peltier modules are used to regulate the energy source temperature by acting on the external case. The optimized design considers using 20 modules: 6 on the top, 6 on the bottom, 4 on the right side, and 4 on the left side, as follows:

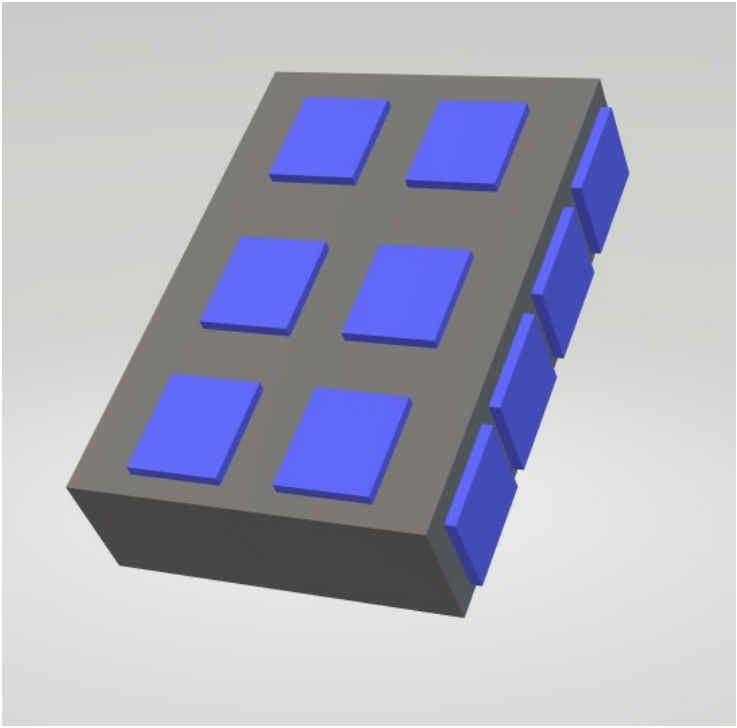

Figure 4.8: Peltier modules system visualization.

The considered modules are squared with 55 mm sides and are made of copper on the outside. The maximum accepted voltage and current are 15.7 V, 8 A, respectively.

The following assumptions are made to integrate the Peltier modules into the model:

- The outer plates are made of copper with a heat transfer coefficient of 385 W/mK.
- All modules act collectively, meaning if one is activated then they are all activated. Therefore, they generate and exchange heat as if they were one single unit whose effect is given by the sum of the individual influences on the model.
- The heat generated/absorbed is calculated for one module and then multiplied by the number of modules. The total heat is then exchanged with the case, which is also considered a single body.
- The initial temperature of the modules is equal to the overall starting temperature.
- The outer surface exchanges heat only with the outside air. The inner surface exchanges heat only with the case.

Implementation
The implementation of the Peltier modules is presented in this subsection. The process followed uses the formulas below to recreate the behaviour of a thermoelectric module, according to Palacios et al. [45].

Each surface of the module either absorbs (Q_c) or generates (Q_g) heat according to the following equations, respectively:

$$Q_c = \alpha \cdot T_{cold} \cdot i_P - 0.5 \cdot \beta \cdot i^2 - \gamma \cdot (T_{hot} - T_{cold}) \tag{4.8}$$

$$Q_g = \alpha \cdot T_{hot} \cdot i_P + 0.5 \cdot \beta \cdot i^2 - \gamma \cdot (T_{hot} - T_{cold}) \tag{4.9}$$

where:

- T_{cold}, T_{hot} = temperature of the cold and hot surface of the module [K]
- i = current delivered to the module [A]

The parameters α, β, and γ adjust the system to the specific modules and conditions. The starting values of the parameters are obtained as follows:

$$\begin{aligned} \beta &= V/i, \\ \alpha &= \frac{Qc + 0.5 \cdot \beta \cdot i^2}{i \cdot T_{hot}}, \\ \gamma &= \frac{\alpha \cdot i \cdot T_{cold} - 0.5 \cdot \beta \cdot i^2}{T_{hot} - T_{cold}} \end{aligned} \tag{4.10}$$

β is obtained by considering the values of voltage and current in the voltage plots of the module's specs at a temperature difference between the hot and cold side of the module equal to zero. Once β is defined is then possible to evaluate α considering values at ΔT = 0 in the plot for the heat removed. Finally, γ is calculated using any pair of values from the curve corresponding to Qc = 0 in the heat removed plot. To facilitate understanding, the values to consider to evaluate the parameters are indicated in the three rectangles in Figure 4.9.

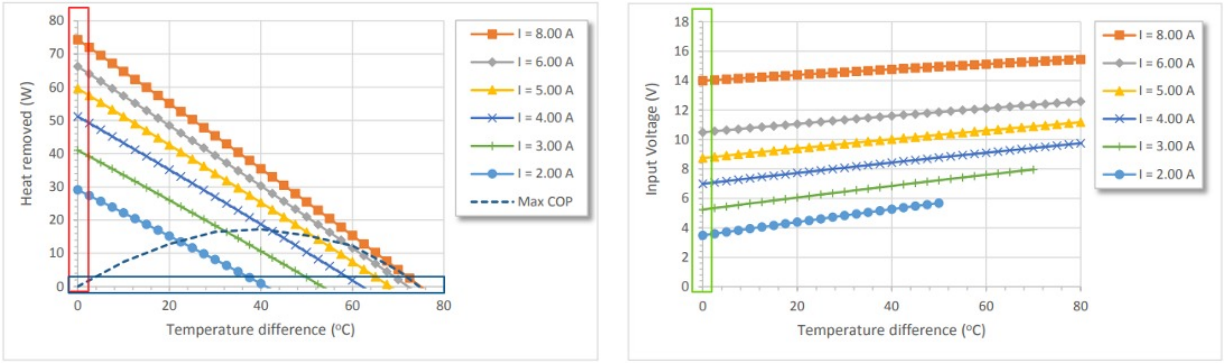

Figure 4.9: Visualization of the data to consider to define the parameters α (red rectangle), β (green rectangle), and γ (blue rectangle) for the Peltier modules.

The parameters are evaluated with a hot side temperature of 25°C, 50°C, and 75°C. From these values is then possible to define a delta for each parameter as the mean of the difference between the values for 25°C-50°C and 50°C-75°C. Considering then the temperature difference from the starting conditions (T_{hot} = 25°C) is possible to obtain the parameters at any given hot side temperature.

Once the parameters are defined, is then possible to determine how much current must be delivered to the module, based on the optimization shown below. The heat generation and absorption are evaluated and the case and Peltier temperature (on both sides) are updated. Finally, the heat exchange between the outer surface and outside air is calculated and the temperatures are updated again.

Control architecture
The thermoelectric modules are regulated with the following control architecture:

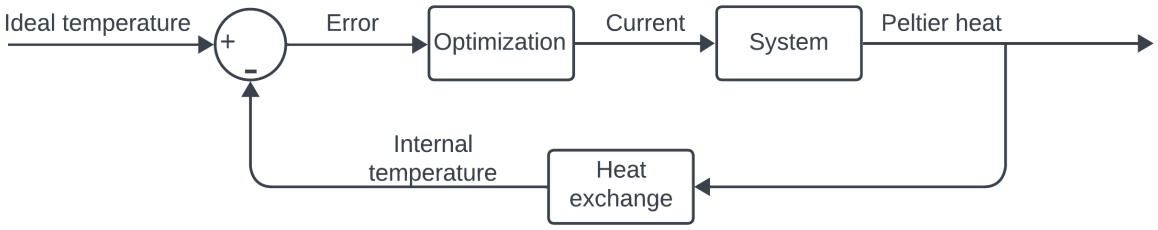

Figure 4.10: Peltier modules control architecture

The system activates when the internal battery temperature, calculated as the average temperature of all cells, falls outside the acceptable range. Even though the literature review in Chapter 2 showed the optimal range for LIBs to be 20-40°C, the selected range for the control architecture is set to be 15-35°C. This is decided to reduced energy consumption in terms of heating by reducing the lower threshold, and for safety concerns to avoid ever reaching the upper limit of 40°C. Once the internal temperature falls outside the range, the system activates and defines the error for the optimization problem. The error is defined as the difference between a predefined ideal temperature of 25°C and the instant case temperature. The optimization then identifies the optimal value of current to deliver to the modules. Consequently, the modules will absorb and release heat on opposite sides, in accordance with the system requirements. The case and internal temperature are reevaluated and utilized for the next iteration.

The amount of current required by the Peltier module is defined with an optimization problem. The latter is divided into two parts based on whether cooling or heating of the supply is needed. Both problems have as decision variables the current i_P delivered to the module and the time Δt required for the case to reach the desired temperature. The two optimizations are presented hereafter in Equation 4.11 and Equation 4.12, which refer to cooling and heating conditions, respectively.

$$\begin{aligned} Q_c &= \alpha \cdot T_{cold} \cdot i_P - 0.5 \cdot \beta \cdot i_P^2 - \gamma \cdot (T_{hot} - T_{cold}), \\ T_{final} &= T_{start} - Qc \cdot \Delta t / (cs_{case} \cdot m_{case}), \\ obj &= (T_{final} - T_{ideal})^2; \end{aligned} \tag{4.11}$$

$$\begin{aligned} Q_g &= \alpha \cdot T_{hot} \cdot i_P + 0.5 \cdot \beta \cdot i_P^2 - \gamma \cdot (T_{hot} - T_{cold}), \\ T_{final} &= T_{start} + Qg \cdot \Delta t / (cs_{case} \cdot m_{case}), \\ obj &= (T_{final} - T_{ideal})^2 + \Delta t \cdot 10; \end{aligned} \tag{4.12}$$

The two optimizations present different objective functions because during heating conditions it is necessary that the energy source is available as soon as possible for user comfort. In cooling conditions instead, the only requirement is to bring the energy source into the acceptable temperature range while reducing power consumption and therefore time is not minimized.

4.5. Model accuracy

The accuracy of the model must be verified. It is decided to test the accuracy of the governing equation, the heat generation of the cells, and the Peltier thermal behaviour. By doing so, the full electrical behavior

of the battery is verified as the governing equation indirectly relies on the current and discharged capacity calculations as well. For what concerns the thermal model, the heat transfer modes are already verified [17] and therefore the heat exchange from the heat pipes as well. Thus, only the heat generation from each cell and the thermoelectric behavior of the Peltier modules must be checked. To analyze the accuracy, the values obtained from the models are compared with reference values. The reference values used to verify the governing equation and the Peltier modules behavior are obtained from their respective data sheet. For what concerns the heat generation of the cells, the reference values are obtained from literature.

By verifying the accuracy of the governing equation, we assure an overall correct electrical behaviour. This happens because to check the equation it is decided to consider the full discharge behaviour of one cell for different conditions, in particular the output voltage as a function of the discharged capacity. The plot is compared to data gathered from the data sheet of the cell and the deviation between the plots is considered. This verification not only considers the equation itself but also the way current and discharge capacity are evaluated in the model since they are needed by the model to define the output voltage for the next iteration. As visible in Appendix A, the plots differ from each other mostly by less than a standard deviation, for which the model is considered accurate.

Considering the thermal model, the internal heat generation of the cell is verified analogously to the governing equation. Data from Giammichele et al. [46] are used for comparison, where a similar cell is experimented. This comparison is shown in Appendix B. The heat exchange model follows the process expressed by Gartner [17], who verified the accuracy.

Finally, the behaviour of the Peltier module is analysed. The same method used for the other elements is considered. Both the heat generation and absorption values obtained from the model are compared to the technical data available and the comparison is shown in Appendix C. As shown, the method used to simulate the thermoelectric behaviour of the modules is accurate and in line with the technical data. The accuracy of the heat pipes is not verified as they simply rely on the heat exchange formulas, for which their behaviour is considered correct.

4.6. Conclusions

In this chapter, the development of the simulation model is presented. As shown, the model recreates the electrical behaviour of the energy source without relating to its internal processes. It is possible to use the same governing equation to recreate the functioning of a different energy source with similar discharge behavior, otherwise a more appropriate one must be selected. The same goes for the thermal behavior, in particular for internal heat generation formula. On the other hand, the rest of the model can be utilized for any other type of EES.

The model functions both with and without the thermal regulator implemented, for which it is possible to evaluate the electrical and thermal behavior of the energy source in different configurations, highlighting the influence of both HPs and Peltier modules on the battery performance. This analysis is shown in the following chapter.

5

Results and discussion

In this chapter, the performance of the novel thermal regulator is presented and analyzed under various conditions. The objective is to evaluate the design according to the assessment parameters, in particular considering thermal efficiency, time response, and energy consumption.

The optimized design of the Peltier regulator, composed of 20 Peltier modules and 6 heat pipes, is tested on a 42 Ah 12.8 V LiFePo4 battery with 4s7p connections and 6 Ah 3.3 V cells. The system is tested in the simulation model described in Chapter 4. The new component is evaluated for different conditions, specifically with different discharge rates and different starting temperature. It is good to remember that the hood air will be at a temperature equal to the starting temperature throughout the whole simulation. Moreover, even though the optimal working range was defined as 20-40°C in Chapter 2, the controller is tuned to maintain the energy sources in a range of 15-35°C.

The cases reported are the following:

- Initial temperature -20°C, energy source inactive: this case aims to determine how long it takes to heat up the energy source to an operational range and how much energy is consumed to do so.

- Initial temperature 50°C, energy source inactive: this case aims to determine how long it takes to cool down the energy source to an operational range and how much energy is consumed to do so.

- Comparison at initial temperature -20°C, discharge rate 30A: this case shows a comparison between the performance of the energy source while working with and without the thermal regulator. The objective is to highlight the influence the regulator has on the EES performance.

Before delving into further discussion, the behavior of the battery alone in different conditions is shown in the following charts. Specifically, Figure 5.1, Figure 5.2, Figure 5.3 show the behavior of the EES with 30 A discharge rate starting from -20°C, 30°C, and 50°C. The figures show the electrical and thermal behavior of the energy source, specifically the voltage output, internal temperature (defined as the average of all cells' temperature), and the case temperature as a function of time. The model is set to allow the battery to run at any temperature, although the working range is considered as 0-35°C.

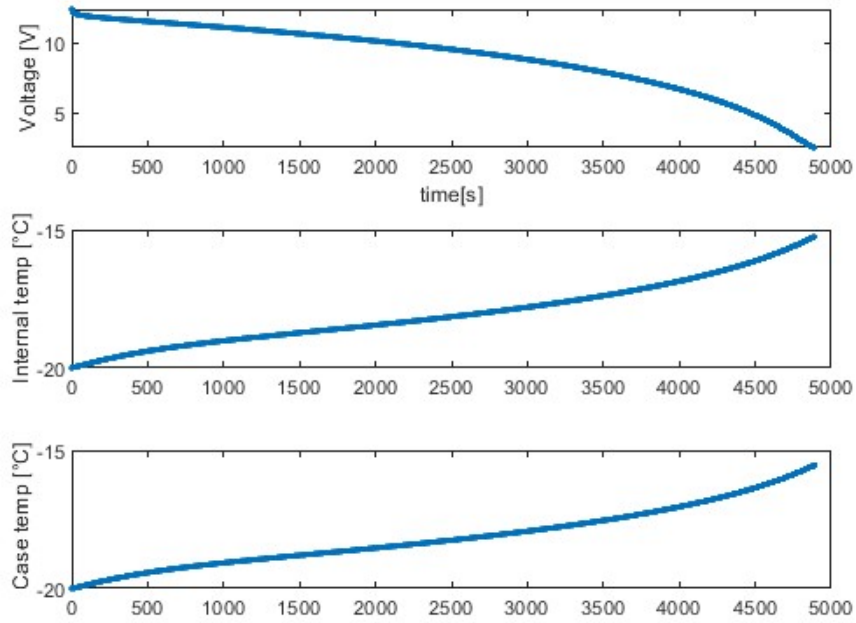

Figure 5.1: Battery without TR, 30A discharge, starting temperature -20°C.

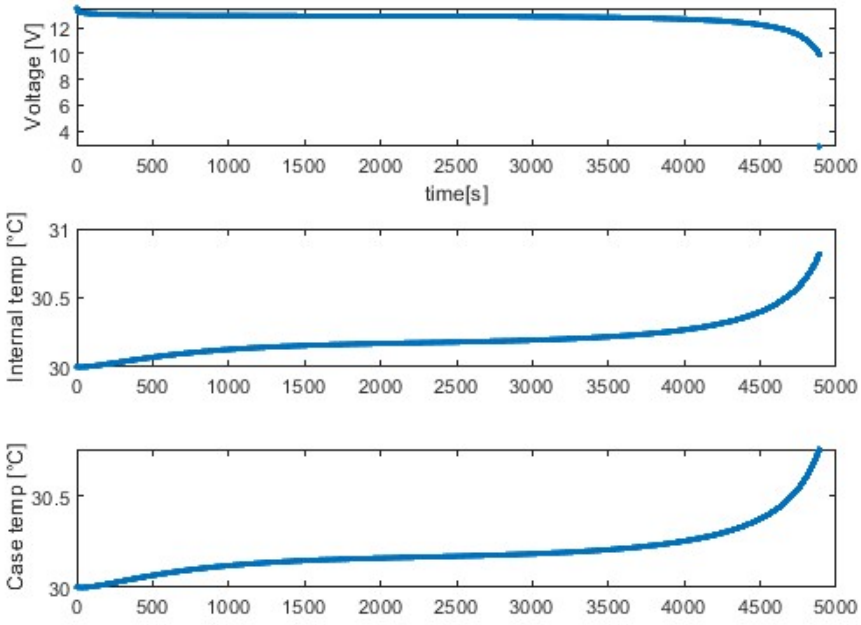

Figure 5.2: Battery without TR, 30A discharge, starting temperature 30°C.

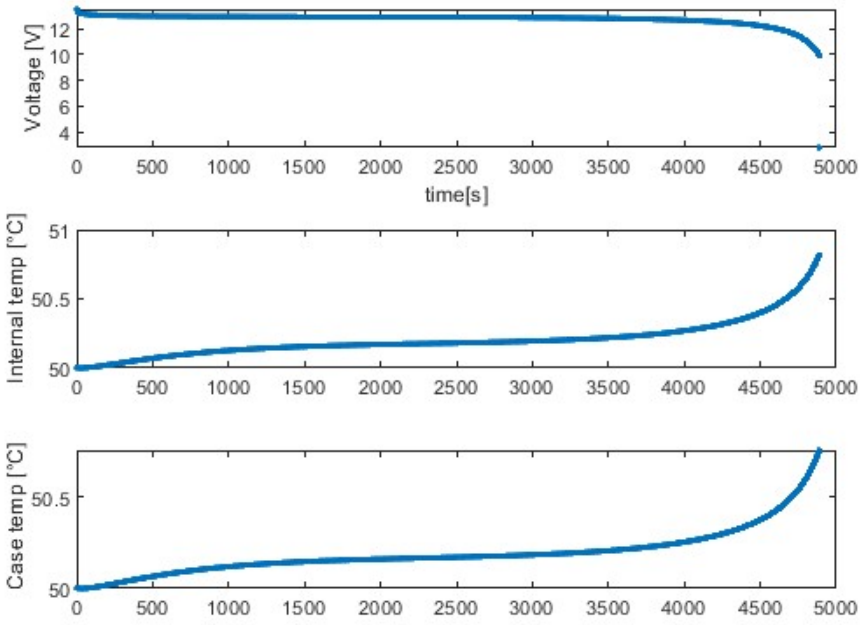

Figure 5.3: Battery without TR, 30A discharge rate, starting temperature 50°C.

5.1. T_{start} = -20°C, energy source inactive

The following three different configurations are considered for these conditions: 1) only the Peltier modules implemented, 2) only the heat pipes implemented, 3) full thermal regulator implemented. The objective is to understand the effect of the two methods used in the new design and how they influence each other.

In this scenario, the main concern is the time needed to bring the energy source to the minimum optimal temperature of 15°C.

5.1.1. HP only

The electrical and thermal behavior of the energy source is shown in Figure 5.4. The internal temperature refers to the average of all cells' temperatures.

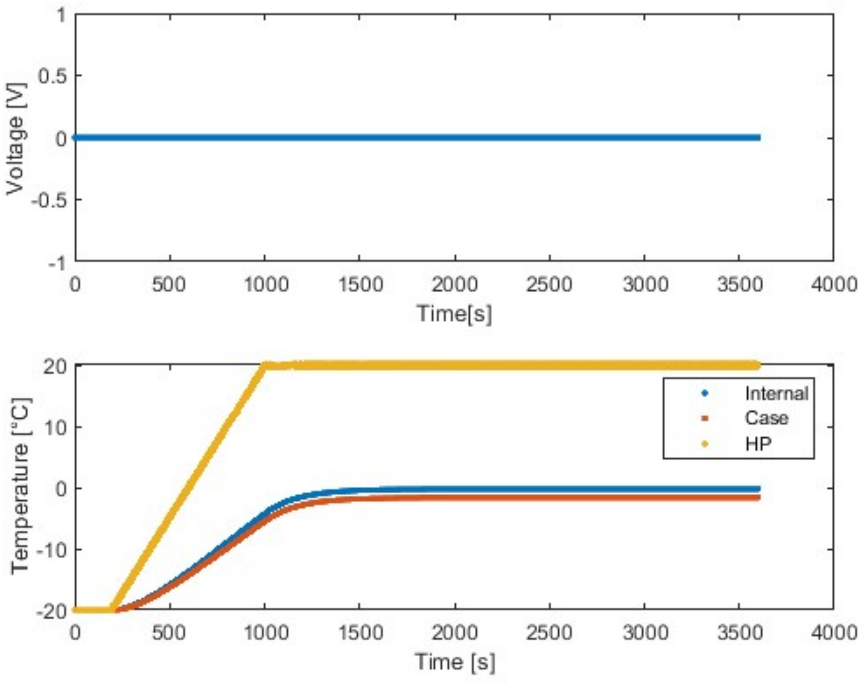

Figure 5.4: Battery details with battery inactive, starting temperature -20°C, only HPs implemented. The T_{HP} temperature of the heat pipes is shown in yellow, the case temperature in red, the internal temperature in blue.

As seen in Figure 5.4, the addition of heat pipes allows the energy source to reach 0°C after approximately 20 minutes and then maintains it at the same temperature. Thus, the heat pipe system alone can maintain the EES in the working range 0-35°C, but it cannot reach the optimal one.

The case's temperature is lower than the internal one because of the heat exchange with the hood air and the inside of the energy source. The same is for the temperature difference between the heat pipes and the battery. The linear behavior of the temperature starts when a balance is met between the heating effect of the heat pipes and the cooling effect of the hood air.

The heating effect could be sped up and improved by changing the behavior of the hot side temperature shown in Figure 4.7, thus by gathering more heat from the HV side.

5.1.2. Peltier only

In this subsection, the influence of the Peltier modules and their performance are discussed.

As shown in Figure 5.5, the internal temperature of the energy source reaches the optimal working range in about 75 s thanks to the Peltier modules. To do so, the control architecture defines high initial current values for the modules to make the process as fast as possible. Even when the minimum working temperature (0°C) is reached, heat is still delivered by the modules as they are designed to maintain the range of 15-35°C to obtain close-to-optimal performance.

In order to meet the time requirements, the initial power delivered is higher than the average after reaching the operating temperature. The power usage decreases after reaching the working temperature as the internal temperature is already at an accepted value, so the modules only need to maintain it. The cyclical path in the i_P seen after 100 s is due to the controller architecture that activates the modules as soon as the cells' average temperature falls below the 15°C threshold. Even though Figure 5.5 shows the behavior

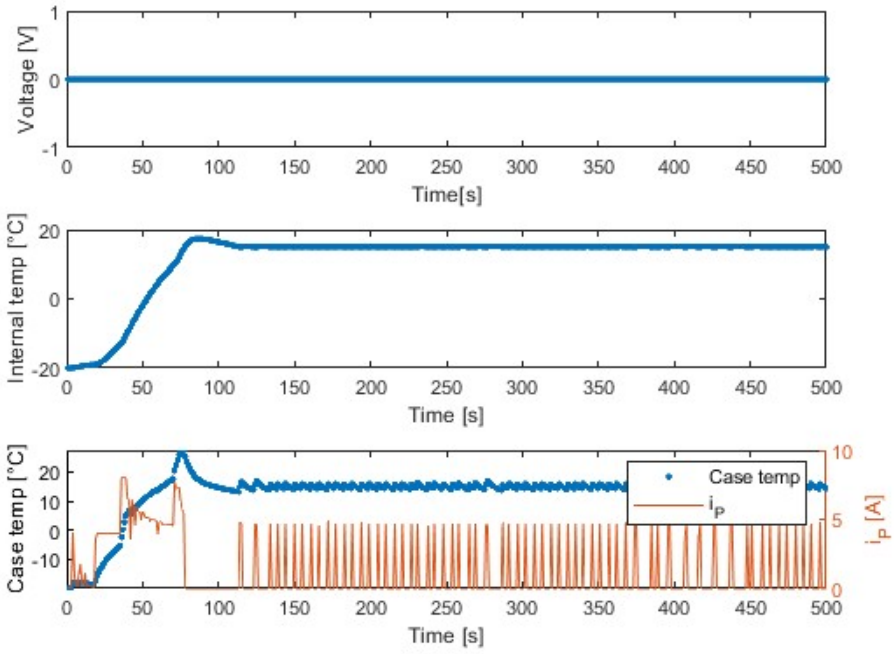

Figure 5.5: Battery details with battery inactive, starting temperature -20°C, only Peltier modules implemented. In the third subplot, the current i_P delivered to each Peltier module is shown in red.

only up to 500s, the total energy consumption for regulating the energy source for 3 hours is approximately 506Wh.

5.1.3. Peltier and heat pipes

In this subsection, the effect of the full thermal regulator is presented.

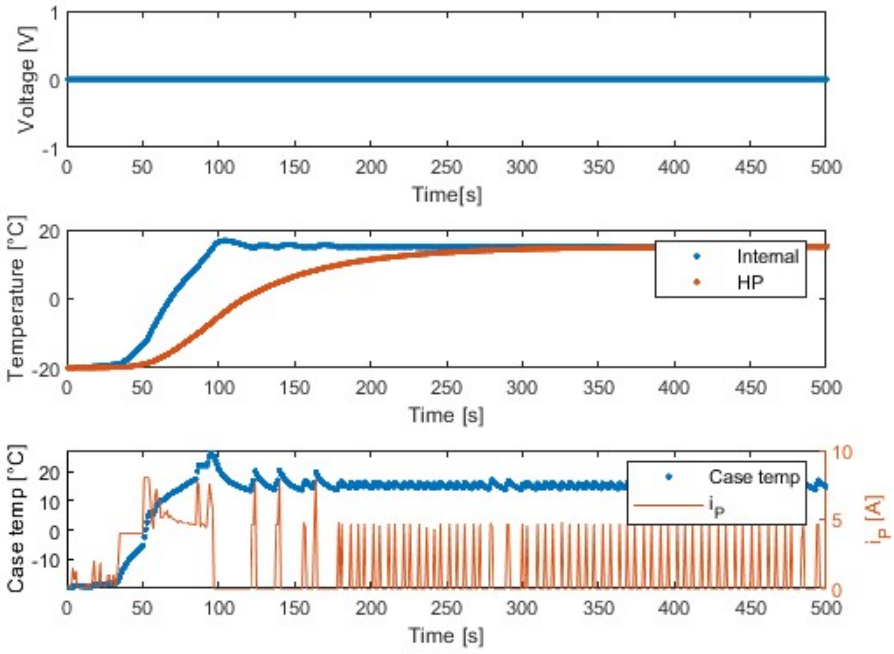

Figure 5.6: Battery details with battery inactive, starting temperature -20°C, full TR implemented. In the second subplot, the internal temperature is shown in blue and T_{HP} in red. In the third subplot, the case temperature is shown in blue and the current i_P delivered to each Peltier module in red.

As shown in Figure 5.6, the heat pipes temperature increases more slowly than the battery internal temperature, meaning the heat pipes are initially working against the Peltier modules as they are cooling the cells. This leads to a slowdown in the heating process, as the temperature of 15°C is met only after about 80s. On the other hand, the presence of the heat pipes helps reduce the overall power consumption. In fact, once the HV side of the heat pipe reaches 30°C, the heat pipe system helps maintain the energy source in a working range. Given that heat pipes are a passive system, the overall energy consumption for three hours of regulation is reduced to 443 Wh, about 15% less then the case with no heat pipes system.

5.2. T_{start} = 50°C, energy source inactive

Two different scenarios are considered for these conditions, 1) only with Peltier modules implemented, 2) with the full TR implemented. The case with only heat pipes is not considered as the heat pipes system is only useful for heating the supply, while in these conditions cooling is needed. The objective is to understand how the two natures of the thermal regulator influence each other and evaluate how detrimental the effect of the heat pipes is on the overall cooling performance. In this scenario, the main concerns are the energy and time needed to cool down the energy source and maintain it in the optimal working range.

5.2.1. Peltier only

The thermal and electrical behavior of the battery, along with the Peltier modules' performance are presented in Figure 5.7.

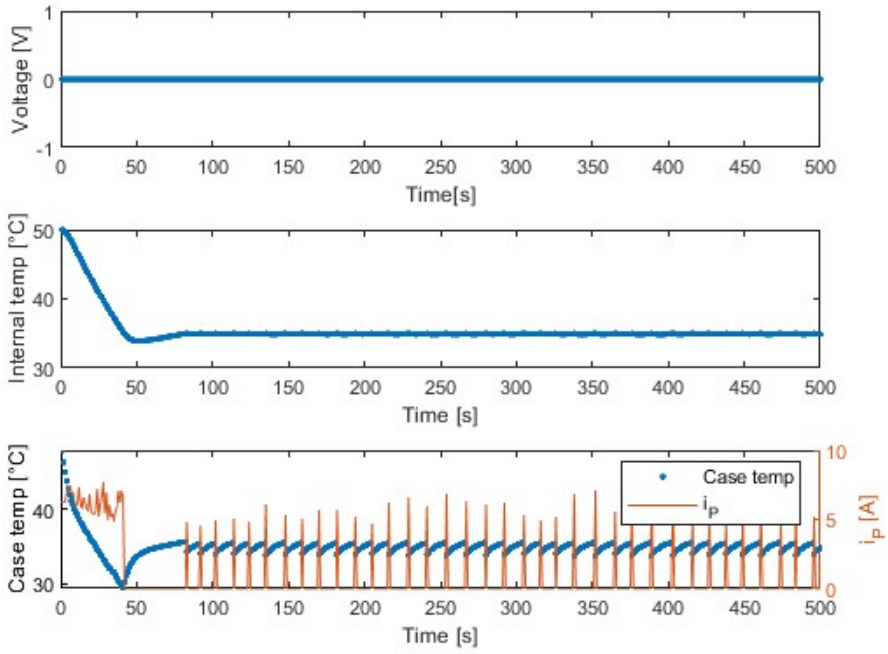

Figure 5.7: Battery details with battery inactive, starting temperature 50°C, only Peltier modules implemented.

As seen from the plot, the energy source is brought into the working range in less than 50 s.

The power consumed by the modules to maintain the energy source in the working range for three hours is 348 Wh.

5.2.2. Peltier and heat pipes

The full thermal regulator design is analyzed to understand how the heat pipe system influences the cooling process.

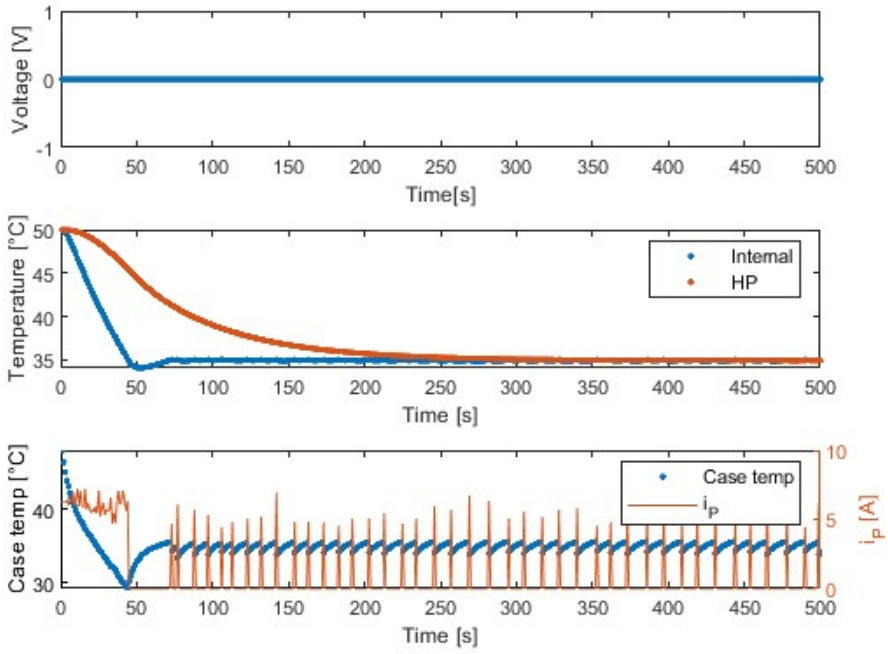

Figure 5.8: Battery details with battery inactive, starting temperature 50°C, full TR implemented.

In this case, the use of the heat pipes actually hinders the initial performance of the design. This is due to the specific requirements of this scenario, in which the heat pipes are heating up the battery unnecessarily, causing the modules to spend more energy to cool down the supply. This is also seen in the third subplot of Figure 5.8 from 0 to about 50 s, where the power consumption is higher than the case with no heat pipes. However, as the internal temperature is lowered, the heat pipes help maintain the system at an accepted temperature as they reach the working range themselves, for which the energy used is only slightly increased compared to the case with thermoelectric modules only, for a total of around 350 Wh.

5.3. Comparison at -20, 30A

In this last section, a comparison of the performance of the energy source with and without the new thermal regulator is presented. A good comparison can be obtained when considering an initial temperature of -20°C and a discharge rate of 30A. In fact, in these conditions, the energy source without regulation shows low efficiency and the power output is much lower than the expected one.

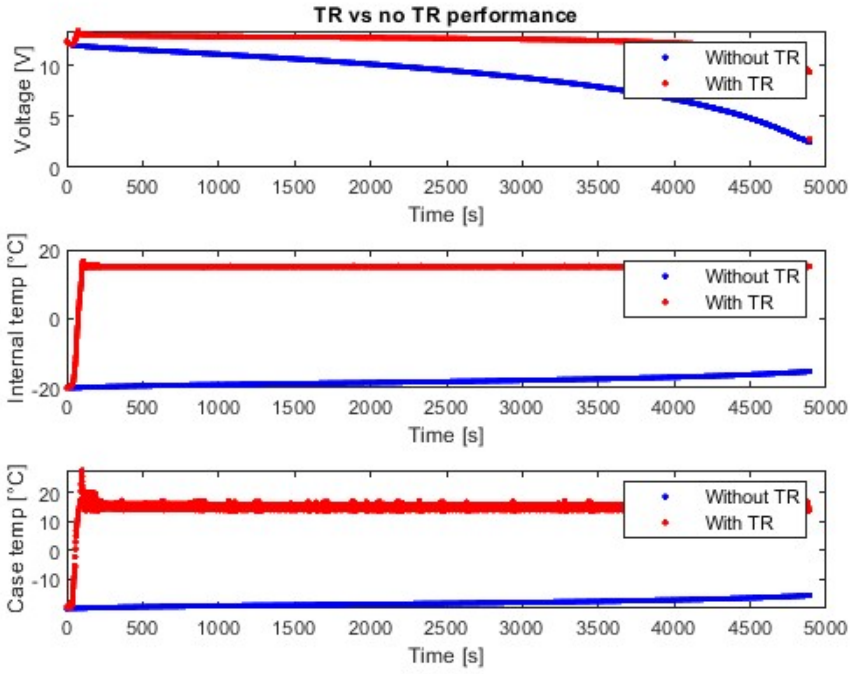

Figure 5.9: Comparison of the performance of the supply with and without TR installed. The plots show the performance of the EES with the TR installed in blue and withouth the TR in red.

As shown in Figure 5.9, the behavior of the energy source is strongly influenced by the presence of the thermal regulator. In fact, given that the output voltage varies based on the battery temperature, it is possible to see that without the TR the middle part of the voltage plot, which should be close to constant, is strongly decreasing as the low temperature reduces the overall efficiency. On the other hand, the presence of the TR allows for a fast warm-up, thus leading to a close-to-optimal behavior of the energy source and a linear output.

5.4. Conclusions

This chapter showed the behavior of the thermal regulator and its influence on the EES performance. As shown in Section 5.1, the Peltier regulator fulfills the expectations and works correctly to maintain the EES in the desired range. In fact, the system can rapidly bring the EES to a working temperature during both cold and hot starts, showing high levels of thermal efficiency. This allows to let the energy source be at any temperature when the car is not being used and still be able to operate it by waiting only 75s, exceeding the expectations of 2 min mentioned for the time response assessment parameter. The system can then maintain the energy source in the defined operating range, assuring optimal performance of the EES.

The combination of both passive and active thermal regulating technologies allows to reduce the energy consumption while efficiently and accurately regulate the battery's temperature. The heat pipes alone can maintain the energy source in a working range while operating the vehicle, improving energy savings. This improves the cost of ownership of the design, as the energy consumption is reduced. Furthermore, the Peltier modules are not being used at full power in the module to reduce energy consumption, meaning there is a chance for further design improvement, thus reduction in terms of manufacturing costs, and that the system can regulate the EES for even more extreme cases.

During cold starts at -20°C the heat pipes alone can bring the energy source to about 0°C, although they cannot heat the battery to the range of 15-35°C. The heat pipes also have a general negative influence on

the time required to bring the energy source to the working range as part of the heat removed/released from the modules has to be used to cool/heat the pipes themselves. However, when they reach the working temperature, the HPs help maintaining the battery in the correct range, reducing the usage of the thermoelectric modules, thus the overall energy consumption.

The Peltier module can maintain the energy source in the desired temperature range. In fact, during cold start ups it takes only about 80s to bring the battery to 15°C, and during warm start ups it takes about 50s to reach the acceptable upper threshold of 35°C. The designed control architecture efficiently works for its purpose, although it could be improved to reduce energy consumption and dictate a more linear behavior of the modules.

The new design shows good performance and capability to regulate the battery temperature in different condition. Both the active and passive nature of the design are important since the Peltier modules speed up and improve the overall regulating process, while the heat pipes reduce the overall energy consumption by passively maintaining the energy source in the working range.

6

Conclusions and recommendations

The goal of this thesis was to understand what types of electrical storage systems perform best in low-voltage nets and how to thermally integrate them into autonomous electric vehicles. In this closing chapter, a section for general conclusion is presented, where the main research question is answered. The following section instead considers the research subquestions and gives an answer to each of them. The chapter is then closed with a set of suggestions for future development.

6.1. General conclusions

The main research questions for this project was the following:

> What types of electrical energy storage systems should be used in the low voltage nets and how can they be efficiently thermally regulated and integrated into the autonomous electric vehicle?

It was determined that lithium-ion batteries should be used as primary low-voltage energy source for their higher energy density, while supercapacitors are a better fit for the secondary low-voltage energy source because of their high power density. Two different temperature ranges are selected for the supplies. It was decided that LIBs must be maintained in a close-to-optimal range of [20°C, 40°C], while supercapacitor have to be regulated into a working range of [-20°C, 70°C]. Because of the narrower range, it was decided to only focus on LIBs regulation.

To control the EES, three different designs were developed, namely the Smart battery, the Magnetic regulator, and the Peltier regulator. To evaluate the designs and select the best option for this application, an assessment was carried out and the Peltier regulator showed to be the best option. This design shows good thermal efficiency, intended as the capability of the component to bring and maintain the energy source into a predefined temperature range when starting at either high or low temperatures. Furthermore, given the system is partly active, it is possible to not only maintain the energy source in a broad temperature range but even to a specific temperature value.

Considering energy consumption for the cost of ownership, the design performed as second best in the assessment, which is possible thanks to the passive nature of the heat pipes that help reducing the energy consumption. However, the component uses 443 Wh and 350 Wh to regulate the energy source for three hours when starting at -20°C and 50°C, which is above the expected values from the assessment and shall then be improved. However, it is essential to consider that the high energy consumption is partly due to the assumption of the hood air to have a constant temperature. This negatively increases the energy consumption as, for instance, when at low temperature, the hood air will keep cooling the battery, enhancing the heating requirements. In reality, the hood air temperature will change along with the rest of the system, approaching a thermal equilibrium, thus reducing the regulating needs and energy consumption.

Regarding the manufacturing costs, the initial design considered for the assessment was further optimized to reduce the manufacturing price by 17%, for a total cost of approximately 1090 €. The lightweight of the system is also beneficial as its weight influences the overall vehicle performance. Also, the Peltier

regulator does not need maintenance, which reduces the overall cost of ownership.

Looking at the response time, the system exceeded the expectations of 2 min to bring the energy source to a working temperature when starting at -20°C as it only takes 75 s. This is important as it improves user comfort by reducing the waiting time.

The main downside to the new design is that it has to rely on the HV battery as the LV one might be fully frozen when the vehicle is started and regulation is needed. Therefore, if the main battery fails, the thermal regulator cannot be activated and only its passive nature will operate. However, to operate the vehicle, the LV battery must be available, thus when failure of the HV one happens, the LV battery will be in the optimal range since it has been regulated until then. As shown in Figure 5.2, when used at 30°C, the LIB does not require regulation. Thus, considering that the energy source and the overall energy system under the hood have been regulated until failure of the HV battery, it can be assumed that the overall hood temperature will be approximately at 30°C when the LV EES must be activated, for which regulation shall not be necessary during usage. Although, further analysis of these conditions shall be conducted.

6.2. Research questions

This section considers the subquestions mentioned in Section 1.3.

- What are the system specifications in terms of power and energy requirements for the low-voltage nets?
  The electrical requirements were outlined in collaboration with the company Audi AG according to the expected average and peak loads in the system. In particular, 480 Wh and 360 W are required for the primary LV EES, while the requirements for the second one are 12 Wh and 2400 W. Both EESs must be available at all times when the vehicle is being operated and thus must be in a working temperature range. However, temperature regulation is not required when the vehicle is not being used.
- How can the low-voltage electrical energy sources be assessed for correct selection for this application?
  The energy source assessment was based on the effect that temperature has on the specific EES and the system electrical requirements. It is decided to use LIBs in the primary LV net and SCs in the secondary one because of their high energy and power density, respectively.
- What are the effects of temperature on the electrical energy sources in the electric autonomous vehicle?
  The effects of temperature on the considered EESs were defined with the literature review developed in Chapter 2. Low temperature cause LIBs to lose active material, alter the battery chemistry, and increase electrolyte viscosity, leading to a risk of freezing of the electrolyte and making the battery inoperable. High temperatures increase the thickness of the solid electrolyte interface, increasing the internal resistance and overall risk of thermal runaway. Considering SCs, low temperatures may freeze the electrolyte, while high temperatures speed up the aging process of the electrode, the decomposition of the electrolyte and can even lead to the evaporation of the electrolyte.
- What are acceptable working temperature ranges for the low-voltage nets energy sources?
  Based on the system requirements and the effect temperature has on the EESs, it was decided to maintain LIBs in a close-to-optimal working range of [20°C, 40°C], while SCs are only maintained in a working range of [-20°C, 70°C].
- How can the thermal regulators of the low-voltage electrical energy sources for autonomous electric vehicles be assessed for correct selection?
  The assessment methodology used is shown in Chapter 3 and considers thermal efficiency, time required to bring the EES to a working temperature when starting at -20°C, cost of ownership, and maintenance requirements. Based on these parameters, it was possible to evaluate the three designs developed and select the best option, namely the Peltier regulator. This design is a combination of passive and active methods, specifically heat pipes in direct contact with the cells and Peltier modules installed on the case.

- How can acceptable levels of efficiency of the thermal regulator be achieved in terms of time and energy required to make the energy source reach the desired temperature?
  The Peltier regulator was the best option out of the three designed because of its high cooling and heating capabilities and fast responsiveness, requiring only 75 s and 50 s to reach a working temperature when starting at -20°C at 50°C, respectively. Considering energy consumption, to bring the energy source to the optimal range and then maintain it at such temperature for three hours, the system requires 443 Wh and 350 Wh when starting at -20°C and 50°C, respectively. These values are higher then the ones expected from the assessment presented in Section 3.2.3, thus improvements are required.
- What control architecture should be used for monitoring the thermal regulators of the low-voltage energy sources?
  The control architecture used to regulate the Peltier modules was a closed loop control system with different control objective based on whether heating or cooling was required. When heating was needed the architecture focused on reducing the waiting time and improve customer comfort, while in cooling conditions it prioritized energy saving.

6.3. Future development

There are two recommendations to improve the model's accuracy. First, heat exchange between the battery and the air under the car's hood should be implemented. Considering the air as always at a constant temperature, thus as an infinite heat sink, limits the accuracy as the air temperature actually varies significantly along with the components' temperature. This will likely have a noticeable impact on the overall performance of the system, specifically on the regulating needs and energy consumption of the regulator.

Second, temperature gradients for each body should be introduced rather than considering each body as a lumped thermal mass. The inclusion of temperature gradients would allow for the identification of potential hotspots that could hinder performance.

Further work on the simulation should also include model validation to expand the system accuracy to other work cases, such as batteries with other geometries and electrical specifications or different ambient temperatures and discharge rates.

Introducing temperature gradients in the simulation model would also introduce heterogeneity in the behavior of Peltier modules, as diverse amounts of heat would be demanded by each module as the energy source would require different levels of regulation at different points. Thus, a different control architecture would be needed.

Different control architectures and optimization techniques for activating the thermoelectric modules shall be investigated to improve the energy efficiency of the regulator. For instance, the implementation of a predictive controller has the potential to reduce energy consumption by analyzing the past thermal performance of the energy source and forecasting future behavior. With this information, the controller could make informed decisions, such as delivering higher initial current levels to create significant temperature variations in the supply. The implemented architecture instead, creates an oscillating behavior as it activates the modules whenever a temperature outside the specified range is detected. Introducing a more sophisticated architecture could reduce energy use and lead to a more uniform thermal behavior.

Improvements can be made with respect to the heat exchange mechanism of the heat pipes. Higher temperatures can develop in the LV energy source and therefore heat should transfer to the HV side as well. The model limits heat exchange within the heat pipe to a single direction, from the HV to the LV side. This constraint strongly reduces the cooling effect of the heat pipes, which could further reduce the energy usage of the Peltier modules.

Finally, the Peltier regulator uses large amounts of energy to maintain the energy source in the desired range. Thus, methods for improvement of the energy efficiency must be analyzed to reduce consumption.

References

[1] Francesco Bella et al. “Safety of Autonomous Vehicles”. In: *Journal of Advanced Transportation* 2020 (2020), p. 8867757. DOI: 10.1155/2020/8867757.

[2] On-Road Automated Driving (ORAD) Committee. *Taxonomy and Definitions for Terms Related to Driving Automation Systems for On-Road Motor Vehicles*. Apr. 2021. DOI: https://doi.org/10.4271/J3016_202104.

[3] Trevisan Pietro. “Analysis of low-voltage energy supply networks in x-by-wire autonomous electric vehicles and the thermal integration of the NV storage”. Literature Review.

[4] Michael Horn et al. “Supercapacitors: A new source of power for electric cars?” In: *Economic Analysis and Policy* 61 (2019). Special issue on: Future of transport, pp. 93–103. DOI: https://doi.org/10.1016/j.eap.2018.08.003.

[5] Mahammad A. Hannan et al. “State-of-the-Art and Energy Management System of Lithium-Ion Batteries in Electric Vehicle Applications: Issues and Recommendations”. In: *IEEE Access* 6 (2018), pp. 19362–19378. DOI: 10.1109/ACCESS.2018.2817655.

[6] Wei Liu et al. “Overview of batteries and battery management for electric vehicles”. In: *Energy Reports* 8 (2022), pp. 4058–4084. DOI: https://doi.org/10.1016/j.egyr.2022.03.016.

[7] Amir Babak Ansari et al. “Thermal-electrochemical simulation of lead-acid battery using reduced-order model based on proper orthogonal decomposition for real-time monitoring purposes”. In: *Journal of Energy Storage* 44 (2021), p. 103491. DOI: https://doi.org/10.1016/j.est.2021.103491.

[8] Bruno Scrosati et al. “Lithium batteries: Status, prospects and future”. In: *Journal of Power Sources* 195.9 (2010), pp. 2419–2430. DOI: https://doi.org/10.1016/j.jpowsour.2009.11.048.

[9] D.A.J. Rand et al. “3 - Lead–acid battery fundamentals”. In: *Lead-Acid Batteries for Future Automobiles*. Ed. by Jürgen Garche et al. Amsterdam: Elsevier, 2017, pp. 97–132. DOI: https://doi.org/10.1016/B978-0-444-63700-0.00003-9.

[10] Xiaopeng Chen et al. “An overview of lithium-ion batteries for electric vehicles”. In: *2012 10th International Power and Energy Conference (IPEC)*. 2012, pp. 230–235. DOI: 10.1109/ASSCC.2012.6523269.

[11] Da Deng. “Li-ion batteries: basics, progress, and challenges”. In: *Energy Science & Engineering* 3.5 (2015), pp. 385–418. DOI: https://doi.org/10.1002/ese3.95. eprint: https://onlinelibrary.wiley.com/doi/pdf/10.1002/ese3.95.

[12] Daniela Galatro et al. “Thermal behavior of lithium-ion batteries: Aging, heat generation, thermal management and failure”. In: *Frontiers in Heat and Mass Transfer (FHMT)* 14 (2020).

[13] Xinghui Zhang et al. “A review on thermal management of lithium-ion batteries for electric vehicles”. In: *Energy* 238 (2022), p. 121652. DOI: https://doi.org/10.1016/j.energy.2021.121652.

[14] Xiyue He et al. “A comprehensive review of supercapacitors: Properties, electrodes, electrolytes and thermal management systems based on phase change materials”. In: *Journal of Energy Storage* 56 (2022), p. 106023. DOI: https://doi.org/10.1016/j.est.2022.106023.

[15] Ander González et al. “Review on supercapacitors: Technologies and materials”. In: *Renewable and Sustainable Energy Reviews* 58 (2016), pp. 1189–1206. DOI: https://doi.org/10.1016/j.rser.2015.12.249.

[16] Sandhya Lavety et al. “A dynamic battery model and parameter extraction for discharge behavior of a valve regulated lead-acid battery”. In: *Journal of Energy Storage* 33 (2021), p. 102031. DOI: https://doi.org/10.1016/j.est.2020.102031.

[17] Niels Gartner. “Thermal behaviour of lithium-ion batteries and the implications on submarine system design”. Master’s Thesis. Delft University of Technology, 2021.

[18] Jackleen S Same et al. “Effect of Thermal Parameters on Behaviour of A Lithium-Ion Battery: Simulation Study”. In: *Int. J. Electrochem. Sci* 17.220951 (2022), p. 2.

[19] Monzer Al Sakka et al. “Thermal modeling and heat management of supercapacitor modules for vehicle applications”. In: *Journal of Power Sources* 194.2 (2009), pp. 581–587. DOI: https://doi.org/10.1016/j.jpowsour.2009.06.038.

[20] Sanjeev Kumar Gupta et al. “A review on recent development of nanofluid utilization in shell and tube heat exchanger for saving of energy”. In: *Materials Today: Proceedings* 54 (2022). International Conference on ”Materials Science and Mathematics for Advanced Technology” ”(MSMAT 2021), pp. 579–589. DOI: https://doi.org/10.1016/j.matpr.2021.09.455.

[21] Zu-Guo Shen et al. “A review on thermal management performance enhancement of phase change materials for vehicle lithium-ion batteries”. In: *Renewable and Sustainable Energy Reviews* 148 (2021), p. 111301. DOI: https://doi.org/10.1016/j.rser.2021.111301.

[22] Oleg Satanovsky Alexander Schmuck. *Audi Media Center*. 2022. URL: https://www.audi-mediacenter.com/en/models-4.

[23] Oleg Satanovsky Alexander Schmuck. *The New 2022 BMW iX xDrive50*. 2022. URL: https://www.bmwusanews.com/newsrelease.do?id=3749&mid=.

[24] Qian Wang et al. “A critical review of thermal management models and solutions of lithium-ion batteries for the development of pure electric vehicles”. In: *Renewable and Sustainable Energy Reviews* 64 (2016), pp. 106–128. DOI: https://doi.org/10.1016/j.rser.2016.05.033.

[25] Zhonghao Rao et al. “A review of power battery thermal energy management”. In: *Renewable and Sustainable Energy Reviews* 15.9 (2011), pp. 4554–4571. DOI: https://doi.org/10.1016/j.rser.2011.07.096.

[26] S. Al Hallaj et al. “Novel thermal management system for electric vehicle batteries using phase-change material”. In: *Journal of the Electrochemical Society* 147.9 (2000). Cited by: 382, pp. 3231–3236. DOI: 10.1149/1.1393888.

[27] Ekkes Brück. “Developments in magnetocaloric refrigeration”. In: *Journal of Physics D: Applied Physics* 38.23 (2005), R381.

[28] A Fly et al. “System thermal and water balance in an evaporatively cooled PEM fuel cell vehicle”. In: *Vehicle Thermal Management Systems Conference Proceedings (VTMS11)*. Woodhead Publishing, 2013, pp. 267–277. DOI: https://doi.org/10.1533/9780857094735.6.267.

[29] N Raghu Ram et al. “Review on magnetocaloric effect and materials”. In: *Journal of Superconductivity and Novel Magnetism* 31 (2018), pp. 1971–1979.

[30] William J Joost. “Reducing vehicle weight and improving US energy efficiency using integrated computational materials engineering”. In: *Jom* 64 (2012), pp. 1032–1038.

[31] Zhiqiang Sun et al. “Thermal management of the lithium-ion battery by the composite PCM-Fin structures”. In: *International Journal of Heat and Mass Transfer* 145 (2019), p. 118739.

[32] Wen Yang et al. “Thermal performance of honeycomb-type cylindrical lithium-ion battery pack with air distribution plate and bionic heat sinks”. In: *Applied Thermal Engineering* 218 (2023), p. 119299.

[33] Julia Lyubina. “Magnetocaloric materials for energy efficient cooling”. In: *Journal of Physics D: Applied Physics* 50.5 (2017), p. 053002.

[34] Y Maral et al. “An examinaion about thermal capacities of thermoelectric coolers in battery cooling systems”. In: *Journal of Engineering Research and Applied Science* 6.2 (2017), pp. 703–710.

[35] Chakib Alaoui. “Solid-state thermal management for lithium-ion EV batteries”. In: *IEEE Transactions on Vehicular Technology* 62.1 (2012), pp. 98–107.

[36] Nazdaneh Yarahmadi et al. “Improved maintenance strategies for district heating pipe lines”. In: *Proceedings of the 14th International Symposium on District Heating and Cooling, Stockholm, Sweden*. 2014, pp. 6–10.

[37] *LiFePO4 Battery Packs - 12.8V-12V LiFePo4 battery Packs*. URL: https://www.litechpower.com/product-detail/LP4S7P6A6AF001.html.

[38] *HT327 IFR32700N60 6000mAh LiFePo4 Battery Cell*. URL: https://www.litechpower.com/product-detail/batterycellHT327IFR32700n60.html.

[39] Dieter Oehler et al. “Investigation of the Effective Thermal Conductivity of Cell Stacks of Li-Ion Batteries”. In: *Energy Technology* 9.6 (2021), p. 2000722.

[40] Marcus Auch et al. “Simple experimental method to determine the specific heat capacity of cylindrical Lithium-Ion-Battery cells”. In: *Applied Thermal Engineering* 234 (2023), p. 121212.

[41] Jinhao Meng et al. “Overview of lithium-ion battery modeling methods for state-of-charge estimation in electrical vehicles”. In: *Applied sciences* 8.5 (2018), p. 659.

[42] Shuai Ma et al. “Temperature effect and thermal impact in lithium-ion batteries: A review”. In: *Progress in Natural Science: Materials International* 28.6 (2018), pp. 653–666.

[43] Nur Hazima Faezaa Ismail et al. “Simplified heat generation model for lithium ion battery used in electric vehicle”. In: *IOP Conference Series: Materials Science and Engineering*. Vol. 53. 1. IOP Publishing. 2013, p. 012014.

[44] *124681 30W 600mm heat pipe*. URL: https://www.digikey.it/en/products/detail/wakefield-vette/124681/9356469.

[45] R Palacios et al. “Analytical procedure to obtain internal parameters from performance curves of commercial thermoelectric modules”. In: *Applied Thermal Engineering* 29.17-18 (2009), pp. 3501–3505.

[46] Luca Giammichele et al. “Thermal behaviour assessment and electrical characterisation of a cylindrical Lithium-ion battery using infrared thermography”. In: *Applied Thermal Engineering* 205 (2022), p. 117974.

A

Governing equation accuracy

In this appendix, the verification process of the accuracy of the model's governing equation is presented. The latter consists in comparing the reference curves, obtained from the technical data sheet of the cell [38], with the curves obtained with the model. In the plots, the standard deviation is also marked, one above and one below the voltage line. The verification is done for different rates of discharge (0.1C, 0.5C, 1C, 2C, 3C) at a constant temperature of 25°C, and for different temperatures (-20°C, -10°C, 0°C, 10°C, 30°C) with a constant discharge rate of 0.5C.

As shown in the plots below, this verification shows good accuracy of the model, almost always within a standard deviation from the reference values. Considering the verification on the rate of discharge, the model follows the reference values correctly. Higher discrepancies are met in the temperature dependency check. However, the plots show that the EES performance in the model at low temperatures is worse then the reference behavior. This leads to more conservative results in the simulation model as more powerful regulation is required then it would be in reality, so if the system works in this conditions it will also work in reality. Thus, the accuracy level is sufficient.

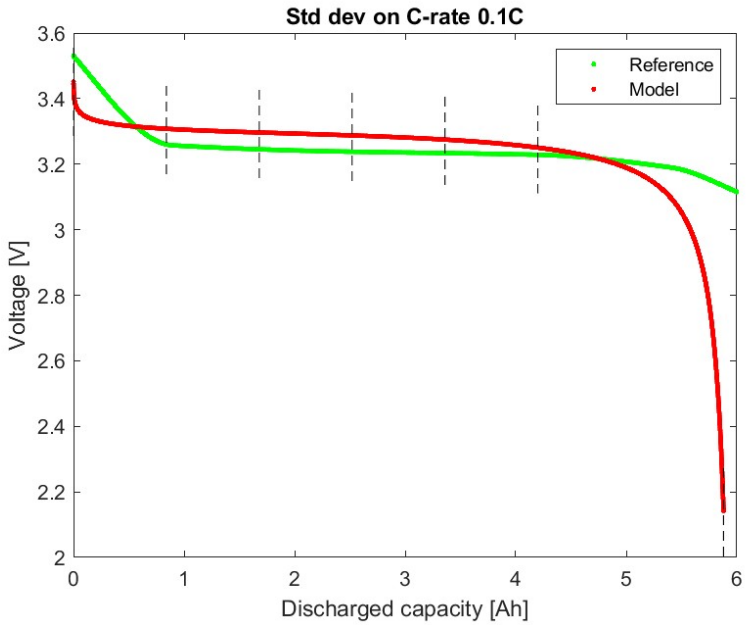

Figure A.1: Standard deviation check for 0.1C C-rate at 25°C.

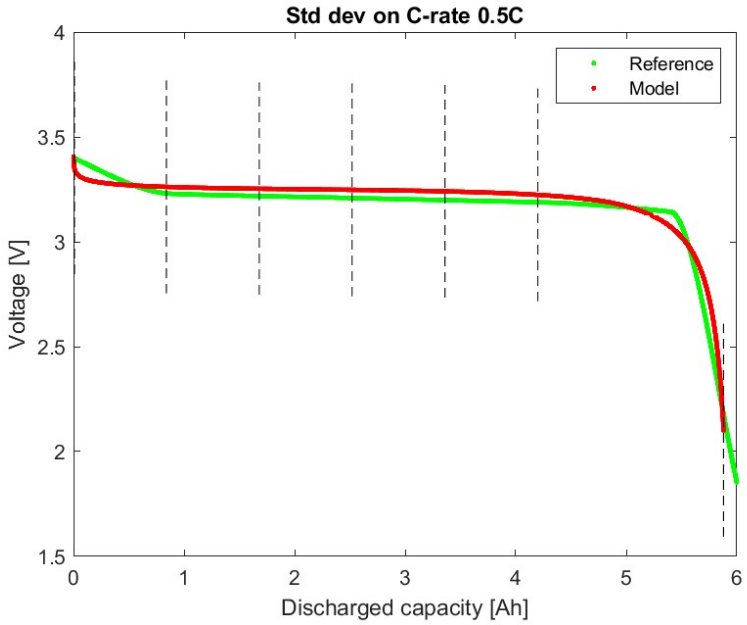

Figure A.2: Standard deviation check for 0.5C C-rate at 25°C.

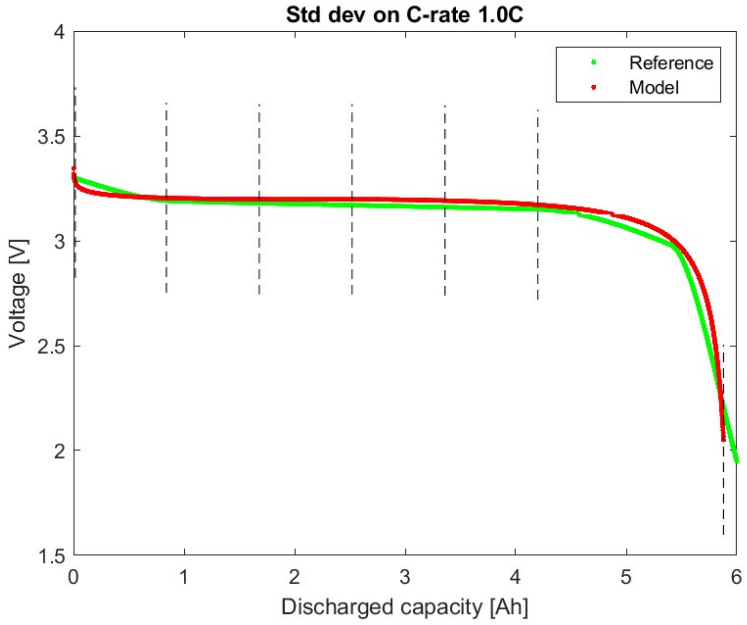

Figure A.3: Standard deviation check for 1C C-rate at 25°C.

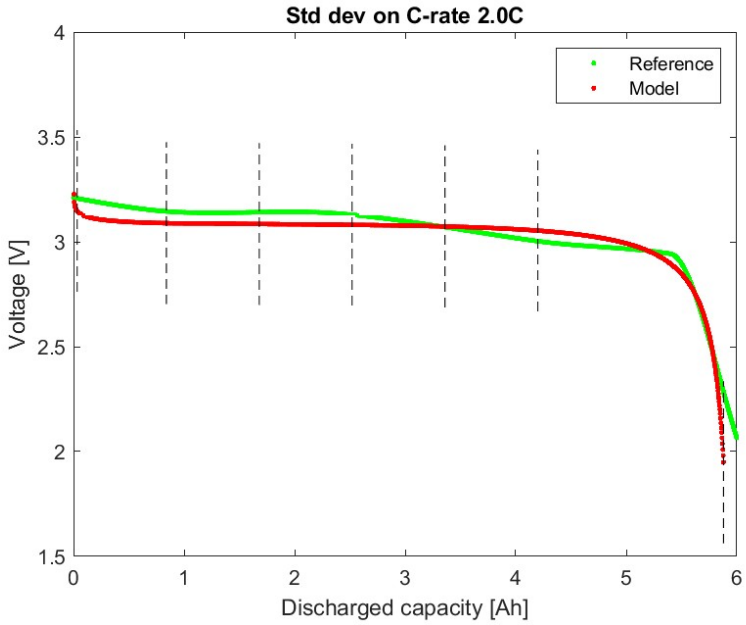

Figure A.4: Standard deviation check for 2C C-rate at 25°C.

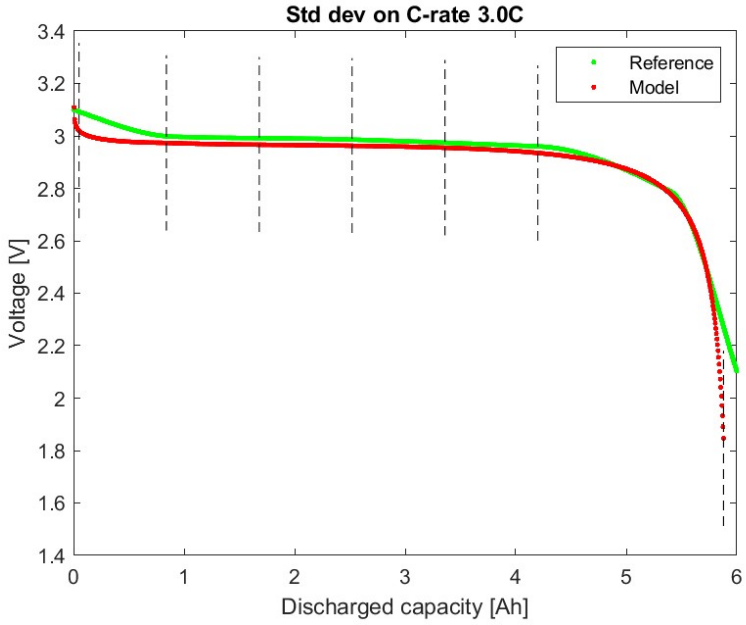

Figure A.5: Standard deviation check for 3C C-rate at 25°C.

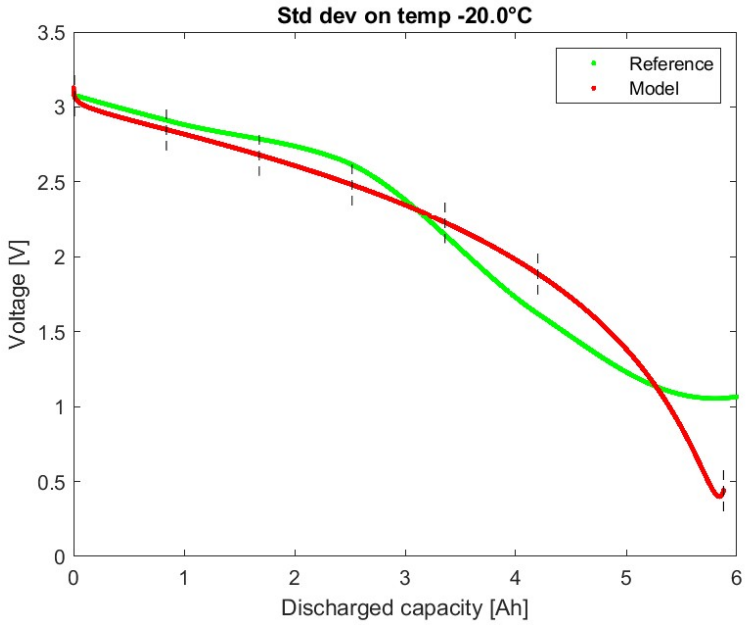

Figure A.6: Standard deviation check at -20°C, 0.5C C-rate.

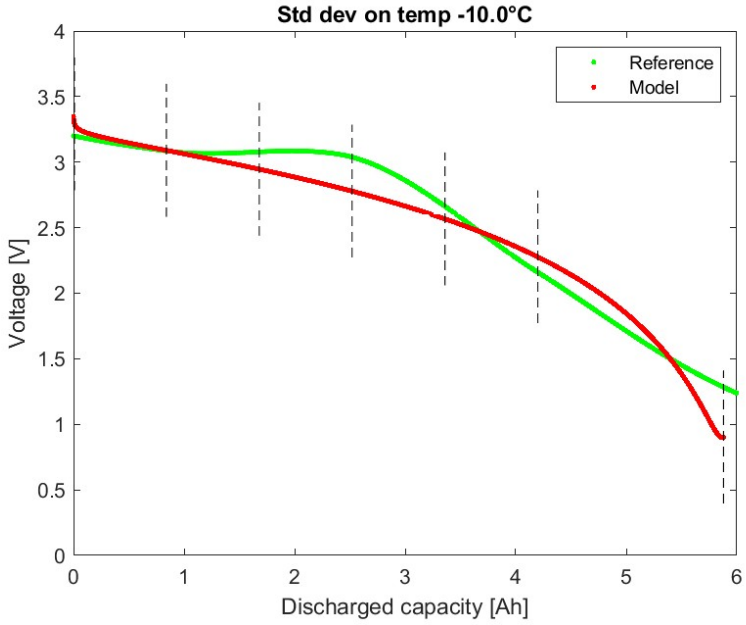

Figure A.7: Standard deviation check at -10°C, 0.5C C-rate.

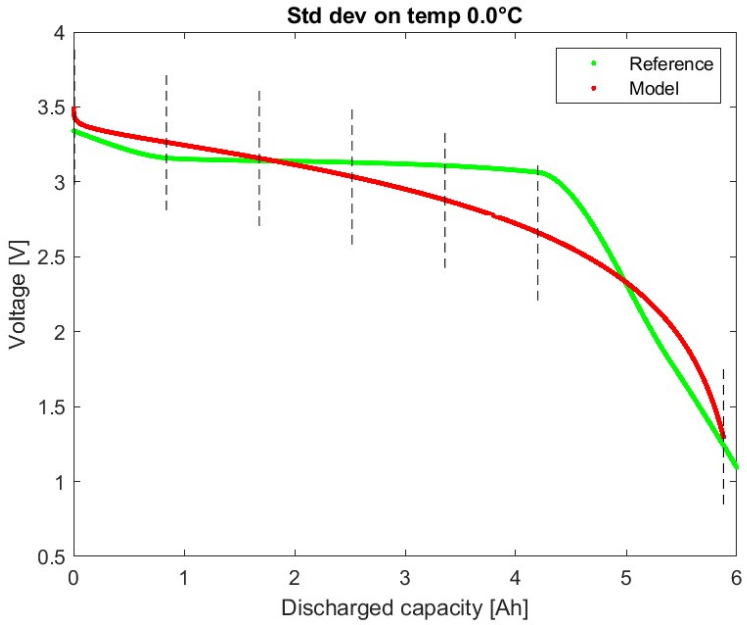

Figure A.8: Standard deviation check at 0°C, 0.5C C-rate.

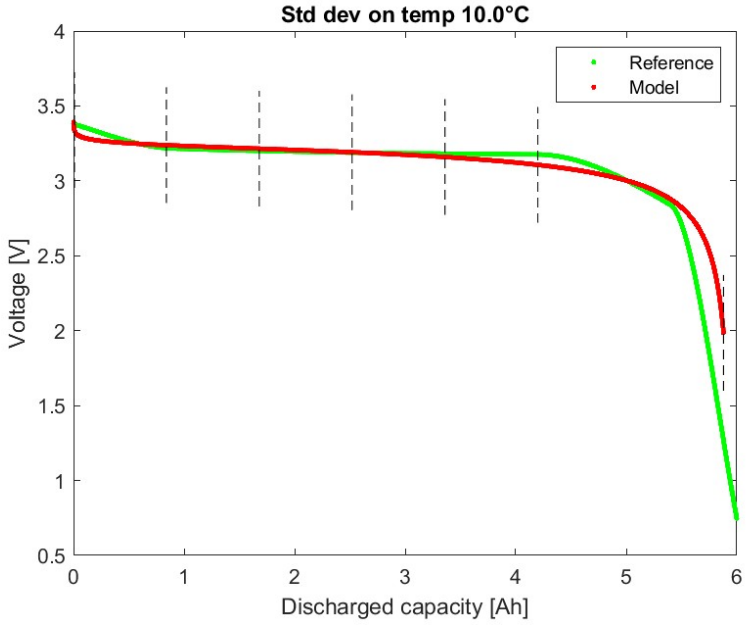

Figure A.9: Standard deviation check at 10°C, 0.5C C-rate.

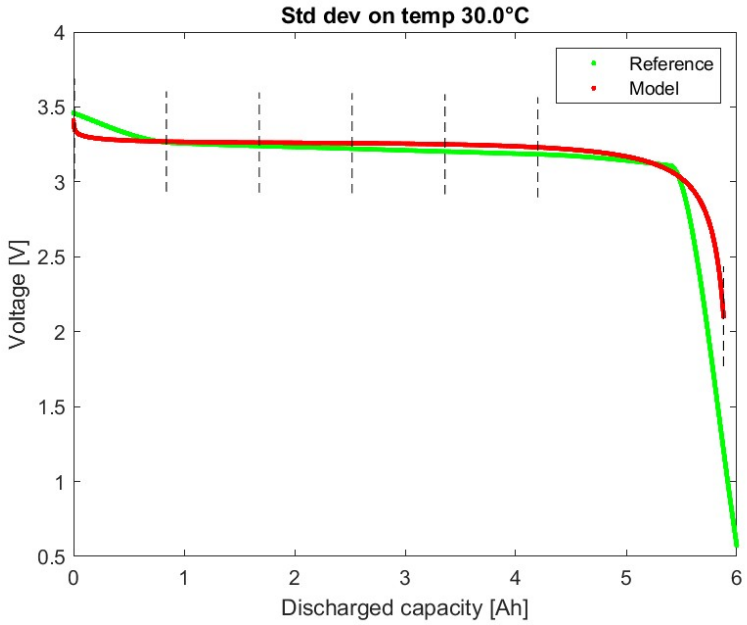

Figure A.10: Standard deviation check at 30°C, 0.5C C-rate.

B

Heat generation accuracy

In this appendix, the verification process of the accuracy of the heat generation model is presented. The latter consists in comparing the reference curves [46] with the curves obtained with the model. In the plots, the standard deviation is also marked, one above and one below the temperature trend. The verification is done for different rates of discharge (0.5C, 1C, 2C, 3C, 4C, 5C, 10C) at a starting temperature of 25°C.

As shown in the comparison plots, the discrepancy is almost always lower then one standard deviation. The plots show higher inaccuracies for low rates of discharge. However, it is essential to recognize, for instance, that the tick interval in the y-axis for Figure B.1 equals 1°C, while in Figure B.7 it equals 10°C. This difference in the gaps is what makes the discrepancy between the model and the reference values more marked for lower discharge rates. Thus, with this consideration, the accuracy of this method is accepted and considered sufficient for all conditions.

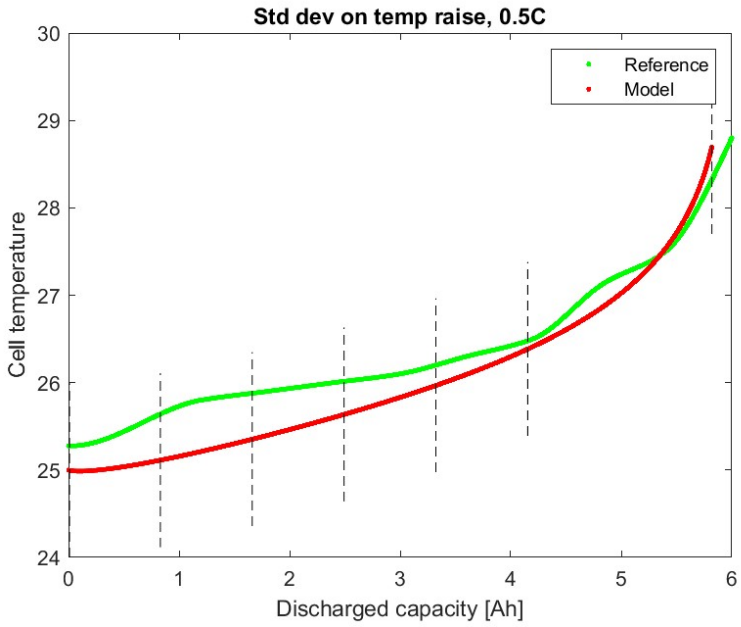

Figure B.1: Standard deviation check for 0.5C C-rate.

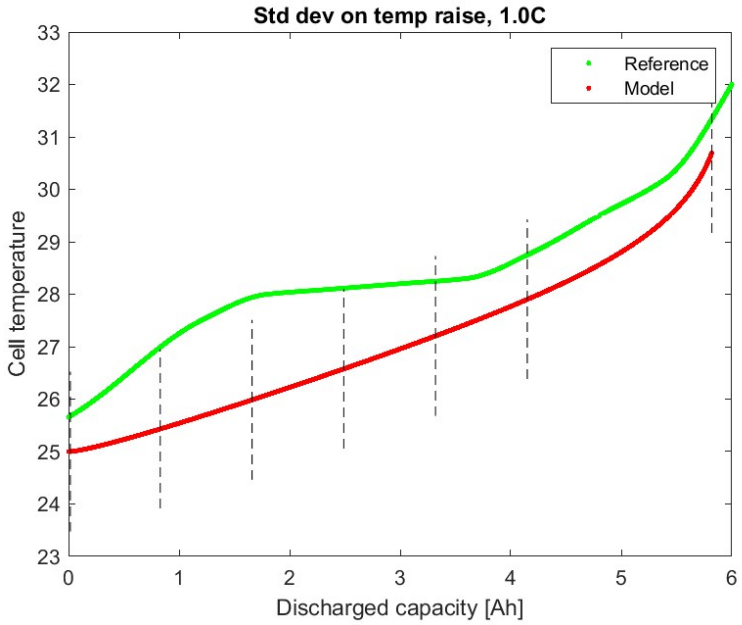

Figure B.2: Standard deviation check for 1C C-rate.

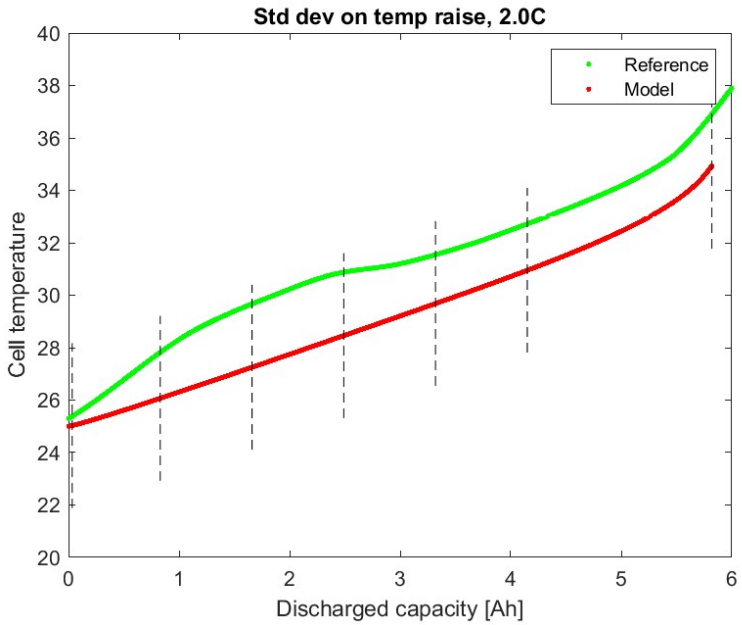

Figure B.3: Standard deviation check for 2C C-rate.

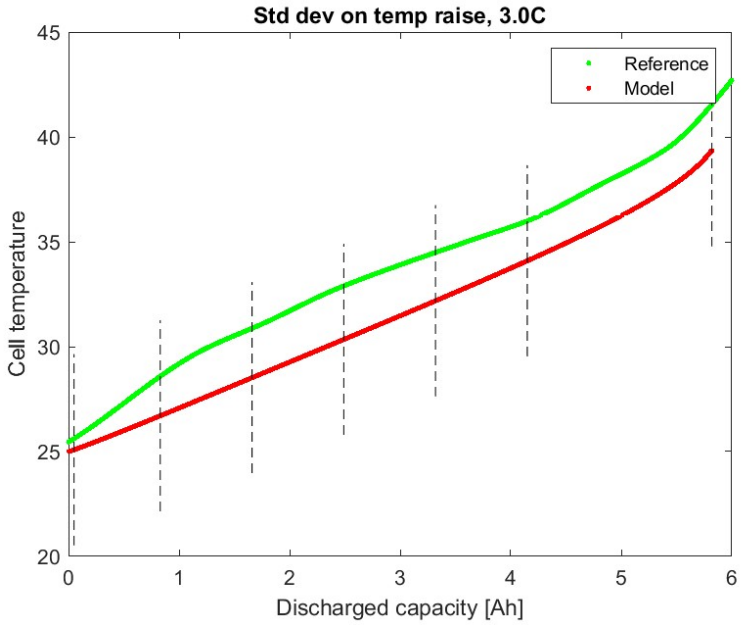

Figure B.4: Standard deviation check for 3C C-rate.

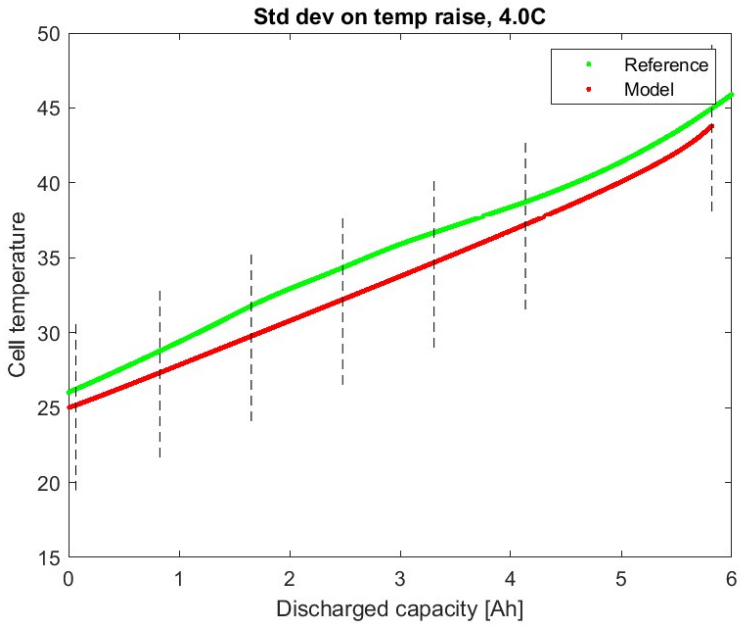

Figure B.5: Standard deviation check for 4C C-rate.

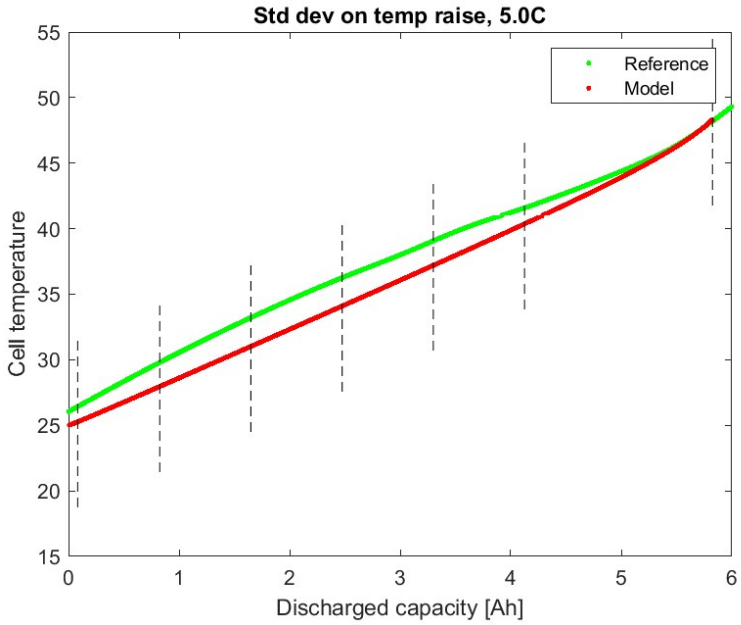

Figure B.6: Standard deviation check for 5C C-rate.

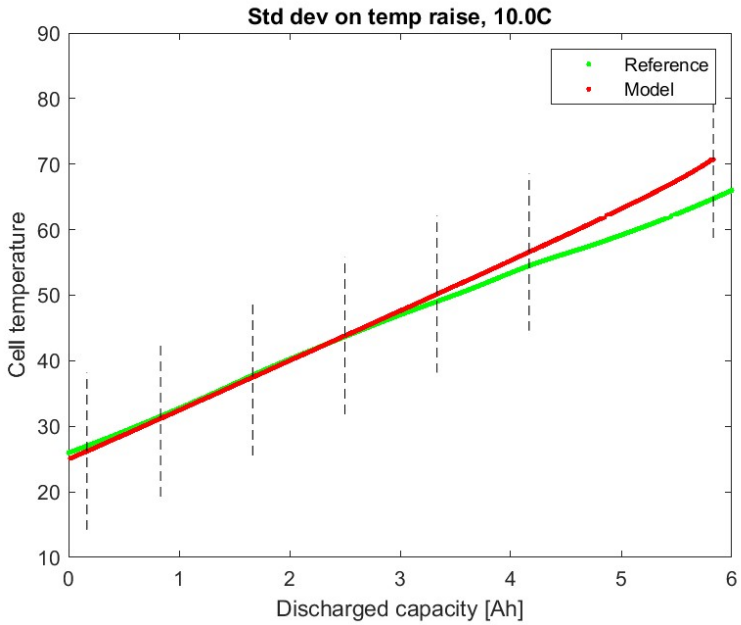

Figure B.7: Standard deviation check for 10C C-rate.

C

Peltier accuracy

In this appendix, the verification process of the accuracy of the Peltier modules model is presented. The latter consists in comparing the reference curves, obtained from the technical data sheet of the modules, with the curves obtained with the model. In the plots, the standard deviation is also marked, one above and one below the heat trend. The verification is done for different current inputs (2A, 3A, 4A, 5A, 6A, 8A) and different temperatures on the hot side of the module, namely 25°C, 50°C, and 75°C. For each combination, the verification is done on both the heat generated (Qg) and the heat absorbed (Qc).

As can be seen, the larger discrepancies appear where the heat generated or absorbed is lower than the one defined by the specs, for which the results are actually more conservative. Thus, if the new component efficiently works in the model then it will also work in reality as even stronger cooling and heating effects can be obtained.

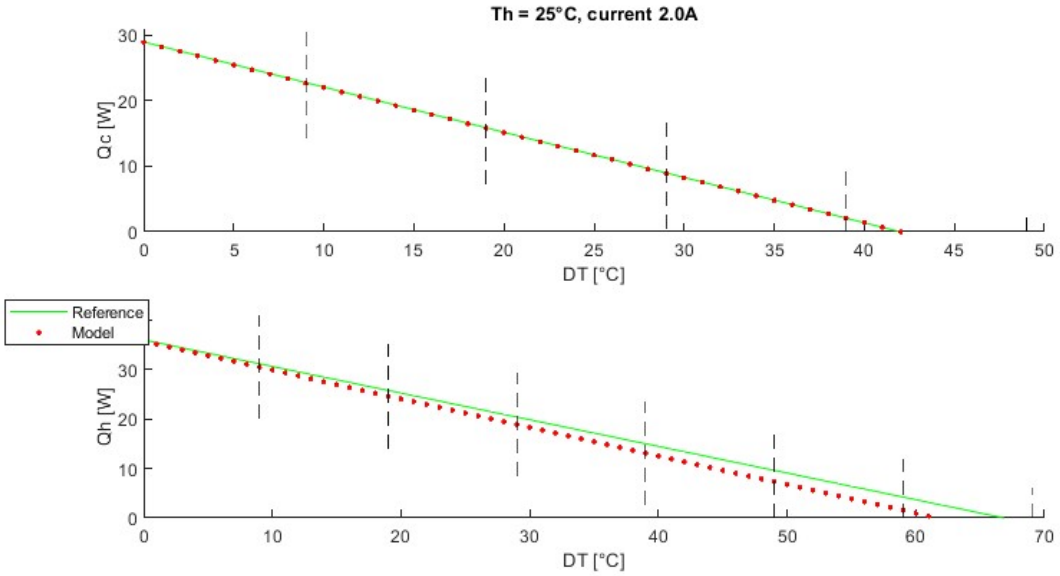

Figure C.1: Standard deviation check for 2A and Thot = 25°C.

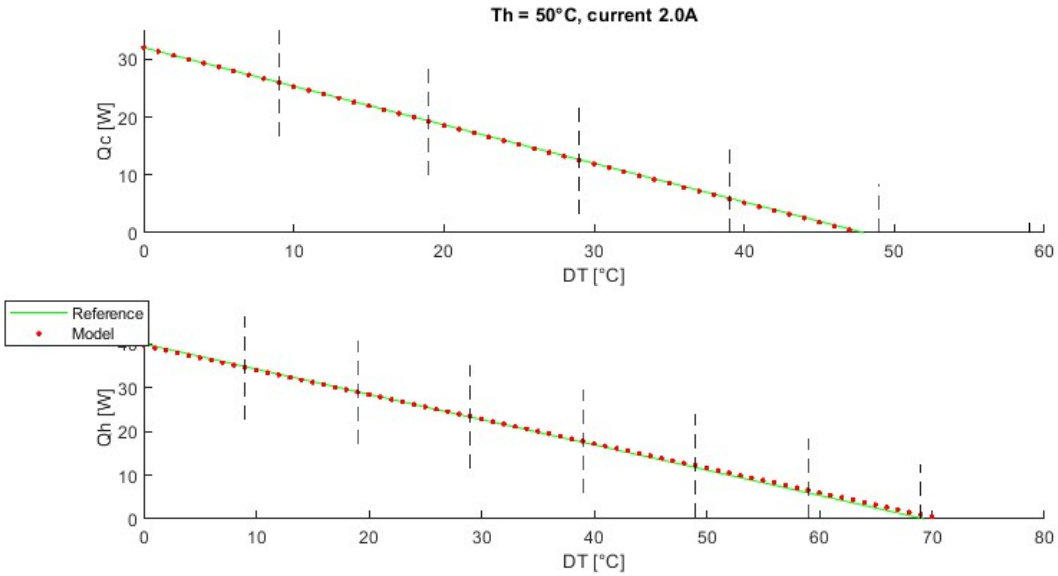

Figure C.2: Standard deviation check for 2A and Thot = 50°C.

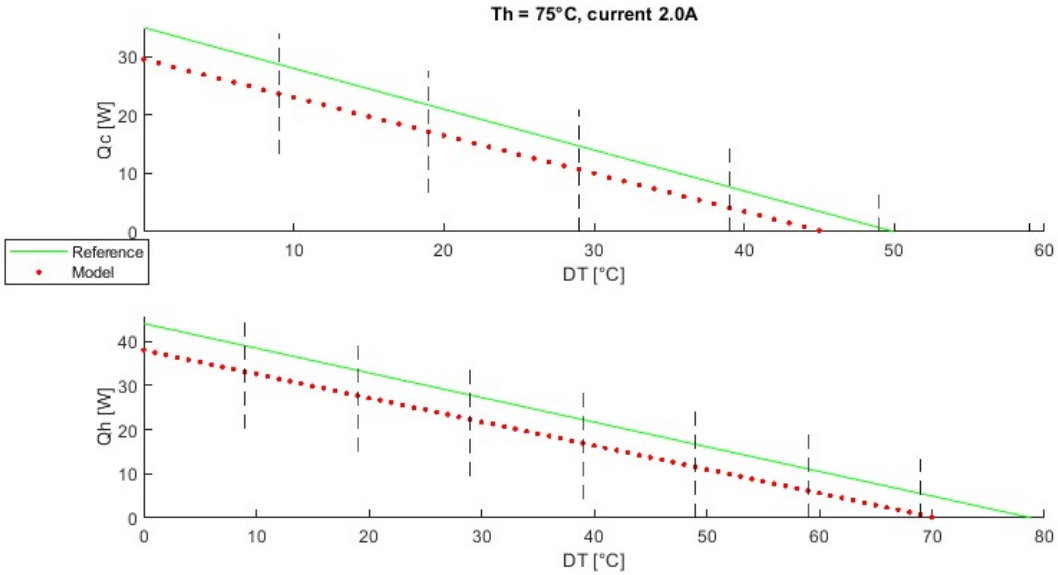

Figure C.3: Standard deviation check for 2A and Thot = 75°C.

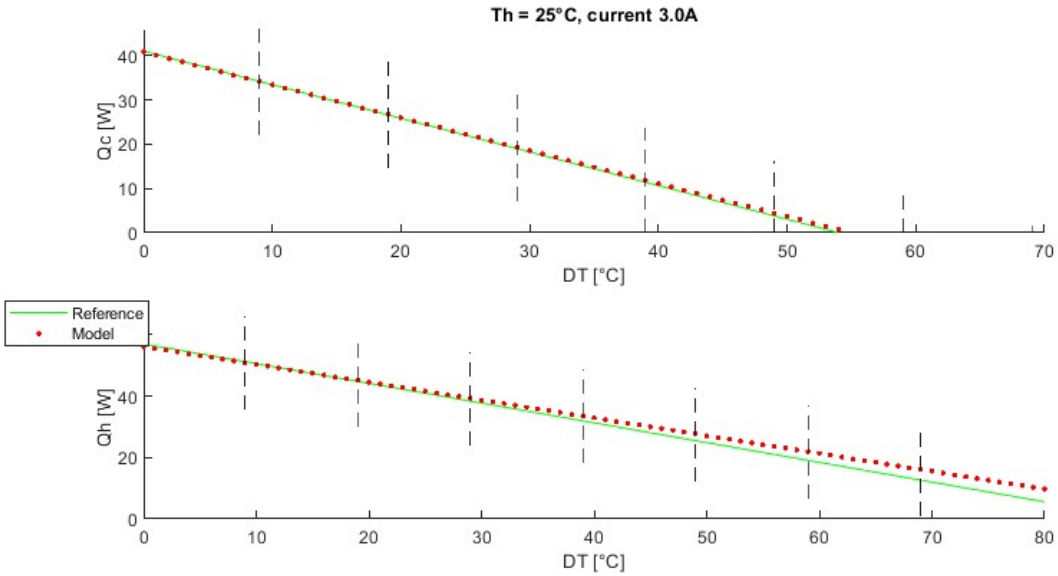

Figure C.4: Standard deviation check for 3A and Thot = 25°C.

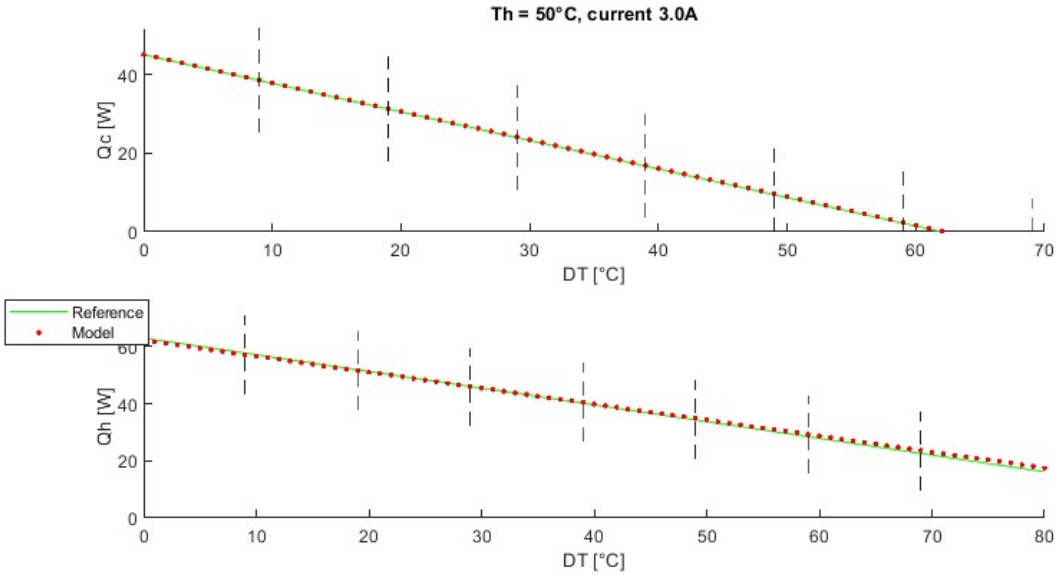

Figure C.5: Standard deviation check for 3A and Thot = 50°C.

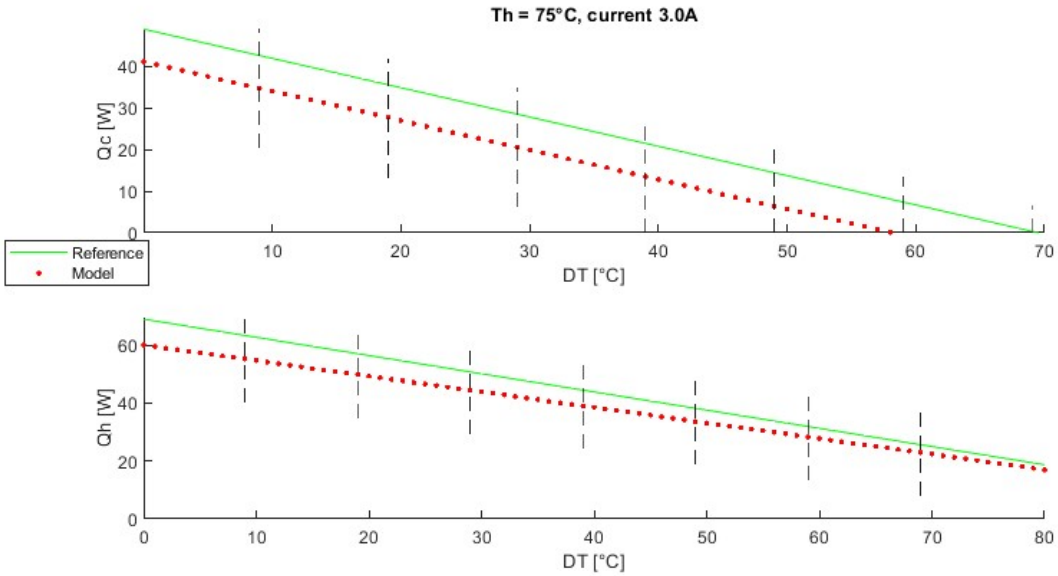

Figure C.6: Standard deviation check for 3A and Thot = 75°C.

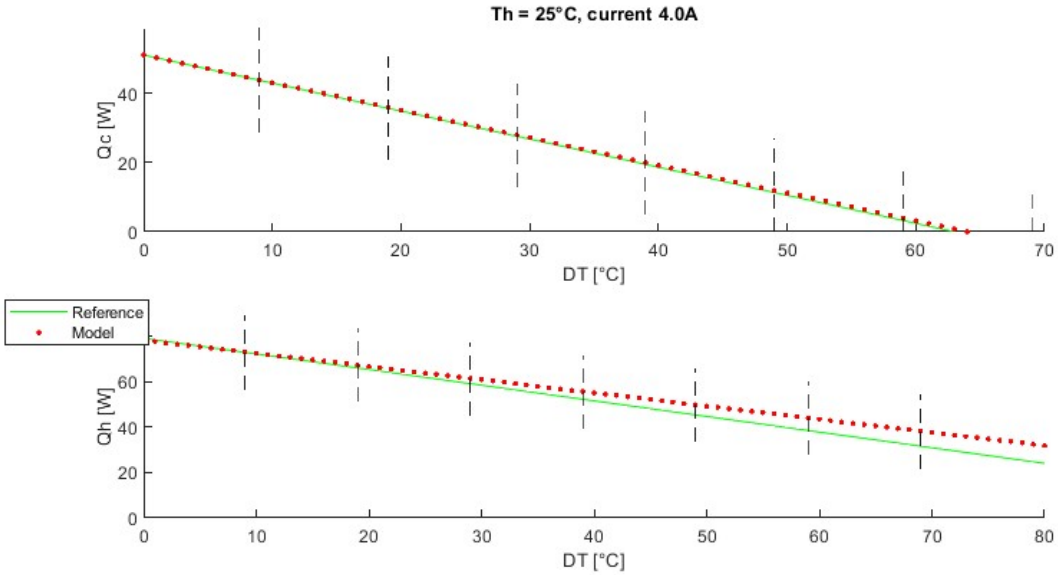

Figure C.7: Standard deviation check for 4A and Thot = 25°C.

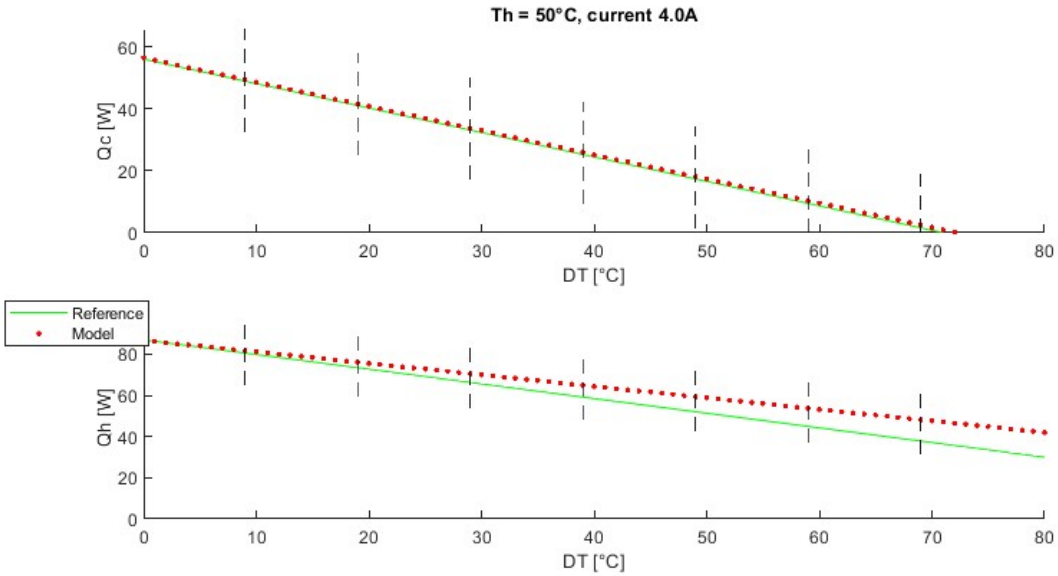

Figure C.8: Standard deviation check for 4A and Thot = 50°C.

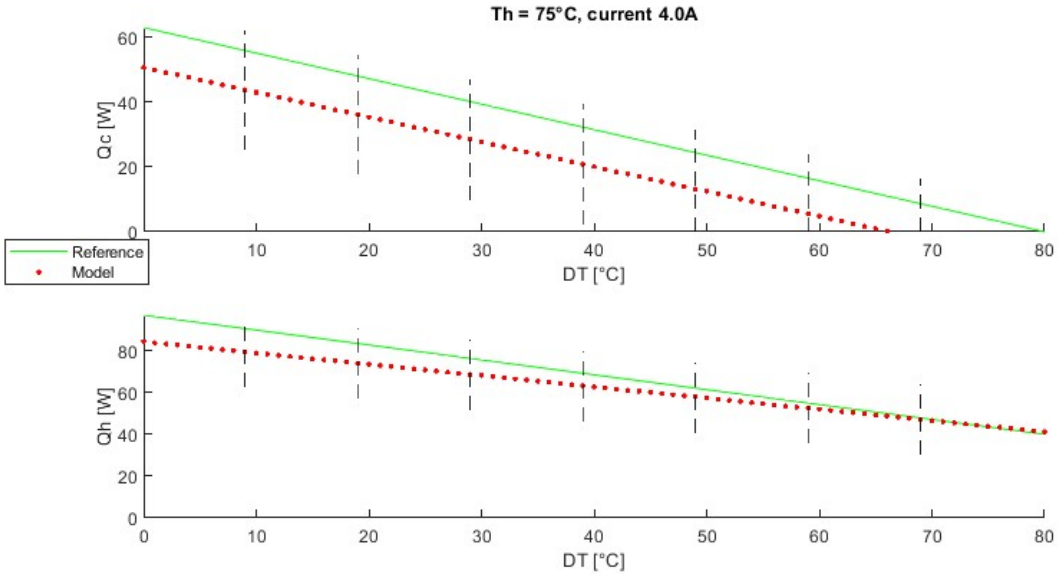

Figure C.9: Standard deviation check for 4A and Thot = 75°C.

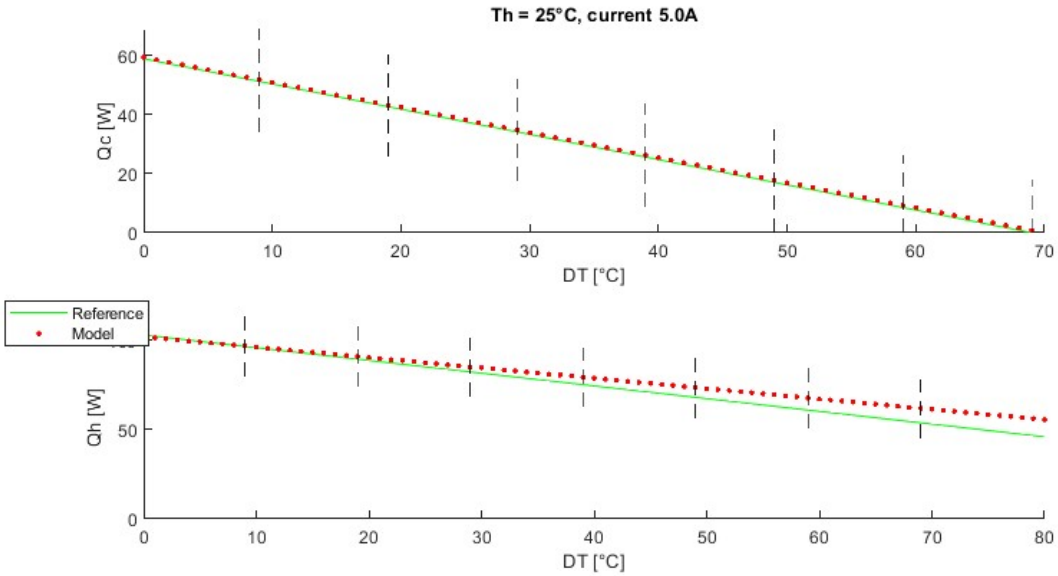

Figure C.10: Standard deviation check for 5A and Thot = 25°C.

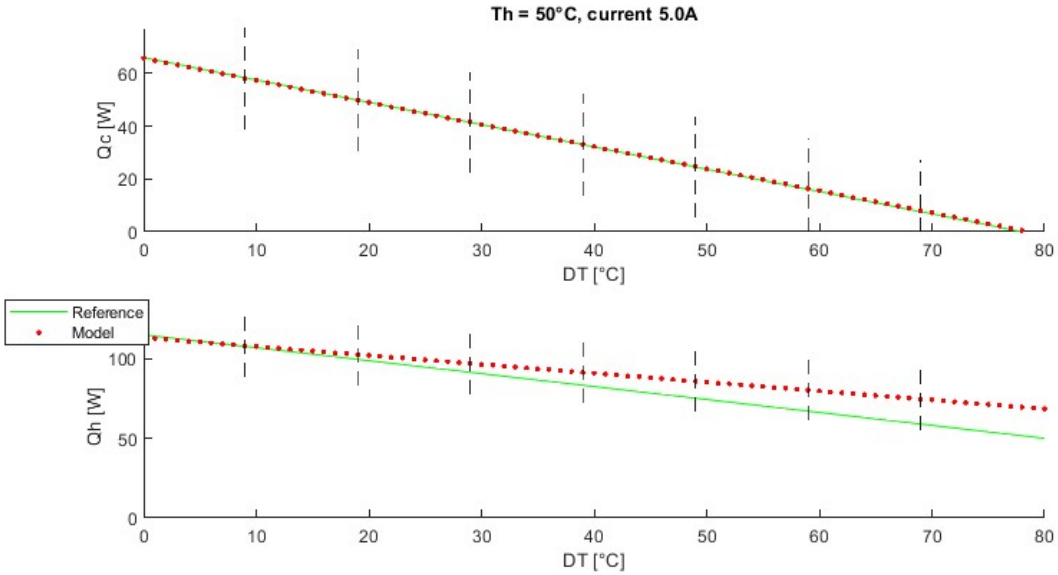

Figure C.11: Standard deviation check for 5A and Thot = 50°C.

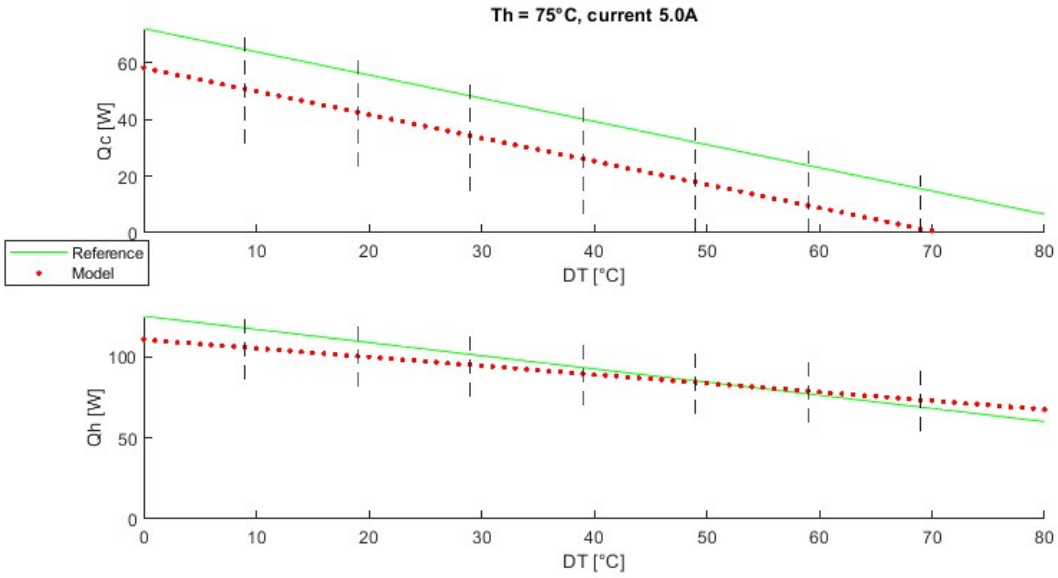

Figure C.12: Standard deviation check for 5A and Thot = 75°C.

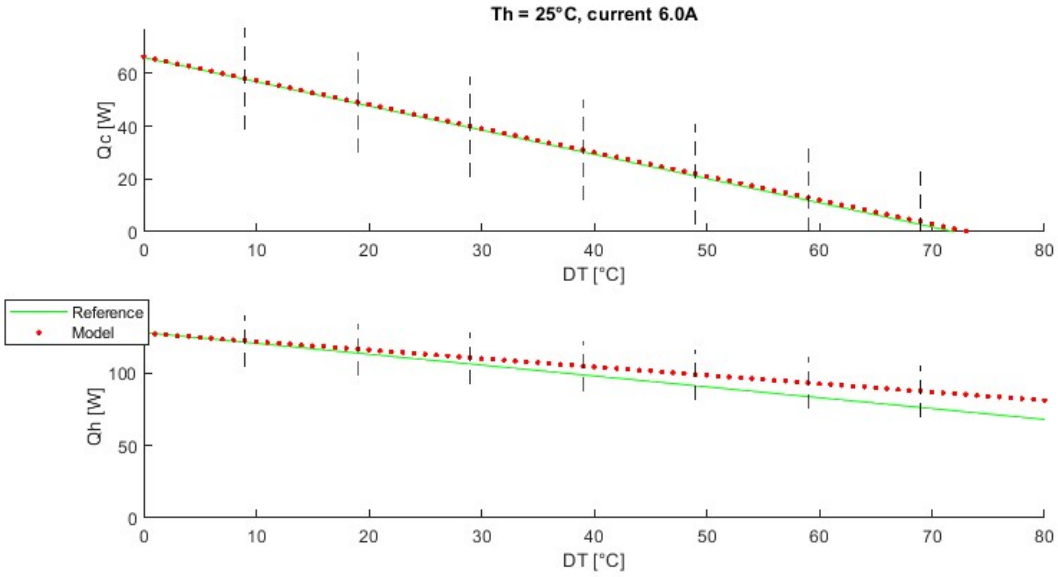

Figure C.13: Standard deviation check for 6A and Thot = 25°C.

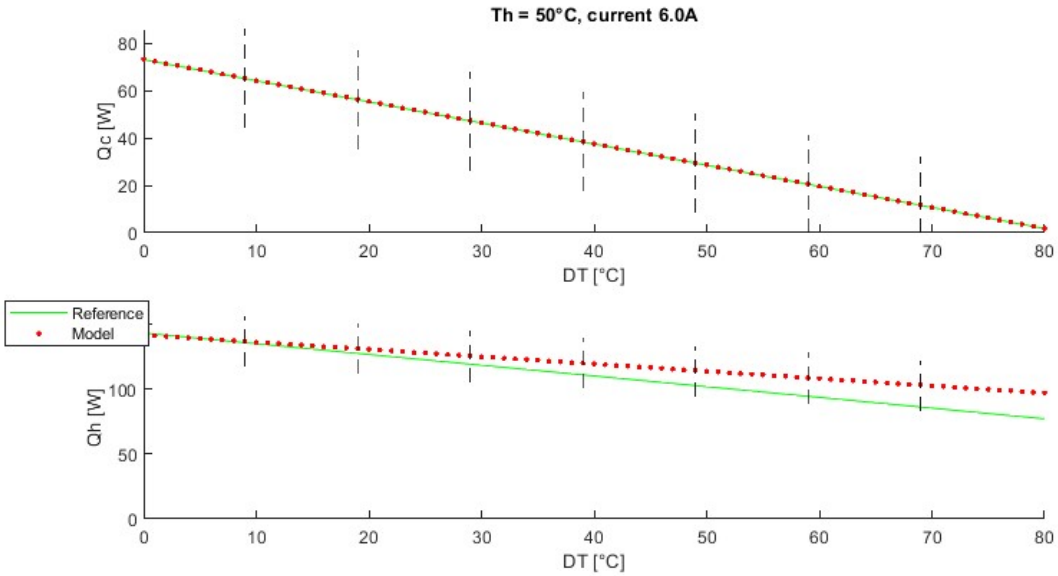

Figure C.14: Standard deviation check for 6A and Thot = 50°C.

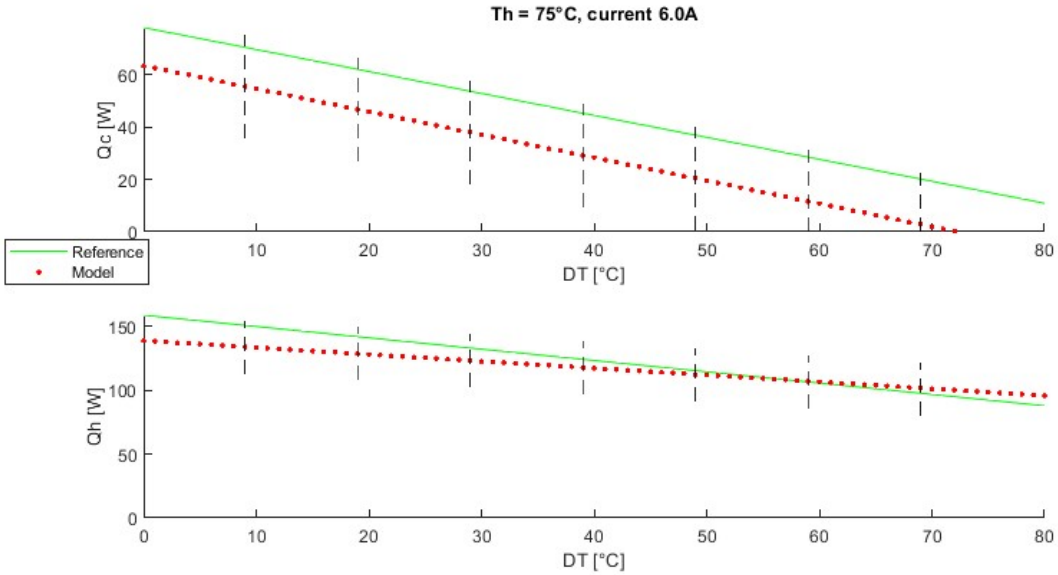

Figure C.15: Standard deviation check for 6A and Thot = 75°C.

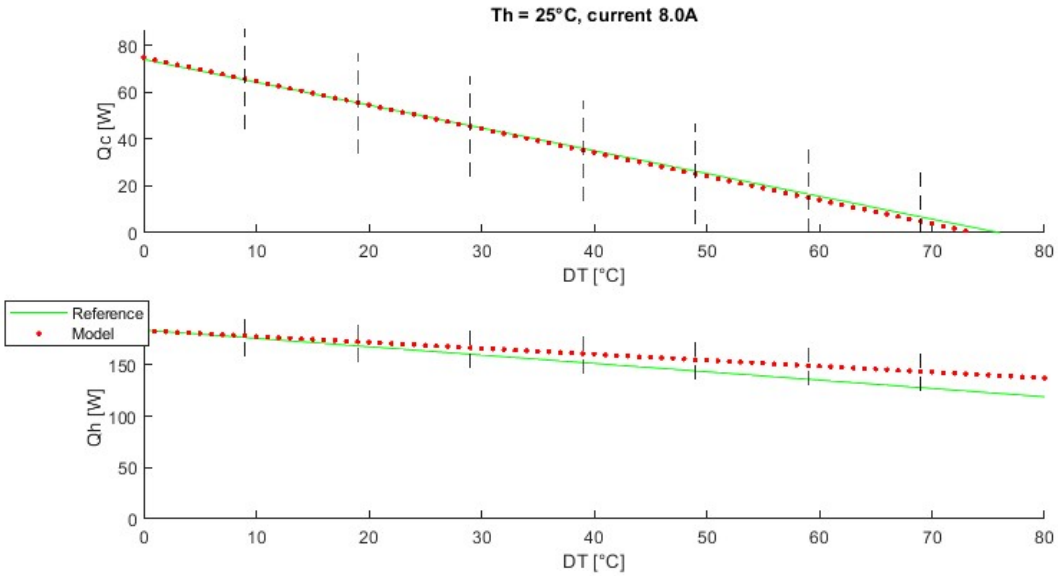

Figure C.16: Standard deviation check for 8A and Thot = 25°C.

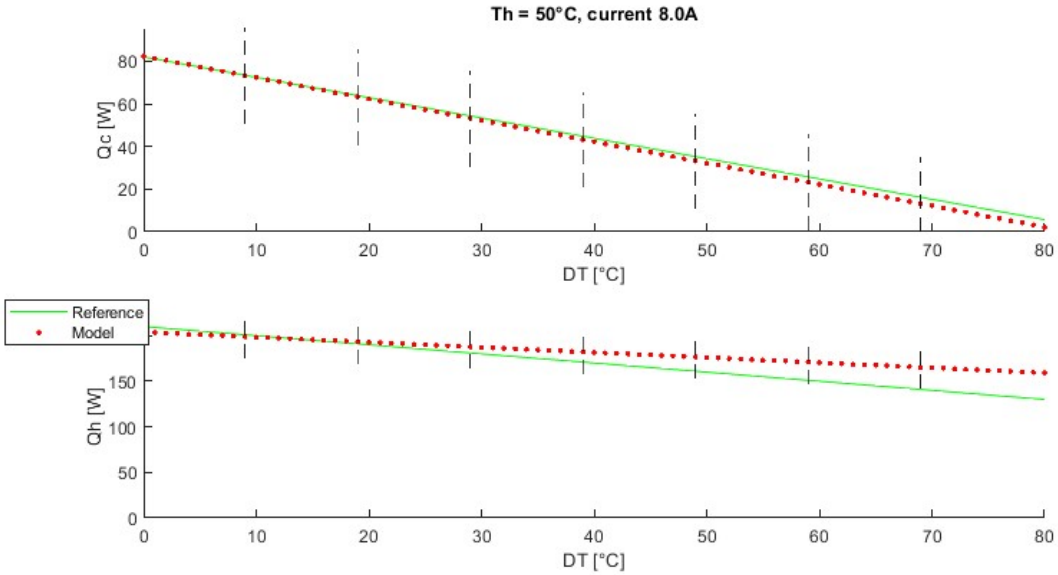

Figure C.17: Standard deviation check for 8A and Thot = 50°C.

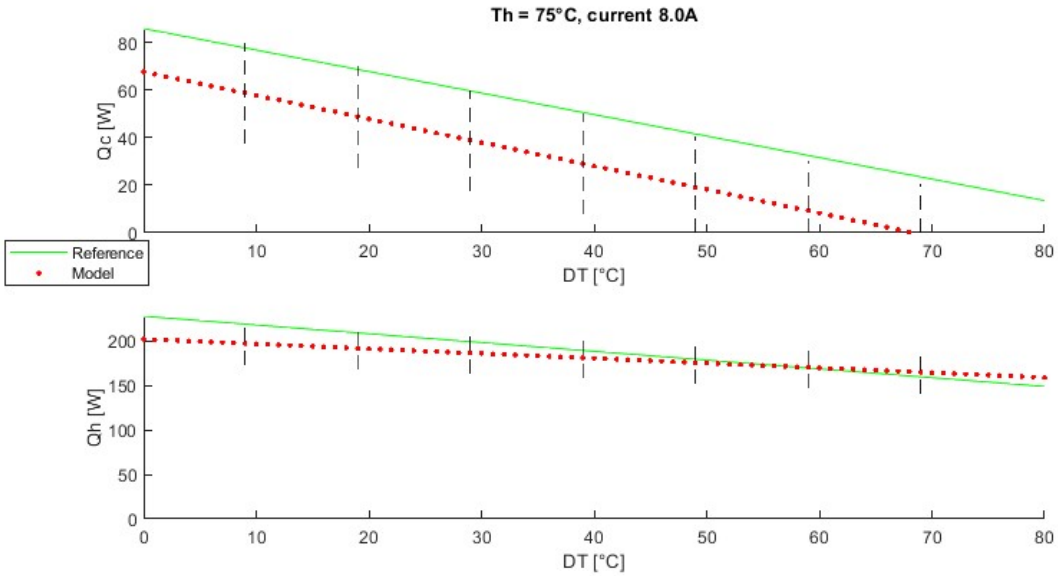

Figure C.18: Standard deviation check for 8A and Thot = 75°C.